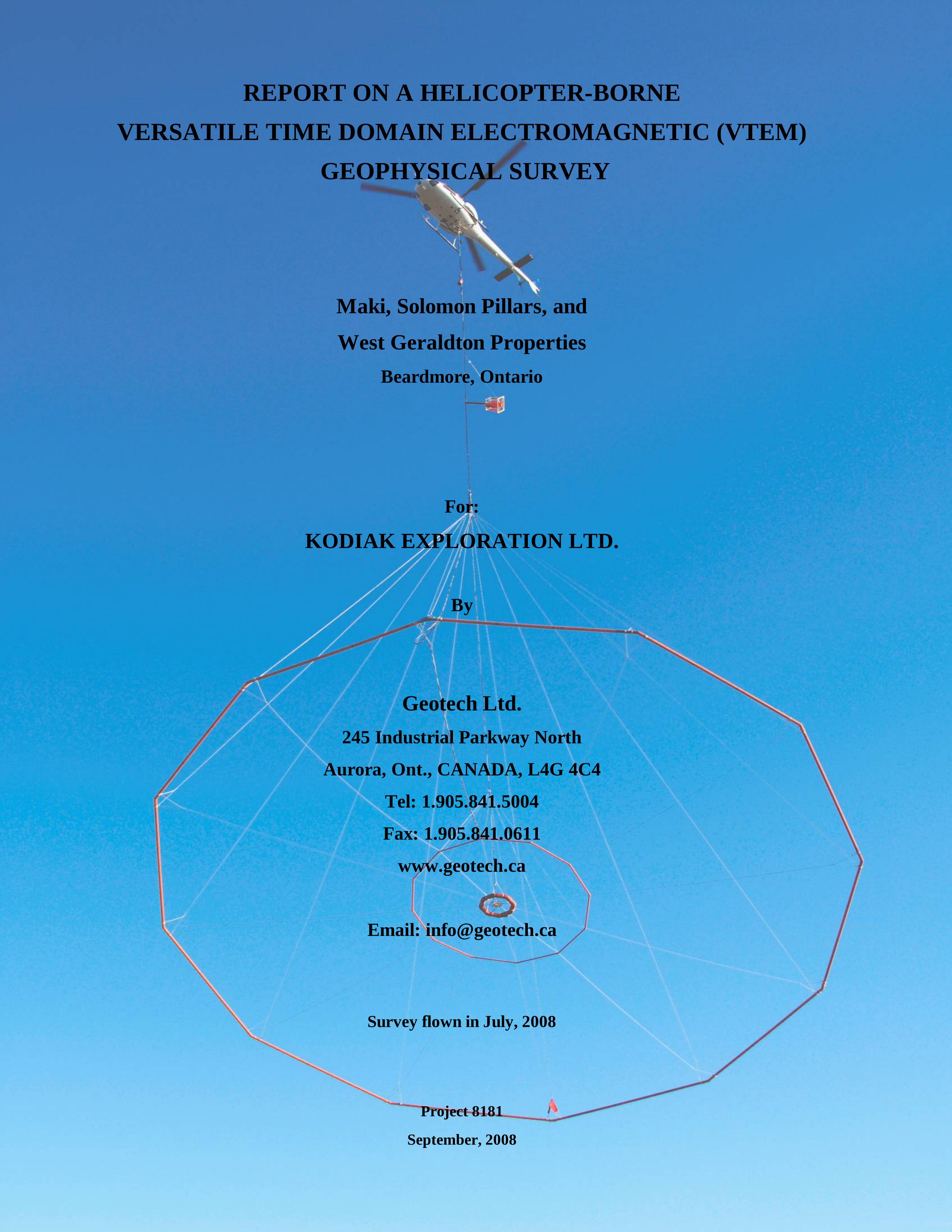

REPORT ON A HELICOPTER-BORNE VERSATILE TIME DOMAIN ELECTROMAGNETIC (VTEM) GEOPHYSICAL SURVEY

Maki, Solomon Pillars, and West Geraldton Properties

Beardmore, Ontario

For:

KODIAK EXPLORATION LTD.

By

Geotech Ltd.

245 Industrial Parkway North

Aurora, Ont., CANADA, L4G 4C4

Tel: 1.905.841.5004

Fax: 1.905.841.0611

www.geotech.ca

Email: info@geotech.ca

Survey flown in July, 2008

Project 8181

September, 2008

TABLE OF CONTENTS

LIST OF FIGURES

LIST OF TABLES

APPENDICES

REPORT ON A HELICOPTER-BORNE VERSATILE TIME DOMAIN ELECTROMAGNETIC SURVEY

Maki, Solomon Pillars, and West Geraldton Properties
Beardmore, Ontario

Executive Summary

During July 18th to 22nd, 2008 Geotech Ltd. carried out a helicopter-borne geophysical survey for Kodiak Exploration Ltd. over three (3) blocks near Beardmore, Ontario, Canada.

Principal geophysical sensors included a versatile time domain electromagnetic (VTEM) system, and a caesium magnetometer. Ancillary equipment included a GPS navigation system and a radar altimeter. A total of 792 line-kilometers were flown.

The survey operations were based in Beardmore, Ontario. In-field data quality assurance and preliminary processing were carried out on a daily basis during the acquisition phase. Preliminary and final data processing, including generation of final digital data and map products were undertaken from the office of Geotech Ltd. in Aurora, Ontario.

The processed survey results are presented as electromagnetic stacked profiles, and as a color contour grid of the B-field EM late time channel, total magnetic intensity, and time constant (Tau).

Digital data includes all electromagnetic and magnetic products, plus ancillary data including the waveform.

The survey report describes the procedures for data acquisition, processing, final image presentation and the specifications for the digital data set. The geophysical results are briefly discussed and interpreted using EM anomaly picking and time constant (Tau) analysis. EM targets are selected for ground follow up.

1. INTRODUCTION

1.1 General Considerations

These services are the result of the Agreement made between Geotech Ltd. and Kodiak Exploration Ltd. to perform a helicopter-borne geophysical survey over the Maki, Solomon Pillars, and West Geralton properties, located near Beardmore, Ontario, Canada.

William Chornobay, President, acted on behalf of Kodiak Exploration Ltd. during the data acquisition and data processing phases of this project.

The geophysical surveys consisted of helicopter borne EM using the versatile time-domain electromagnetic (VTEM) system and aeromagnetics using a caesium magnetometer. A total of 792 line-km of geophysical data were acquired during the survey. The survey area is shown in Figure 1.

The crew was based at the town of Beardmore, Ontario for the acquisition phase of the survey. Survey flying started on July 18th and was completed on July 22nd, 2008

Data quality control and quality assurance, and preliminary data processing were carried out on a daily basis during the acquisition phase of the project. Final data processing followed immediately after the end of the survey. Final reporting, data presentation and archiving were completed from the Aurora office of Geotech Ltd. in September, 2008.

Figure 1 - Property Location

1.2 Survey and System Specifications

The Maki, Solomon Pillars, and West Geraldton properties are located in central Ontario, 60 kilometers east of Lake Nipigon. The base of operations for the survey blocks were in Beardmore, Ontario which is located 10 kilometers south-west from the Maki Property.

The survey blocks were flown in a north-south (N 0° E) direction with a traverse line spacing of 100 meters, as depicted in Figure 2. Tie lines were flown perpendicular to the traverse lines at a spacing of 750 to 950 metres in the direction of N 90° E. For more detailed information on the flight spacing and direction see Table 1.

The helicopter maintained a mean terrain clearance of 75 meters which translates into an average height of 40 meters above ground for the bird-mounted VTEM system and 62 meters for the magnetic sensor.

The survey was flown using an Astar B2 helicopter, registration C-GCYE. The helicopter was operated by Expedition Helicopters Inc. Details of the survey specifications may be found in Section 2 of this report.

1.3 Topographic Relief and Cultural Features

Topographically, the three properties exhibit a shallow relief, with an elevation ranging from 315-411 meters above sea level. The blocks are located 60 kilometers east of Lake Nipigon. There are many small rivers, lakes, and wetlands that run throughout the block. This survey block is covered by NTS (National Topographic Survey) of Canada sheet 042E10, 042E11, 042E12, 042E14, and 042E15.

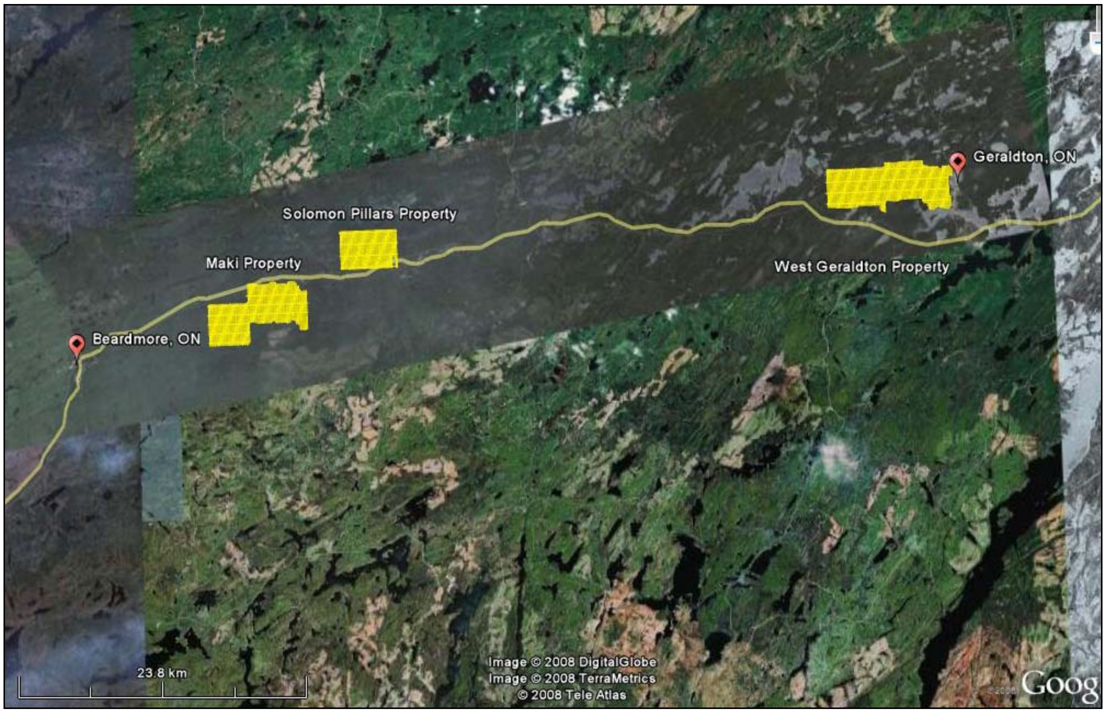

Figure 2 – Google Image of Survey Blocks

2. DATA ACQUISITION

2.1 Survey Area

The survey blocks (see location map, Figure 2) and general flight specifications are as follows:

Table 1 - Survey blocks

Survey block	Traverse Line spacing (m)	Area (Km^2)	Line-km's	Flight direction	Line numbers
Maki	Traverse: 100	29	304	N 0° E	L1000 – L1810
	Tie: 750			N 90° E	T1500 – T1550
Solomon Pillars	Traverse: 100	15	165	N 0° E	L2000 – L2460
	Tie: 950			N 90° E	T2500 – T2530
West Geraldton	Traverse: 100	34	365	N 0° E	L3000 – L4040
	Tie: 900			N 90° E	T4500 – T4531

Survey block boundaries co-ordinates are provided in Appendix B.

2.2 Survey Operations

Survey operations were based out of the Roxy's Motel in Beardmore, Ontario from July 18th to July 22nd, 2008. The following table shows the timing of the flying.

Table 2 - Survey schedule

Date	Flight #	Flown KM	Block	Crew location	Comments
18-July-08				Beardmore, Ontario	No production – rain
19-July-08	1- 3	159	SOLOMON	Beardmore, Ontario	Production
20-July-08	4 - 7	289	WEST GERADTON	Beardmore, Ontario	Production
21-July-08	8 - 10	170	WEST GERADTON / MAKI	Beardmore, Ontario	Production
22-July-08	11 - 13	174	MAKI	Beardmore, Ontario	Production – JOB COMPLETE

2.3 Flight Specifications

The helicopter was maintained at a mean height of 75 meters above the ground with a nominal survey speed of 80 km/hour. This allowed for a nominal EM sensor terrain clearance of 40 meters and a magnetic sensor clearance of 62 meters. The data recording rates of the data acquisition was 0.1 second for electromagnetics, magnetometer and gamma ray spectrometer, 0.2 second for altimeter and GPS. This translates to a geophysical reading about every 2 meters along flight track. Navigation was assisted by a CDGPS receiver and data acquisition system, which reports GPS co-ordinates as latitude/longitude and directs the pilot over a pre-programmed survey grid.

The operator was responsible for monitoring of the system integrity. He also maintained a detailed flight log during the survey, tracking the times of the flight as well as any unusual geophysical or topographic feature.

On return of the aircrew to the base camp the survey data was transferred from a compact flash card (PCMCIA) to the data processing computer. The data were then uploaded via ftp to the Geotech office in Aurora for daily quality assurance and quality control by qualified personnel, operating remotely.

2.4 Aircraft and Equipment

2.4.1 Survey Aircraft

The survey was flown using a Eurocopter Aerospatiale (Astar) B2 helicopter, registration C-GCYE. The helicopter was operated by Expedition Helicopters Inc., based out of Cochrane, Ontario. Installation of the geophysical and ancillary equipment was carried out by Geotech Ltd.

2.4.2 Electromagnetic System

The electromagnetic system was a Geotech Time Domain EM (VTEM) system. The configuration is as indicated in Figure 3 below.

Receiver and transmitter coils are concentric and Z-direction oriented. The coils were towed at a mean distance of 35 meters below the aircraft as shown in Figure 5. The receiver decay recording scheme is shown diagrammatically in Figure 4.

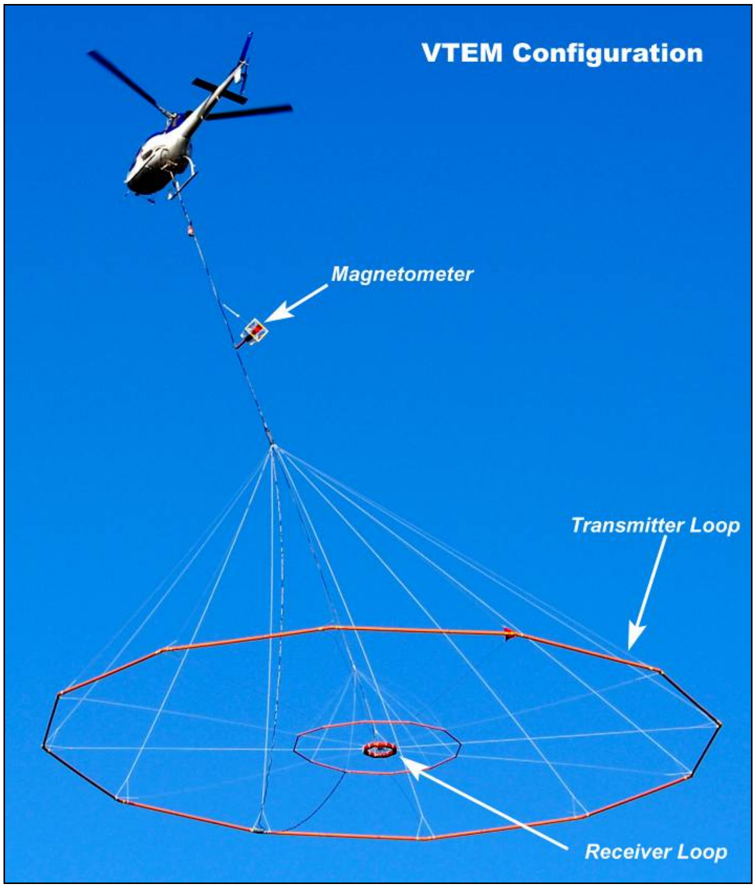

Figure 3 - VTEM Configuration

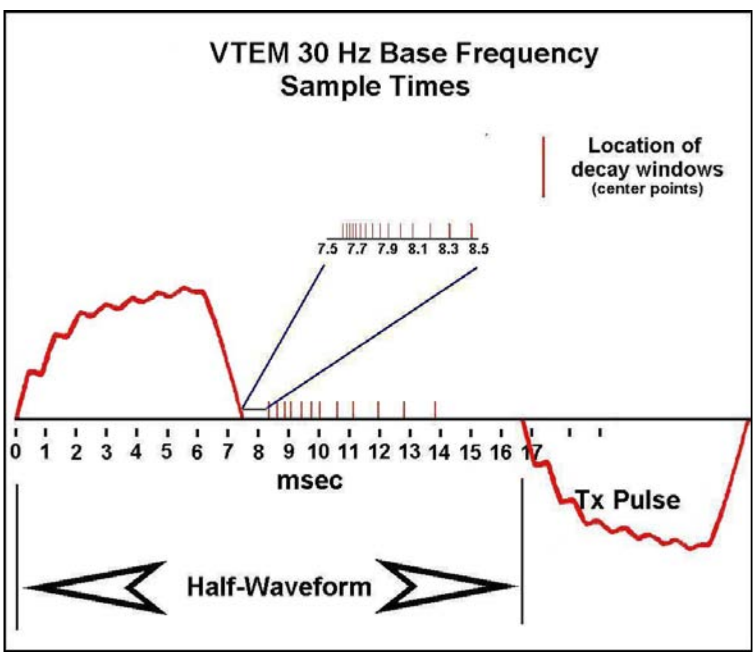

Figure 4 - VTEM Long Pulse 7 ms Waveform & Sample Times.

The complete VTEM decay sampling scheme is shown in Table 3 below. Twenty-four time measurement gates (channels 10 to 33) were used for the final data processing in the range from 120 ms to 6578 ms, as shown in Table 5.

Table 3 – Decay Sampling Scheme

VTEM Time Gates				
Array	Microseconds			
Index	Middle	Start	End	Width
0	0			
1	10	10	21	11
2	21	16	26	11
3	31	26	37	11
4	42	37	47	11
5	52	47	57	10
6	62	57	68	11
7	73	68	78	11
8	83	78	91	13
9	99	91	110	19
10	120	110	131	21
11	141	131	154	24
12	167	154	183	29
13	198	183	216	34
14	234	216	258	42
15	281	258	310	53
16	339	310	373	63
17	406	373	445	73
18	484	445	529	84
19	573	529	628	99
20	682	628	750	123
21	818	750	896	146
22	974	896	1063	167
23	1151	1063	1261	198
24	1370	1261	1506	245
25	1641	1506	1797	292
26	1953	1797	2130	333
27	2307	2130	2526	396
28	2745	2526	3016	490
29	3286	3016	3599	583
30	3911	3599	4266	667
31	4620	4266	5058	792
32	5495	5058	6037	979
33	6578	6037	7203	1167
34	7828	7203	8537	1334
35	9245	8537	10120	1584

VTEM system parameters:

<u>Transmitter Section</u>

- Transmitter coil diameter: 26 m
- Number of turns: 4
- Transmitter base frequency: 30 Hz
- Peak current: 176 A
- Pulse width: 7.3 ms
- Pulse width: Duty cycle: 44%
- Peak dipole moment: 373,600 nIA
- Nominal terrain clearance: 40 m

<u>Receiver Section</u>

- Receiver coil diameter: 1.2 m
- Number of turns: 100.
- Effective coil area: 113.1 m^2
- Wave form shape: trapezoid
- Power Line Monitor: 60 Hz

<u>Magnetometer</u>

- Nominal terrain clearance: 62 m

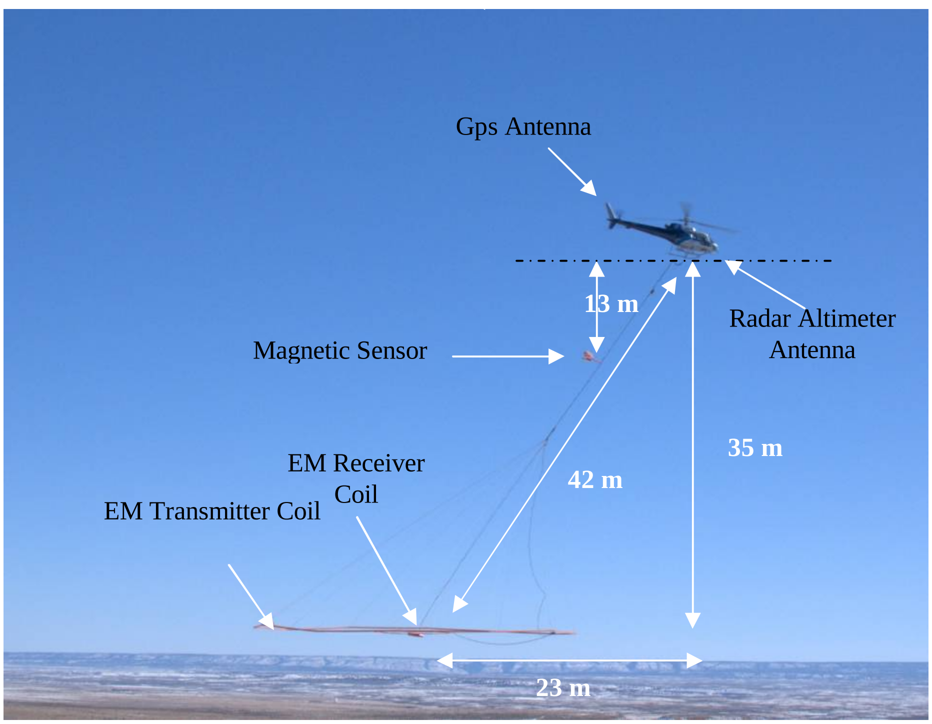

Figure 5 – VTEM system configuration

2.4.3 Airborne magnetometer

The magnetic sensor utilized for the survey was a Geometrics optically pumped caesium vapour magnetic field sensor, mounted in a separated bird, 13 metres below the helicopter, as shown in Figure 5. The sensitivity of the magnetic sensor is 0.02 nanoTesla (nT) at a sampling interval of 0.1 seconds. The magnetometer sends the measured magnetic field strength as nanoTesla to the data acquisition system via the RS-232 port.

2.4.4 Radar Altimeter

A Terra TRA 3000/TRI 40 radar altimeter was used to record terrain clearance. The antenna was mounted beneath the bubble of the helicopter cockpit (Figure 5).

2.4.5 GPS Navigation System

The navigation system used was a Geotech PC104 based navigation system utilizing a NovAtel's CDGPS (Canada-Wide Differential Global Positioning System Correction Service) enable OEM4-G2-3151W GPS receiver, Geotech navigate software, a full screen display with controls in front of the pilot to direct the flight and an NovAtel GPS antenna mounted on the helicopter tail (Figure 5). As many as 11 GPS and two CDGPS satellites may be monitored at any one time. The positional accuracy or circular error probability (CEP) is 1.8 m, with CDGPS active, it is 1.0 m. The co-ordinates of the block were set-up prior to the survey and the information was fed into the airborne navigation system.

2.4.6 Digital Acquisition System

A Geotech data acquisition system recorded the digital survey data on an internal compact flash card. Data is displayed on an LCD screen as traces to allow the operator to monitor the integrity of the system. The data type and sampling interval as provided in Table 4.

Table 4 – Acquisition Sampling Rates

DATA TYPE	SAMPLING
TDEM	0.1 sec
Magnetometer	0.1 sec
GPS Position	0.2 sec
Radar Altimeter	0.2 sec

2.4.7 Base Station

A combined magnetometer/GPS base station was utilized on this project. A Geometrics Caesium vapour magnetometer was used as a magnetic sensor with a sensitivity of 0.001 nT. The base station was recording the magnetic field together with the GPS time at 1 Hz on a base station computer.

The base station magnetometer sensor was installed in an isolated area behind Lodge #6 in Beardmore, Ontario (49˚40'53.49"N, W 87˚32'43.38"W), away from electric transmission lines and moving ferrous objects such as motor vehicles. The base station data were backed-up to the data processing computer at the end of each survey day.

3. PERSONNEL

The following Geotech Ltd. personnel were involved in the project.

Field:

Project Manager:	Peter Cholewa (Office)
Crew chief:	Adrian Srmasag
System Operator:	Alexander Smirnov

The survey pilot and the mechanical engineer were employed directly by the helicopter operator – Expedition Helicopters Inc.

Pilot:	Yvon Benjamin
Mechanical Engineer:	Jonathan Fontaine

Office:

QC/QC:	Emilio Schein
Preliminary Data Processing:	Emilio Schein
Field Data Processing:	Nasreddine Bournas
Interpretation:	Nasreddine Bournas
Reporting/Mapping:	Milica Marich

Data acquisition phases were carried out under the supervision of Andrei Bagrianski, P. Geo, Surveys Manager. Processing phases were carried out under the supervision of Jean Legault, P. Geo, Manager of Processing and Interpretation. The overall contract management and customer relations were by Paolo Berardelli.

4. DATA PROCESSING AND PRESENTATION

Data compilation and processing were carried out by the application of Geosoft OASIS Montaj and programs proprietary to Geotech Ltd.

4.1 Flight Path

The flight path, recorded by the acquisition program as WGS 84 latitude/longitude, was converted into the NAD 83 UTM coordinate system (UTM Zone 16N) in Oasis Montaj.

The flight path was drawn using linear interpolation between x, y positions from the navigation system. Positions are updated every second and expressed as UTM easting's (x) and UTM northing's (y).

4.2 Electromagnetic Data

A three stage digital filtering process was used to reject major sferic events and to reduce system noise. Local sferic activity can produce sharp, large amplitude events that cannot be removed by conventional filtering procedures. Smoothing or stacking will reduce their amplitude but leave a broader residual response that can be confused with geological phenomena. To avoid this possibility, a computer algorithm searches out and rejects the major sferic events. The filter used was a 16 point non-linear filter.

The signal to noise ratio was further improved by the application of a low pass linear digital filter. This filter has zero phase shift which prevents any lag or peak displacement from occurring, and it suppresses only variations with a wavelength of less than roughly 1 second or 15 metres. This filter is a symmetrical 1 second linear filter.

The results are presented as stacked profiles of EM voltages for the time gates, in linear - logarithmic scale for both B-field and dB/dt response. A grid of the B-field time channel, recorded 1.953 milliseconds after the termination of the impulse is also presented as contour colour image.

Generalized modeling results of VTEM data, written by consultant Roger Barlow and Nasreddine Bournas, P. Geo., are shown in Appendix E.

Graphical representations of the VTEM input current waveform and transmitter output voltage of the receiver coil are both shown in Appendix C.

4.3 Anomaly Section

The EM data were subjected to an anomaly recognition process using all time domain geophysical channels and using B-Field and dB/dt profiles. The resulting EM anomaly picks are presented as overlays on all the topographic maps.

Each individual conductor pick is represented by an anomaly symbol classified according to calculated conductance (Figure 6)[1]. Identified anomalies were classified into one of four categories. The anomaly symbol is accompanied by postings denoting the calculated conductance from dB/dt, calculated dB/dT and B-field decay constants (Tau). Each symbol is also given an identification letter label, unique to each flight line. The anomaly symbol legend is given below.

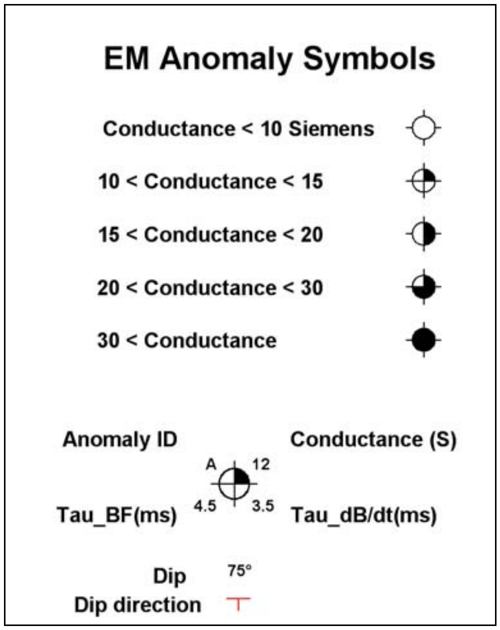

Figure 6 - EM Anomaly Symbols

EM anomaly symbols are presented in all final maps, i.e. VTEM profiles and total magnetic intensity grid. The anomalous responses have been picked on each line, reviewed and edited by a geophysicist on a line by line basis to discriminate between bedrock, overburden and culture conductors. The new channels were created in each of the Geosoft "XYZ" tables for the block. The identified time domain electromagnetic VTEM anomalies are listed in Appendix F.

[1]Note: The conductances were obtained from the EM time constant whose relationship was calculated using Maxwell forward modeling algorithm (EMIT Technology Ltd. Pty. Midland, WA, AU). The conductance model utilized was for a vertical tabular prism, with horizontal dimensions of 10 x 100 metre and 1000 metre vertical (N.Bournas, Geotech Ltd., pers. comm. 09/2008).

4.4 Magnetic Data

The processing of the magnetic data involved the correction for diurnal variations by using the digitally recorded ground base station magnetic values. The base station magnetometer data were edited and merged into the Geosoft GDB database on a daily basis. The aeromagnetic data were corrected for diurnal variations by subtracting the observed magnetic base station deviations.

Tie line levelling was carried out by adjusting intersection points along traverse lines. A micro-levelling procedure was applied to remove persistent low-amplitude components of flight-line noise remaining in the data.

The corrected magnetic data were interpolated between survey lines using a random point gridding method to yield x-y grid values for a standard grid cell size of approximately 0.25 cm at the mapping scale. The Minimum Curvature algorithm was used to interpolate values onto a rectangular regular spaced grid.

5. DELIVERABLES

5.1 Survey Report

The survey report describes the data acquisition, processing, and final presentation of the survey results.

The survey report is provided in two paper copies and digitally in PDF format.

5.2 Maps

Final maps were produced at a scale 1:10,000 (Maki and Solomon Pillars properties) and 1:20,000 (West Geraldton property). The coordinate/projection system used was NAD 83, UTM zone 16 north. All maps show the flight path trace and topographic data; latitude and longitude are also noted on maps.

The preliminary and final results of the survey are presented as EM profiles, a late-time gate gridded EM channel, a color magnetic contour map, and time constant (Tau) color grid. The following maps are presented on paper;

- B-field profiles, Time Gates 0.234 – 6.578 ms in linear logarithmic scale, with TMI colour image.
- B/dt profiles, Time Gates 0.234 – 6.578 ms in linear logarithmic scale.
- B-field mid time, Time Gate 1.953 ms colour image.
- B-field mid time, Time Gate 1.953 ms colour image with EM Anomalies.
- Time constant (Tau) colour image calculated from dB/dt.
- Time constant (Tau) colour image calculated from B-Field.
- Total magnetic intensity colour image and contours.

5.3 Digital Data

- Two copies of the data and maps on DVD-ROM were prepared to accompany the report. Each DVD -ROM contains a digital file of the line data in GDB Geosoft Montaj format as well as the maps in Geosoft Montaj Map format.

- Two copies of DVD-ROMs were prepared.

There are two (2) main directories,

Data contains databases, grids and maps, as described below.
Report contains a copy of the report and appendices in PDF format.

Databases in Geosoft GDB format, containing the channels listed in Table 5.

Table 5 – Geosoft GDB Data Format.

Channel Name	**Description**
Line:	Flight line number with flight number
X:	X positional data (meters – NAD83, UTM zone 16 north)
Y:	Y positional data (meters –NAD83, UTM zone 16 north)
Z:	GPS antenna elevation (meters - ASL)
Radar:	Helicopter terrain clearance from radar altimeter (meters - AGL)
RadarB:	EM Bird terrain clearance from radar altimeter (meters - AGL)
Dist:	Distance between observations (meters)
DEM:	Digital elevation model (meters)
Gtime1:	GPS time (seconds of the day)
Mag1:	Raw Total Magnetic field data (nT)
Mag2:	Diurnal corrected Total Magnetic field data (nT)
Mag_ML:	Leveled Total Magnetic field data (nT)
Basemag:	Magnetic diurnal variation data (nT)
SF[10]:	dB/dt 120 microsecond time channel ($pV/A/m^4$)
SF[11]:	dB/dt 141 microsecond time channel ($pV/A/m^4$)
SF[12]:	dB/dt 167 microsecond time channel ($pV/A/m^4$)
SF[13]:	dB/dt 198 microsecond time channel ($pV/A/m^4$)
SF[14]:	dB/dt 234 microsecond time channel ($pV/A/m^4$)
SF[15]:	dB/dt 281 microsecond time channel ($pV/A/m^4$)
SF[16]:	dB/dt 339 microsecond time channel ($pV/A/m^4$)
SF[17]:	dB/dt 406 microsecond time channel ($pV/A/m^4$)
SF[18]:	dB/dt 484 microsecond time channel ($pV/A/m^4$)
SF[19]:	dB/dt 573 microsecond time channel ($pV/A/m^4$)
SF[20]:	dB/dt 682 microsecond time channel ($pV/A/m^4$)
SF[21]:	dB/dt 818 microsecond time channel ($pV/A/m^4$)
SF[22]:	dB/dt 974 microsecond time channel ($pV/A/m^4$)
SF[23]:	dB/dt 1151 microsecond time channel ($pV/A/m^4$)
SF[24]:	dB/dt 1370 microsecond time channel ($pV/A/m^4$)
SF[25]:	dB/dt 1641 microsecond time channel ($pV/A/m^4$)
SF[26]:	dB/dt 1953 microsecond time channel ($pV/A/m^4$)
SF[27]:	dB/dt 2307 microsecond time channel ($pV/A/m^4$)
SF[28]:	dB/dt 2745 microsecond time channel ($pV/A/m^4$)
SF[29]:	dB/dt 3286 microsecond time channel ($pV/A/m^4$)
SF[30]:	dB/dt 3911 microsecond time channel ($pV/A/m^4$)
SF[31]:	dB/dt 4620 microsecond time channel ($pV/A/m^4$)

Channel Name	Description
SF[32]:	dB/dt 5495 microsecond time channel (pV/A/m^4)
SF[33]:	dB/dt 6578 microsecond time channel (pV/A/m^4)
BF[10]:	B-field 120 microsecond time channel (pVms)/(Am^4)
BF[11]:	B-field 141 microsecond time channel (pVms)/(Am^4)
BF[12]:	B-field 167 microsecond time channel (pVms)/(Am^4)
BF[13]:	B-field 198 microsecond time channel (pVms)/(Am^4)
BF[14]:	B-field 234 microsecond time channel (pVms)/(Am^4)
BF[15]:	B-field 281 microsecond time channel (pVms)/(Am^4)
BF[16]:	B-field 339 microsecond time channel (pVms)/(Am^4)
BF[17]:	B-field 406 microsecond time channel (pVms)/(Am^4)
BF[18]:	B-field 484 microsecond time channel (pVms)/(Am^4)
BF[19]:	B-field 573 microsecond time channel (pVms)/(Am^4)
BF[20]:	B-field 682 microsecond time channel (pVms)/(Am^4)
BF[21]:	B-field 818 microsecond time channel (pVms)/(Am^4)
BF[22]:	B-field 974 microsecond time channel (pVms)/(Am^4)
BF[23]:	B-field 1151 microsecond time channel (pVms)/(Am^4)
BF[24]:	B-field 1370 microsecond time channel (pVms)/(Am^4)
BF[25]:	B-field 1641 microsecond time channel (pVms)/(Am^4)
BF[26]:	B-field 1953 microsecond time channel (pVms)/(Am^4)
BF[27]:	B-field 2307 microsecond time channel (pVms)/(Am^4)
BF[28]:	B-field 2745 microsecond time channel (pVms)/(Am^4)
BF[29]:	B-field 3286 microsecond time channel (pVms)/(Am^4)
BF[30]:	B-field 3911 microsecond time channel (pVms)/(Am^4)
BF[31]:	B-field 4620 microsecond time channel (pVms)/(Am^4)
BF[32]:	B-field 5495 microsecond time channel (pVms)/(Am^4)
BF[33]:	B-field 6578 microsecond time channel (pVms)/(Am^4)
PLM:	60 Hz power line monitor
TauBF:	Time Constant (Tau) calculated from B-field data (milliseconds)
TauSF:	Time Constant (Tau) calculated from dB/dt data (milliseconds)

Electromagnetic B-field and dB/dt data is found in array channel format between indexes 10 – 33, as described above.

- Database of the VTEM Waveform “waveform.gdb” in Geosoft GDB format, containing the following channels:

Time: Sampling rate interval, 10.416 microseconds
RX_Volt: Output voltage of the receiver coil (volt)
TX_Curr: Output current of the transmitter (amps)

- Grids in Geosoft GRD format, as follow,

**_mag:	Total magnetic intensity (TMI) (nT)
**_tauBF:	Time constant (Tau) B-Field (ms)
**_tauSF:	Time constant (Tau) dB/dt (ms)
**_BF26:	B-Field channel 26 (Time Gate 1.953 ms)

  Where ** represents the block (i.e.: "solo_Mag.grd").

  A Geosoft .GRD file has a .GI metadata file associated with it, containing grid projection information. A grid cell size of 25 meters was used for the grids.

- Maps at 1:10,000 and 1:20,00 scale in Geosoft MAP format are as follows:

8181_**_TMI_BF:	B-field profiles, Time Gates 0.234 – 9.245 ms in linear logarithmic scale, with TMI colour image.
8181_**_dBdt:	dB/dt profiles, Time Gates 0.234 – 9.245 ms in linear logarithmic scale.
8181_**_BF26:	B-field mid time, Time Gate 1.953 ms
8181_**_AnomBF26:	B-field mid time, Time Gate 1.953 ms
8181_**_TMI:	Total magnetic intensity (nT)
8181_**_TauBF:	Time constant (Tau) B-Field (ms)
8181_**_TauSF:	Time constant (Tau) dB/dt (ms)

  Where ** represents the block (i.e.: "8181_maki_TMI.map").

  1:50,000 topographic vectors were taken from the NRCAN Geogratis database at; http://geogratis.gc.ca/geogratis/en/index.html.

- Google Earth files 8181_flight.kmz showing the flight path of the blocks.

  Free version of Google Earth software can be downloaded from,
  http://earth.google.com/download-earth.html

6. PRELIMINARY INTERPRETATION

6.1 Geological Context and Mineralization: Solomon Pillars Property

The geologic target model used at Solomon Pillars is a mineralized shear zone located and parallel to a banded iron formation and/or foot wall and hanging wall greywacke. Mineralized sections in stripped outcrop were mapped. They are controlled by crosscutting structures that probably create a rake or plunge to the mineralized zone down dip. [2]

The zones are mapped at the surface and identified in core samples and are composed of alternating layers of massive and disseminated Pyrite with minor Arsenopyrite, Pyrrhotite, Bornite and chalcopyrite. Gold mineralization is believed to be primarily associated with the sulphides.

6.2 EM Analysis: Solomon Pillars Property

Figure 7 shows the B-Field image for a late time channel (1.953 ms after the current shut off). An anomalous zone consisting of double peak anomalies and trending roughly in the east west direction is indicated in the northern portion of the property. The posted EM anomaly centers are related to the top of the sources and indicate the conductor axes.

Conductors located in the eastern portion of the property are characterized by moderate conductance values ranging from 10 to 20 S and the conductor located in the western part has lower conductance values (less than 10 S). The detected conductors axes are probably related to a conductive lithologies or possibly fault structures.

[2]B.Bayat, Kodiak Exploration Ltd., pers. comm., 09/2008.

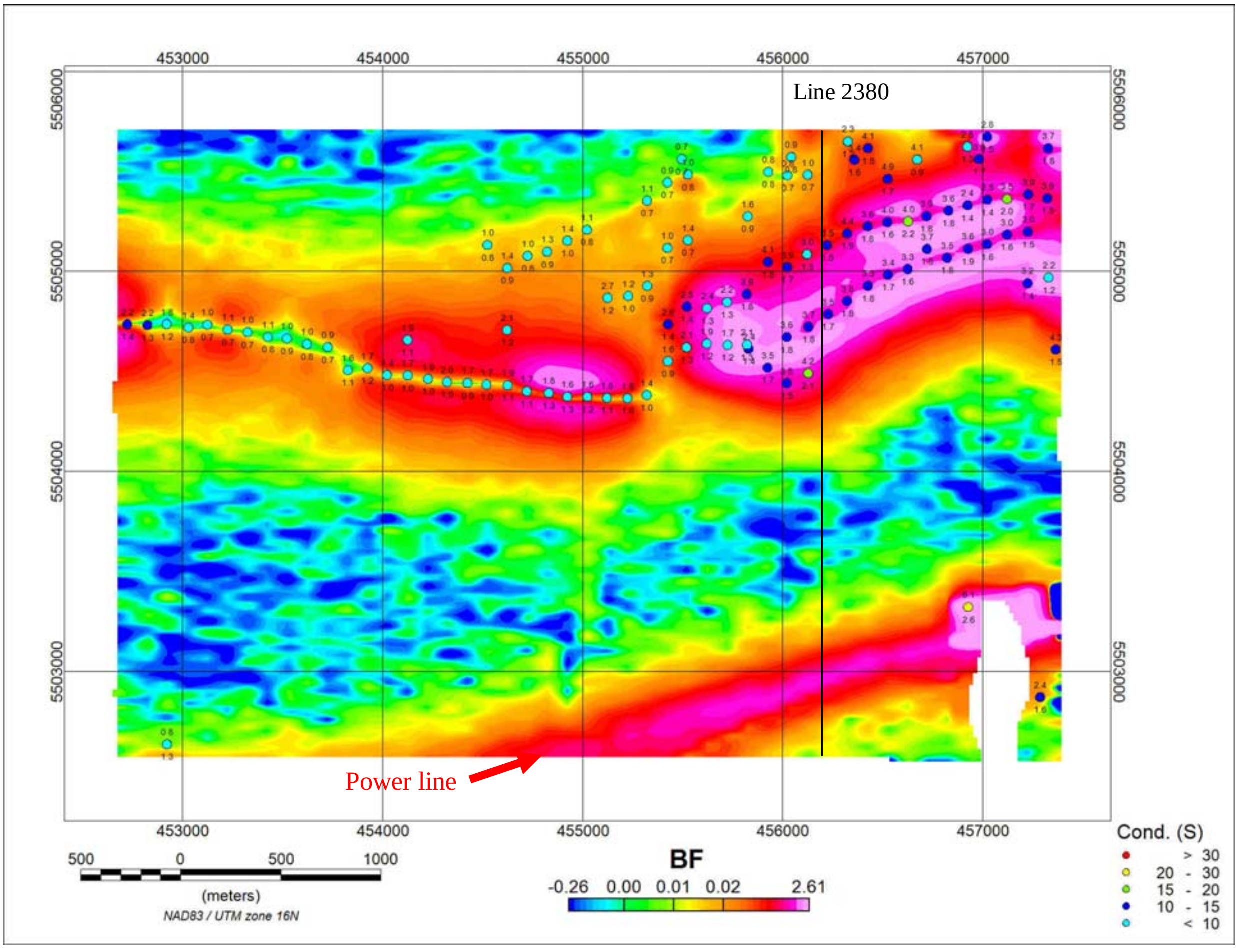

Figure 7 - EM anomaly centers posted on the B-Field (1.953 ms) image.

In Figure 7, the upper value indicates the time constant (Tau) estimated from B-Field, and lower value tau from dB/dt. A CDI section was performed for the line 2380 indicated in black (Figure 8).

6.3 CDI Section: Solomon Pillars Property

A CDI (Conductivity Depth Image) was performed for line 2380 using the EMflow (ENCOM Technology Ltd. Pty., North Sydney, NSN, AU) software. The section illustrated in Figure 8 highlights the presence of shallow and steeply dipping thin conductors that could be associated with mineralized zones.

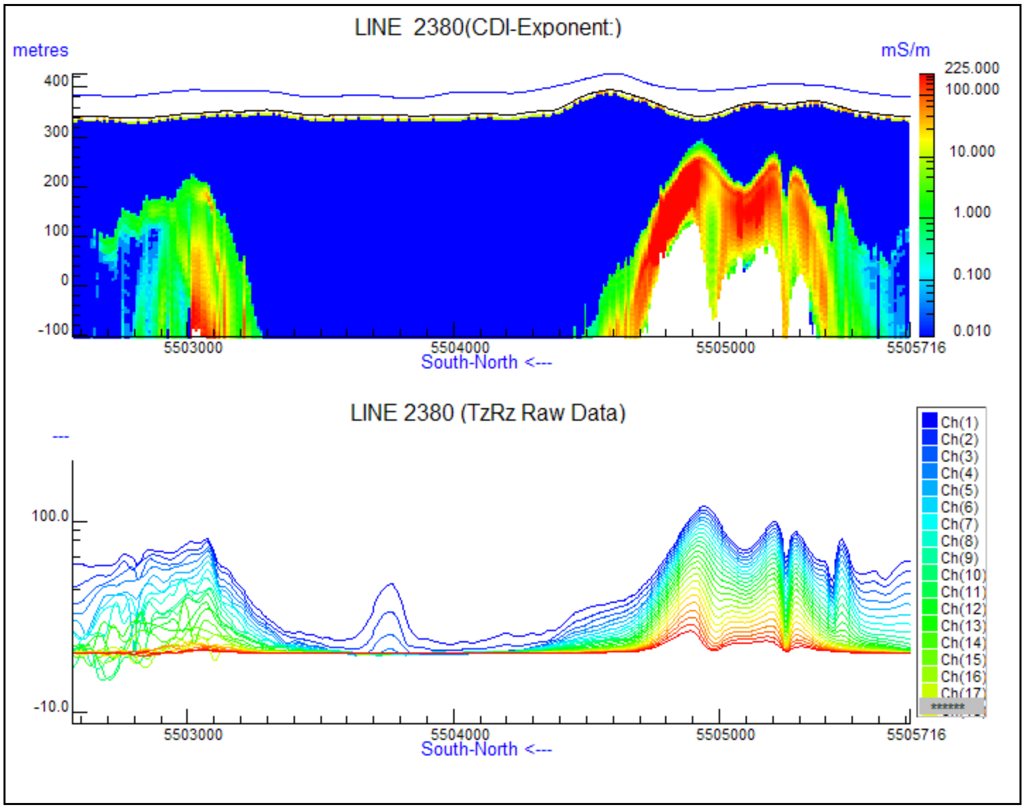

Figure 8 - CDI section for the line 2380 depicting steeply dipping bedrock conductors in the northern portion of the line.

In Figure 8, the noisy profile curves observed in the southern part of the line are related to power-line noise effects that also cause a false conductor artifact in the CDI section.

6.4 Magnetic Data Analysis: Solomon Pillars Property

The Solomon Pillars property is characterized by a high level of magnetic activity as shown in Figure 9. The values of the observed magnetic field range from 57400 to 59800 nT, approximately yielding a difference of 2400 nT. A strong anomaly is observed in the west-central portion of the block. It is probably related to a mafic or ultramafic formation. Several North-easterly trending lineaments are observed in the upper eastern half of the map. It is worth mentioning that one of the detected conductors in this eastern part is closely associated with a magnetic lineament suggesting possible sulphides or banded-iron formations. Other conductors appear to be non-magnetic, suggesting a possible graphitic mineralogy.

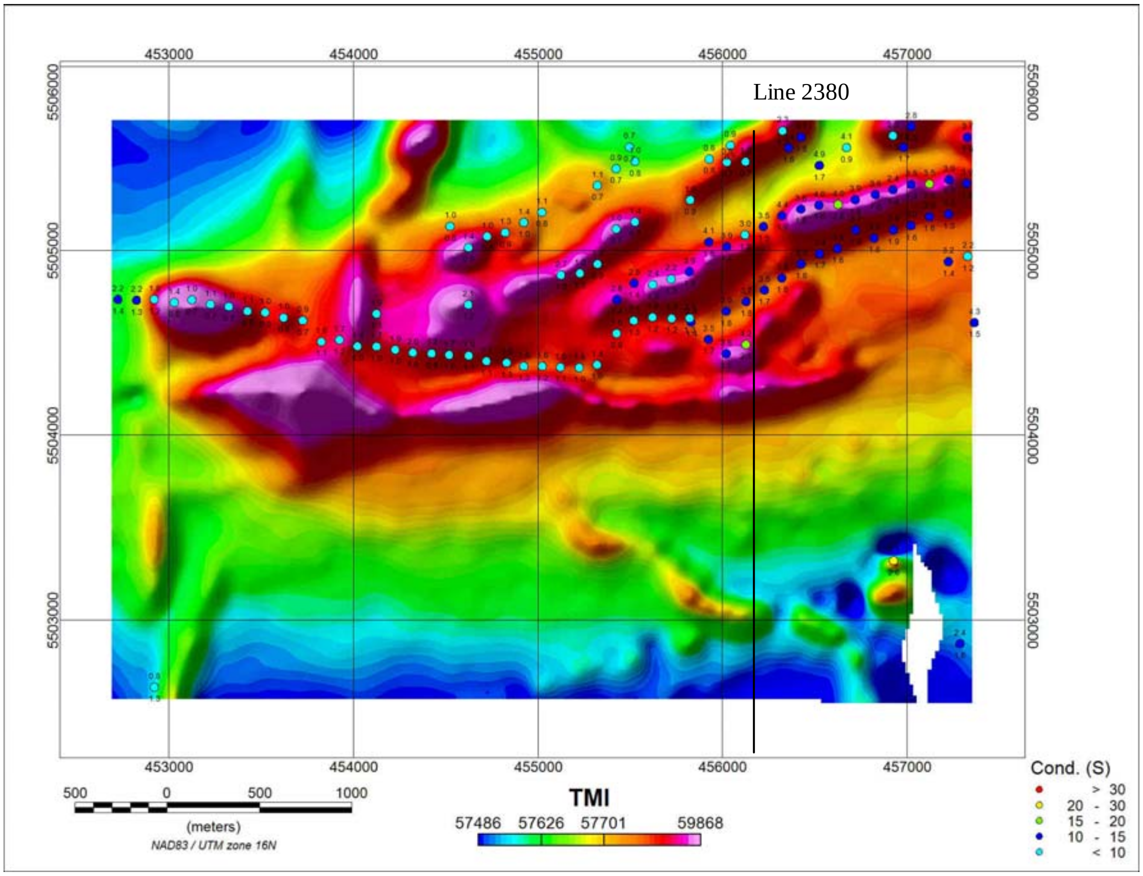

Figure 9 - EM anomaly centers posted on the color shaded relief of the TMI.

In Figure 9, the upper value indicates the time constant (Tau) estimated from B-Field, and lower value tau from dB/dt.

6.5 Geological Context and Mineralization: Maki Property

Maki property is considered as a shear zone type deposit where gold mineralization associated with sulphides occurs within structurally prepared areas controlled parallel to the regional shear. The mineralized zones contain alternating layers of massive and disseminated sulphides with interlayers of quartz, chlorite and silicified rocks. Pyrite is the dominant sulphide with Arsenopyrite and chalcopyrite in lesser amount[3].

[3]B.Bayat, Kodiak Exploration Ltd., pers. comm., 09/2008.

6.6 EM Analysis: Maki Property

Figure 10 shows the B-Field image for a late time channel (1.953 ms). It shows that the Maki property is dominated by a series of linear conductive zones trending roughly in an east-northeast direction. Most of the observed anomalies are caused by long, linear tabular structures and are probably associated with formational conductors, or possibly faults, alteration and shear zones.

The detected bedrock conductors exhibit moderate to high conductance values ranging from 10 to 30S and high time constant values (>3ms) calculated from dB/dt data.

A CDI section was performed for the line1650 shown in black, in Figure 10.

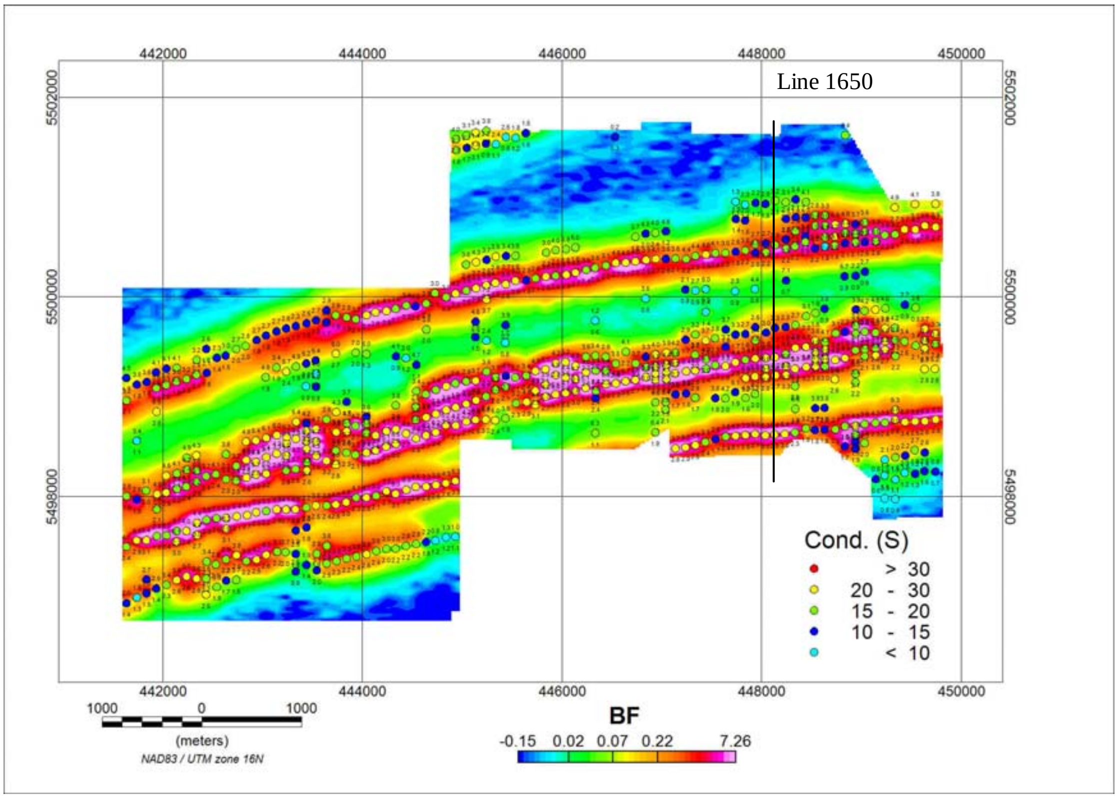

Figure 10 - EM anomaly centers posted on the B-Field (1.953 ms) image.

In Figure 10, the upper value indicates the time constant (Tau) estimated from B-Field, and lower value tau from dB/dt.

6.7 CDI Section: Maki Property

The CDI section obtained using EMFlow for the line 1650 is illustrated in Figure 11. It shows three conductive zones associated with shallow and steeply dipping bedrock conductors, from the three bands defined in Figure 10. Most of the detected conductors are of thin plate type, and probably related to conductive stratigraphies and faults, with a possible sulphide or graphite mineralization association.

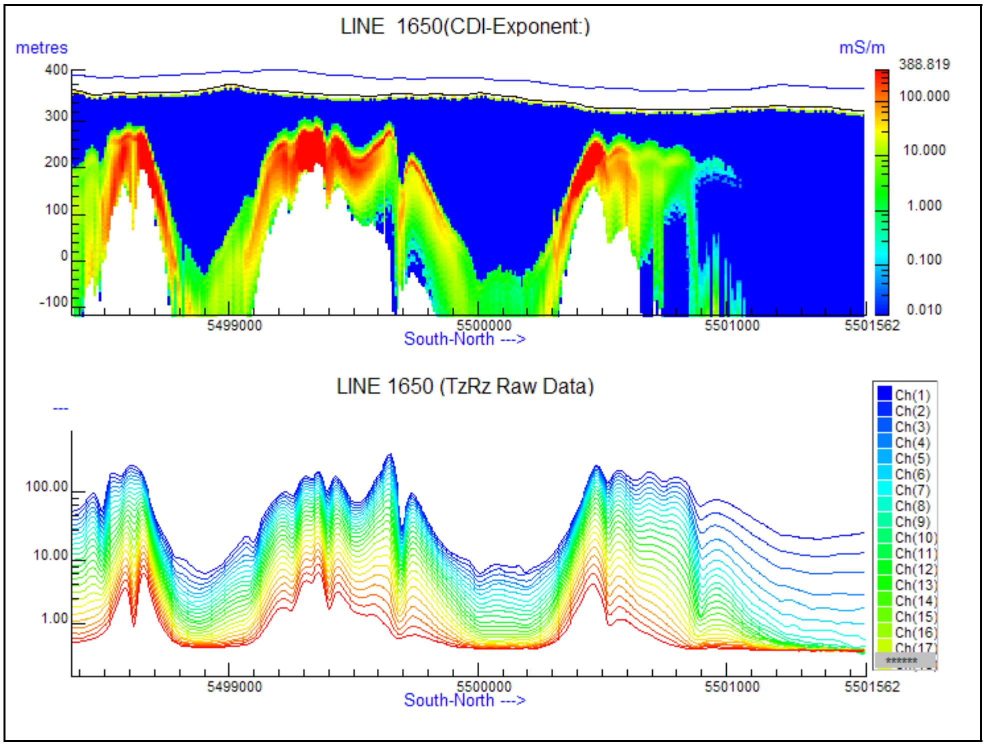

Figure 11 - CDI section for the Line 1650 showing a series of steeply dipping bedrock conductors.

6.8 Magnetic Data Analysis: Maki Property

The total magnetic field intensity (TMI) in Figure 12 shows a series of parallel lineaments trending roughly in the east-west direction. The strongest anomaly with amplitude of more than 2000 nT is associated with the EM conductors in the eastern portion of the property. It is probably closely related with a magnetite rich mafic or ultramafic formation. The observed lineaments are in very good correlation with the detected bedrock conductors, which suggests the presence of sulphides, possibly pyrrhotite.

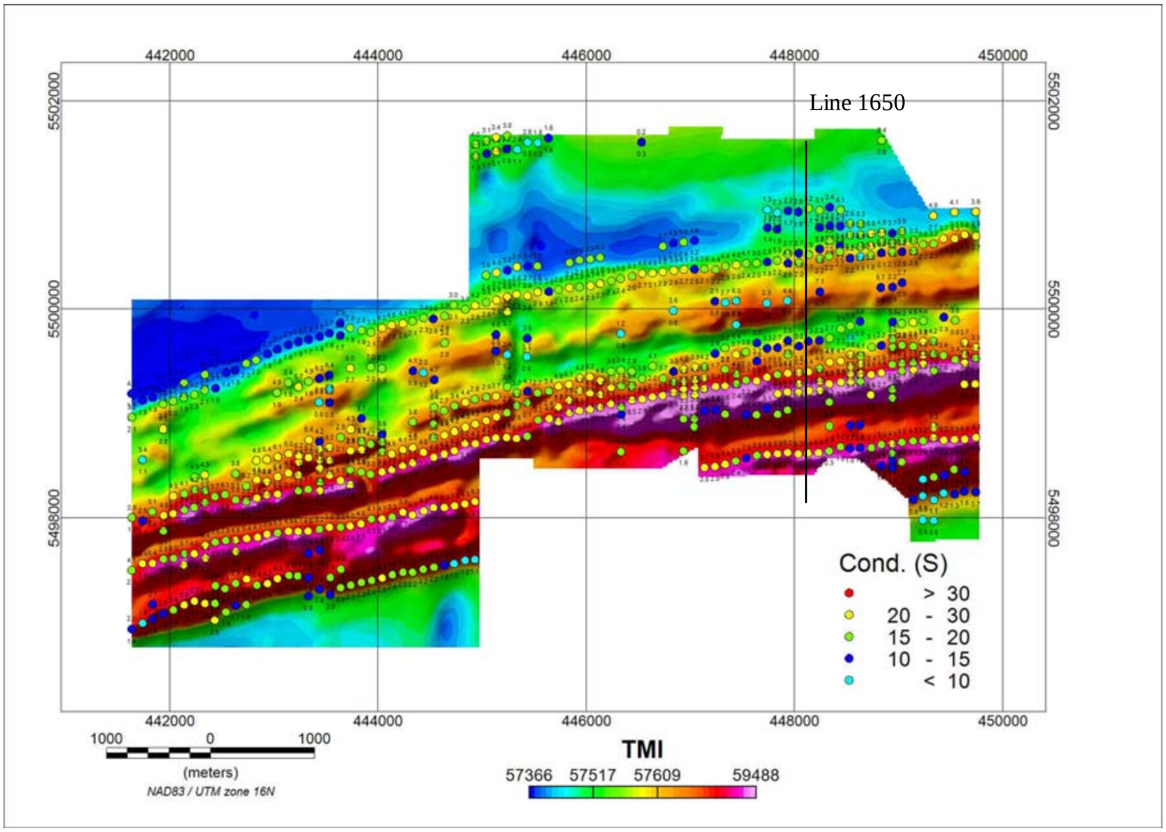

Figure 12 - EM anomaly centers posted on the color shaded relief of the TMI.

In Figure 12, the upper value indicates the time constant (Tau) estimated from B-Field, and lower value tau from dB/dt.

6.9 Geological Context and Mineralization: West Gerldton Property

At West Geraldton, the geologic targets envisioned are expected to be tabular in form and structurally controlled, with high grade mineralization consisting of sulphides zones with a mafic gabbroic association. Other targets may occur with lower grade fractions and as disseminated sulphide mineralization associated with altered intrusions[4].

6.10 EM Analysis: West Geraldton Property

As shown in Figure 13, the West Geraldton property is dominated by a series of banded linear and east-westerly trending EM conductors. The observed anomalies are double peak type caused by steeply dipping thin bedrock conductors. The conductance estimates are in the range of 10 to 30S. The mean time constant estimated from dB/dt is 2ms and from B-Field is 3ms. The anomalies are probably associated with steeply dipping conductive structures, such as formational sulphide, bands, or graphitic sediments, or possibly fault zones.

In Figure 13, the upper value indicates the time constant (Tau) estimated from B-Field, and lower value tau from dB/dt. A CDI section was performed for the line 3840 shown in black.

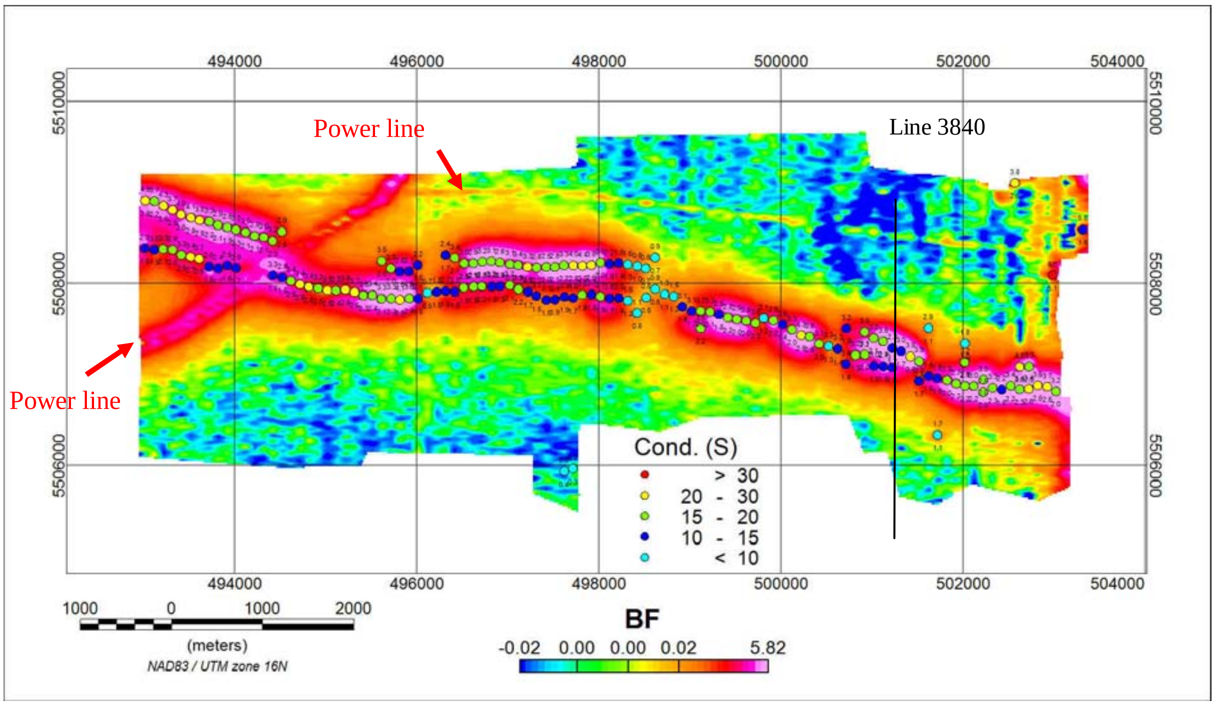

Figure 13 - EM anomaly centers posted on the B-Field (1.953 ms) image.

[4]B.Bayat, Kodiak Exploration Ltd., pers. comm., 09/2008.

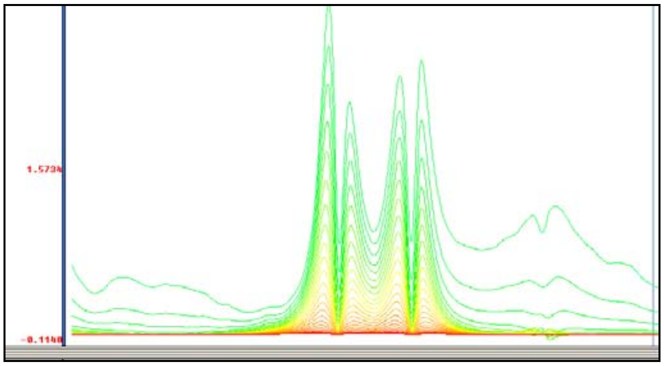

Figure 14 - EM decays observed at the West Geralton property.

6.11 CDI Section: West Geraldton Property

A conductivity depth image section was performed for line 3840 using EMFlow software. The section indicates a shallow and steeply dipping bedrock conductive package in the centre of the line.

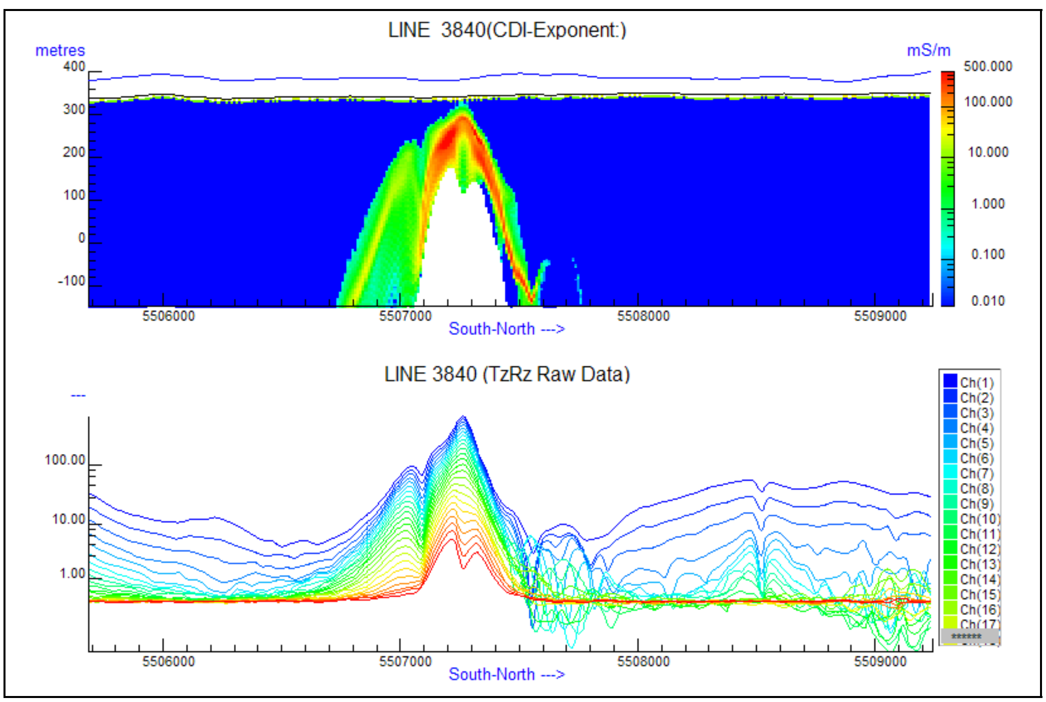

Figure 15 - Conductivity depth section for the Line 3840.

6.12 Magnetic Data Analysis: West Geraldton Property

Figure 16 shows the total magnetic field (TMI) map of the West Geraldton block exhibits a high level of magnetic activity with values ranging from 56000 to 68300 nT. The map shows very strong linear magnetic anomalies with intensities over 10000 nT. These lineaments are likely associated with ultramafic dykes, with high contents of magnetite. The detected bedrock conductors are correlated within magnetic lows, which indicates they are unrelated to magnetite, possibly graphitic or non-magnetic sulphides.

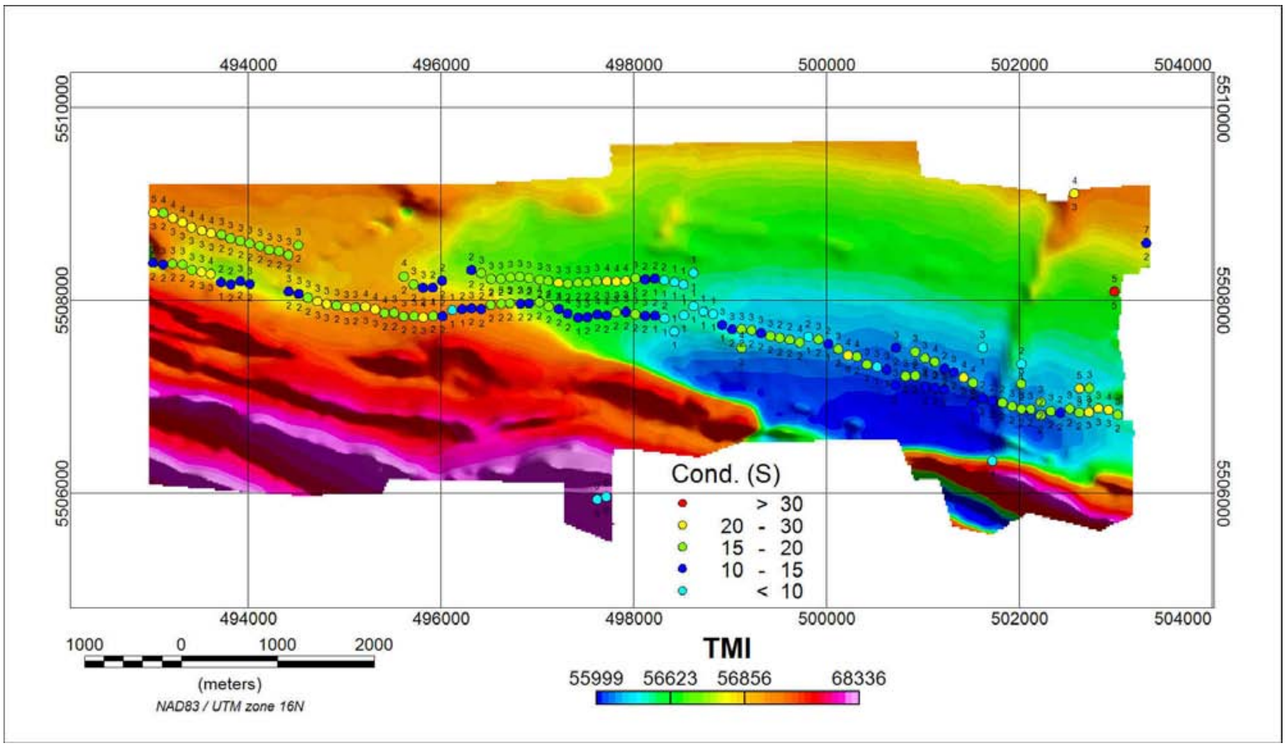

Figure 16 - EM anomaly centers posted on the color shaded relief of the TMI.

In Figure 16, the upper value indicates the time constant (Tau) estimated from B-Field, and lower value tau from dB/dt.

7. CONCLUSIONS AND RECOMMENDATIONS

7.1 Conclusions

A helicopter-borne versatile time domain electromagnetic (VTEM) geophysical survey has been completed over three (3) blocks (Maki, Solomon Pillars, and West Geraldton properties) near Beardmore, Ontario, Canada.

The total area coverage is 78 km^2. Total survey line coverage is 792 line kilometres. The principal sensors included a Time Domain EM system and a magnetometer. Results have been presented as stacked profiles and contour colour images at a scale of 1:10,000 and 1:20,000.

The VTEM survey conducted over the three properties detected many linear bedrock conductors. Most of them are in good correlation with magnetic signatures, suggesting a likely association with sulphide or mixed magnetite mineralized units, or faults or possibly alteration zones. The analysis of the magnetic data over the flown property shows a high level of magnetic activity, likely associated with magnetite and possibly pyrrhotite rich, mafic and ultramafic units or intrusions.

7.2 Recommendations

Based on the geophysical results obtained, a number of interesting EM and magnetic anomaly groupings were identified across the three properties, Maki, Solomon Pillars, and West Geraldton. We therefore recommend a more detailed interpretation of the EM and magnetic data using inversion and modelling techniques to better characterize the observed anomalies and to accurately determine their parametres (depth, conductance, dip, etc.) prior to ground follow-up and drill testing.

We also recommend performing 2D and 3D EM modeling to accurately determine the conductors' parameters (Conductance, Dip, and depth). In depth interpretation of the magnetic data based on structural analysis and 2D and 3D inversion techniques (Euler Deconvolution, analytic signal) is highly recommended to map magnetic structures, faults, shear zones and fractures that particularly control the mineralization.

Respectfully submitted[5],

Milica Marich
Geotech Ltd.

Jean Legault, P. Geo, P. Eng
Geotech Ltd.

Nasreddine Bournas, P.Geo (QC)
Geotech Ltd.

September 2008

[5]Final data processing and interpretation of the EM-magnetic geophysical data were carried out by Nasreddine Bournas, P.Geo (QC), from the office of Geotech Ltd. in Aurora, Ontario, under the supervision of Jean Legault, P. Geo, Manager of Data Processing and Interpretation.

APPENDIX A

SURVEY BLOCK LOCATION MAPS

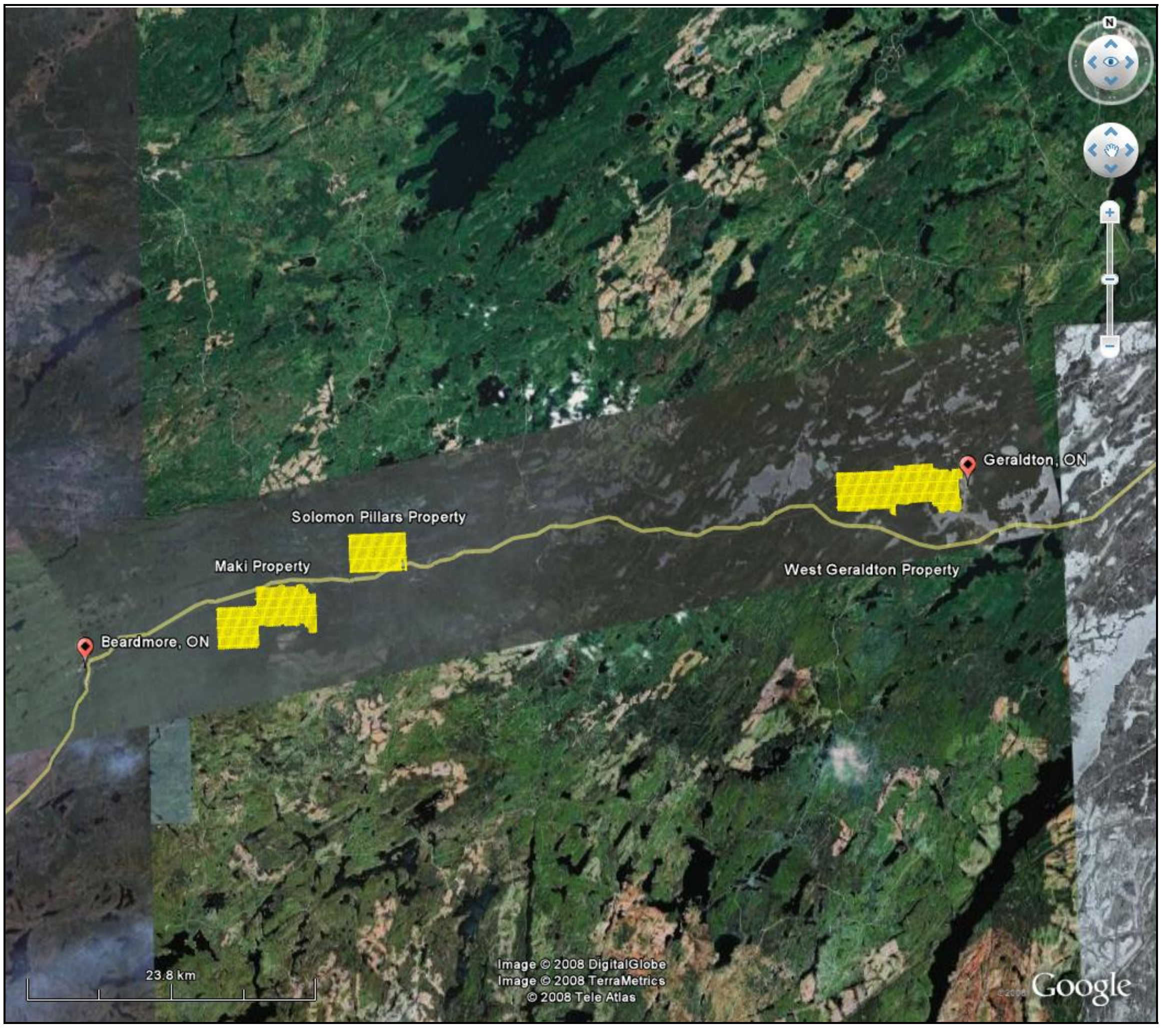

Google Earth Image

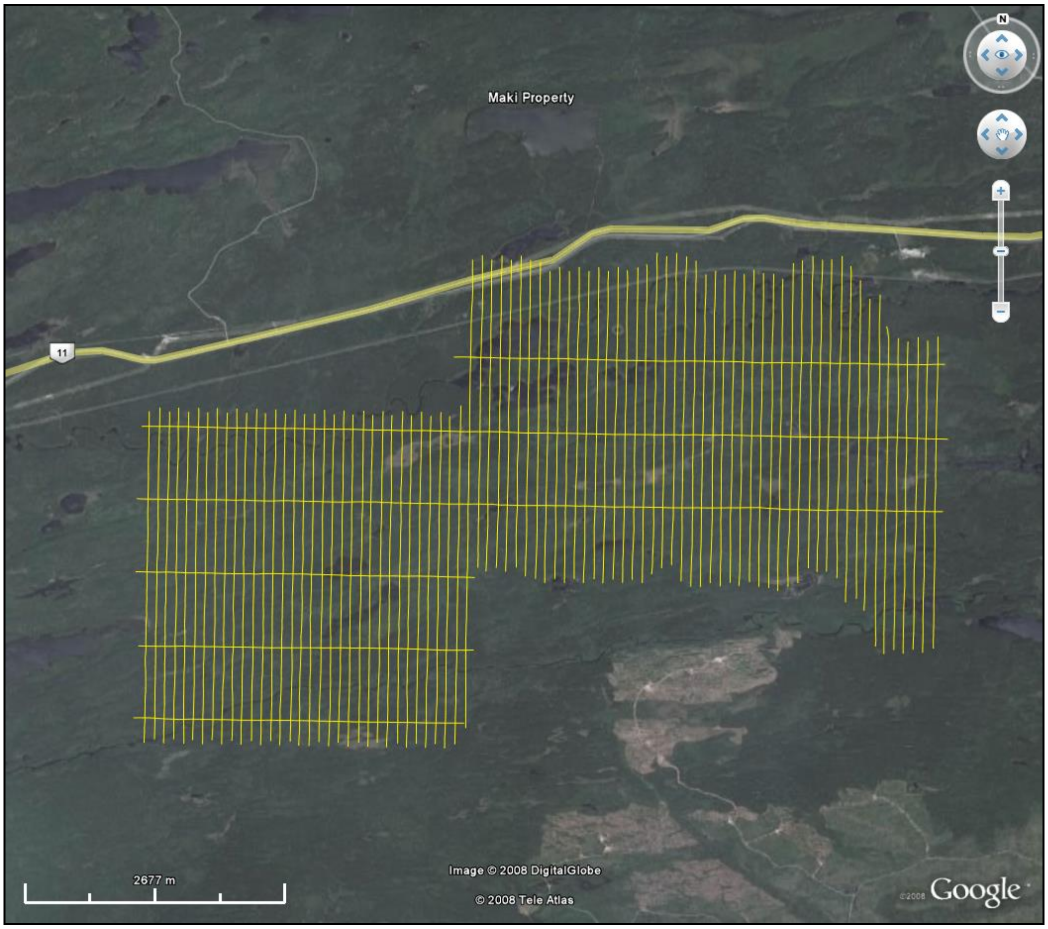

Google Earth Image

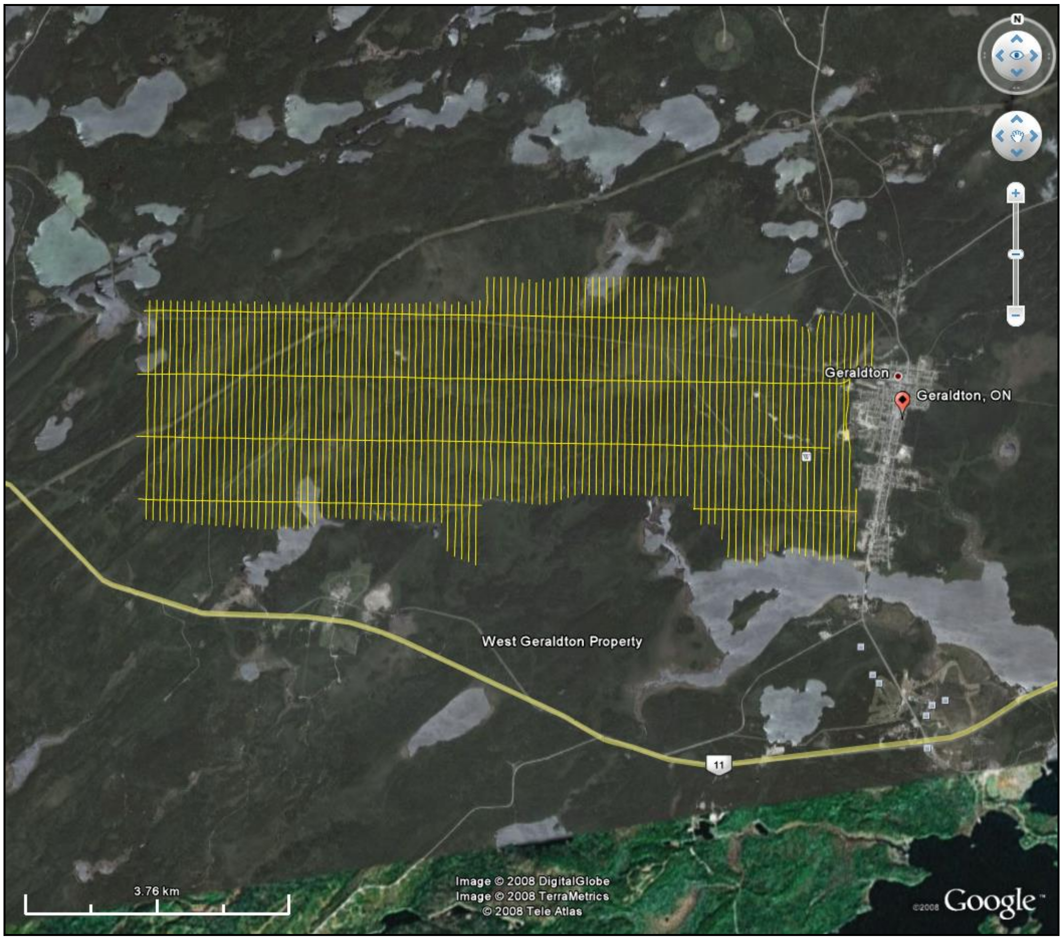

Google Earth Image

Google Earth Image

APPENDIX B

SURVEY BLOCK COORDINATES

(NAD 83, UTM zone 16 north)

Maki Property	
X	Y
441636.9	5496815.4
441636.9	5500020.2
444881.3	5500020.2
444888.7	5500412
446763.9	5500434.5
446752.7	5500850
447153.9	5500843.5
447169.7	5500411
447681.3	5500415.2
447959	5500449.5
448292.2	5500456.5
448275.9	5500818.5
448796.2	5500818.5
448792.7	5500461
449208.8	5500471.5
449222.3	5499563
449750	5499570.5
449740.6	5499178.5
449253	5499130.5
448930.9	5499100
448921.5	5499558.5
448534.3	5499547
448138.9	5499507.5
447998.4	5499492.5
447992.8	5499628.7
447252.9	5499609.5
447254.2	5499546
446771.5	5499533.5
446781.4	5499643
445618.1	5499627.5
445599.3	5499859.5
444881.7	5499848.3
444881.3	5496815.4

West Geraldton Property	
X	Y
492918.8	5507489
493468.7	5507489
493468.7	5509089
496533.8	5509089.1
498131.3	5509166.3
499731.4	5509166.4
501176.1	5509033.1
502176.1	5509033
502104.6	5508835
502511.4	5508871
502556.7	5509050.7
503121.1	5509052.3
503142.5	5508505
502878.5	5508525.5
502579.4	5508469
502489.9	5507964.5
503041.5	5508029
503032.1	5507835.5
502992.5	5507833.5
502979.6	5507565.5
503021.7	5507563.5
502995.6	5507469.5
501870.7	5507967.5
501982.9	5507540.5
502236.3	5507592
502317	5507203.5
502979.6	5507025.5
502800.8	5506757.5
503353	5506744.5
503314.2	5506468.9
503200.8	5506024.5
503004.5	5506079.5
502915.1	5505737.2
502743.1	5505725.2
502691.4	5505741.6
502502.1	5505809.2
502169.1	5505850

Solomon Pillars Property	
X	Y
452724.3	5505642.6
457341.3	5505642.6
457341.3	5502646.9
452724.3	5502646.9

502203.1	5505934
502156.1	5506033
502049.1	5505901
501752.3	5505879
501757	5505681
501354.2	5505711.5
501232.2	5506430.5
500905.5	5506399
500894.3	5506823.5
501196.1	5506774
501152	5507114.5
499399.7	5507086
499383.5	5507144.5
498868.4	5507032.5
498902.4	5506949.6
498921.9	5506832.5
498501.5	5506757.5
498501.5	5506757.5
498141	5506733.3
498135	5507003
497741	5507003.5
497742.9	5505599.2
497350.3	5505740.2
497350.1	5507566.4
496533.8	5507489
496493.7	5507210.4
496489	5506301.8
495450.4	5506420.8
495361	5506077.5
494713.2	5506040.2
494426.7	5506106
493922	5506125.8
492930.2	5506192.3
492979	5506735.1
492918.4	5506731.4

APPENDIX C

VTEM WAVEFORM

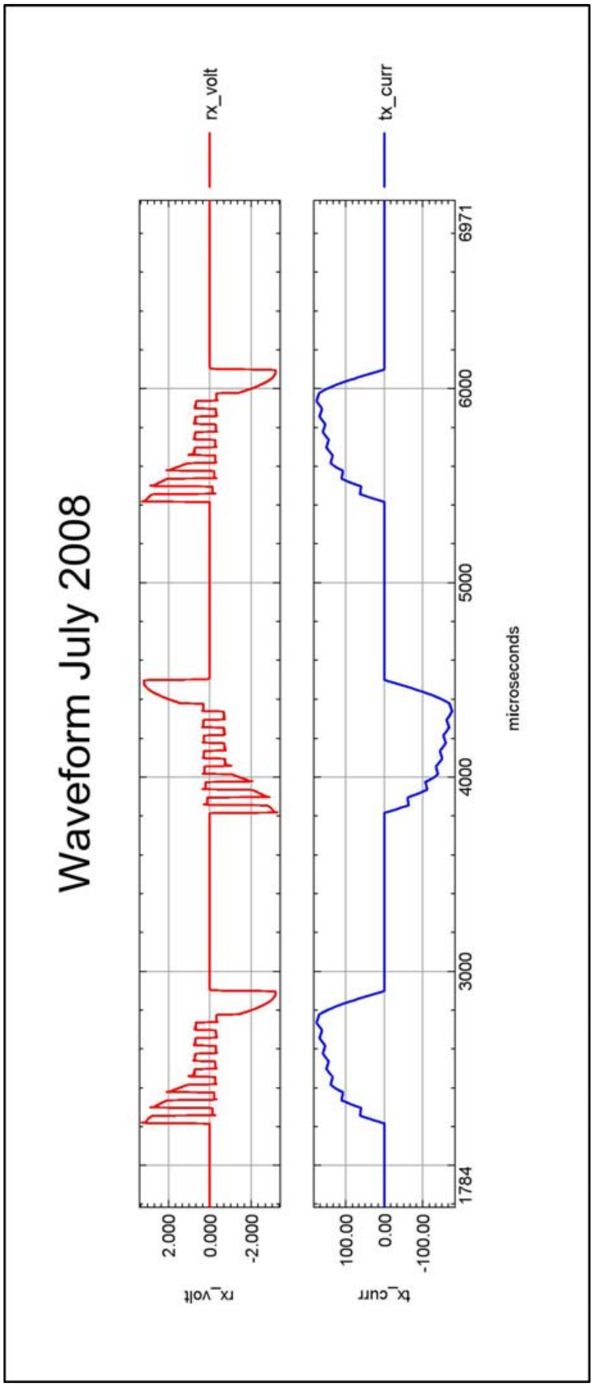

APPENDIX D

GEOPHYSICAL MAPS

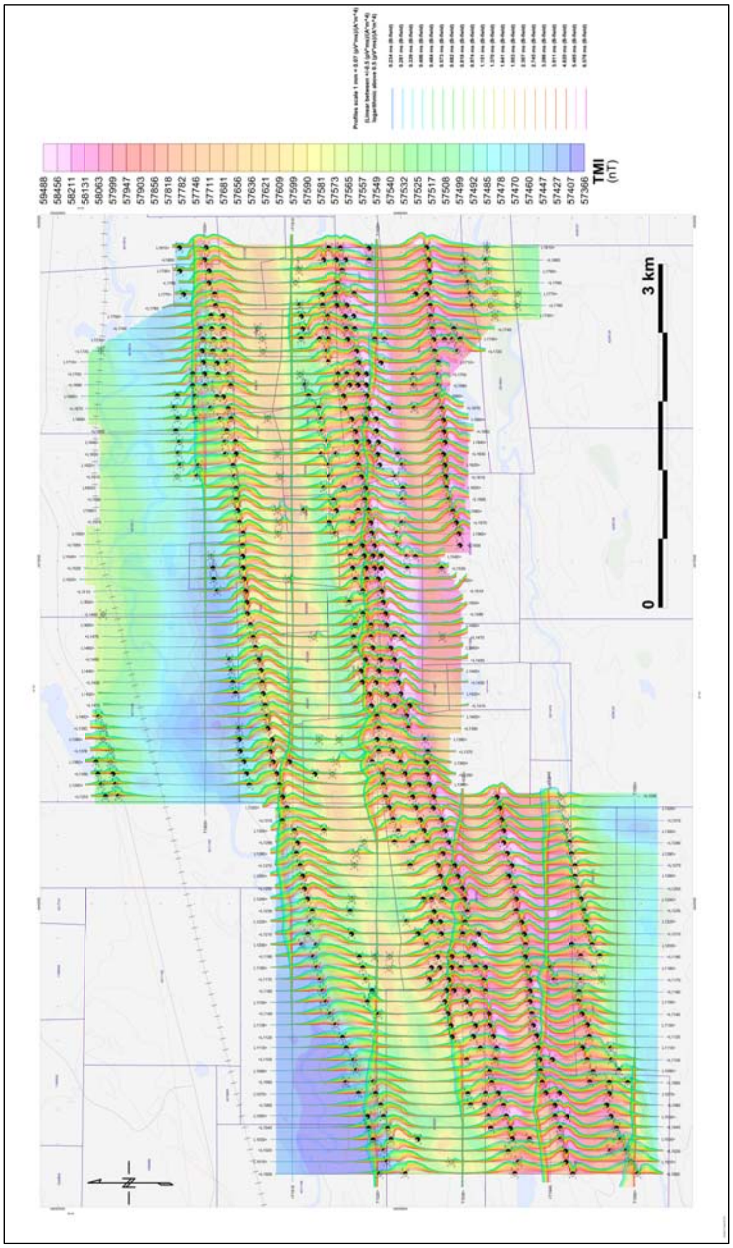

Maki Property: VTEM B-Field Profiles
– Time Gates 0.234 to 6.578 ms., over TMI image with EM Anomalies

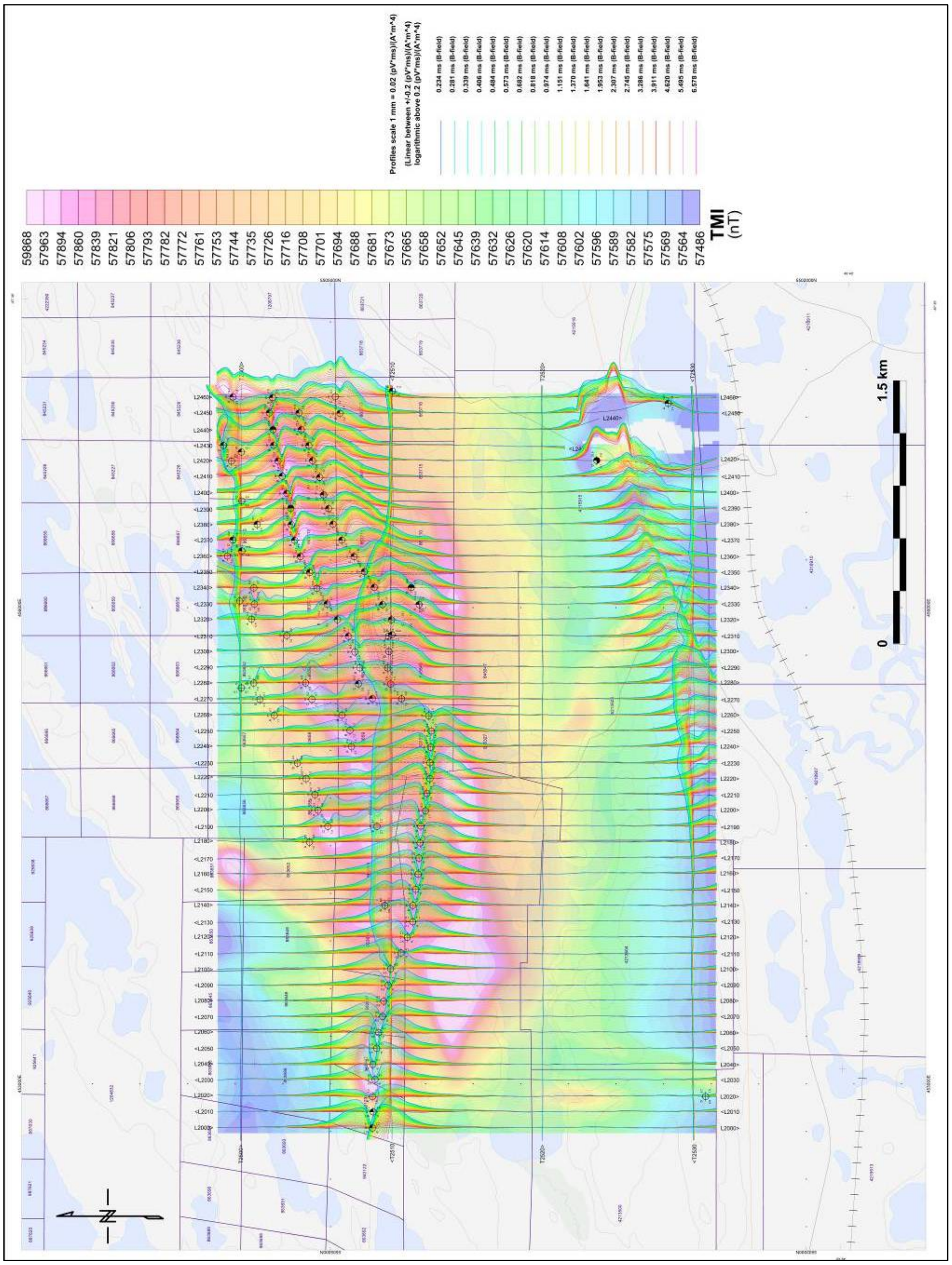

Solomon Pillars Property: VTEM B-Field Profiles
– Time Gates 0.234 to 6.578 ms., over TMI image with EM Anomalies

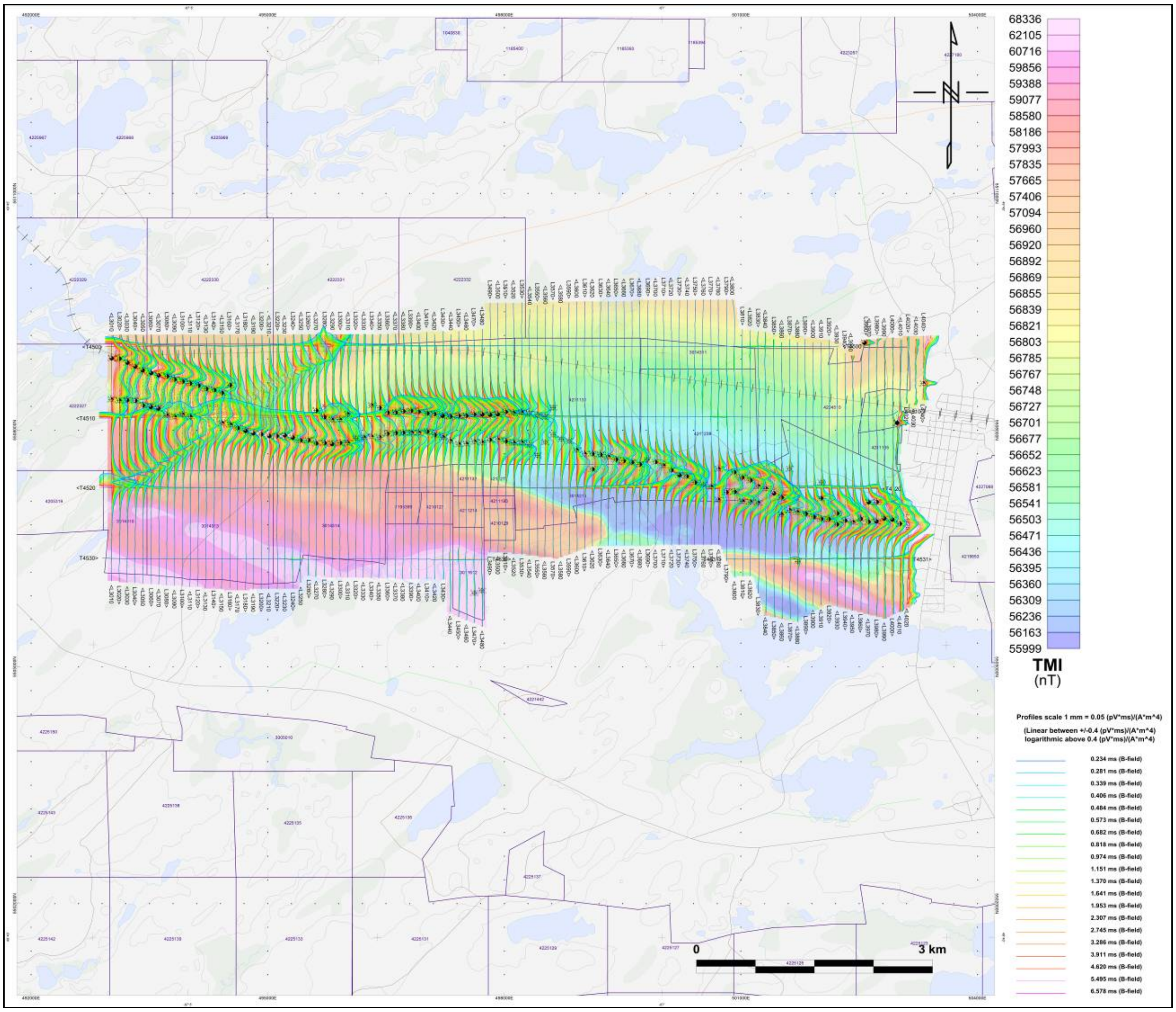

West Geraldton Property: VTEM B-Field Profiles
– Time Gates 0.234 to 6.578 ms., over TMI image with EM Anomalies

APPENDIX E

GENERALIZED MODELING RESULTS OF THE VTEM SYSTEM

Introduction

The VTEM system is based on a concentric or central loop design, whereby, the receiver is positioned at the centre of a 26.1 meters diameter transmitter loop that produces a dipole moment up to 373,600 nIA at peak current. The wave form is a bi-polar, modified square wave with a turn-on and turn-off at each end. With a base frequency of 30 Hz, the duration of each pulse is approximately 7.3 milliseconds followed by an off time where no primary field is present.

During turn-on and turn-off, a time varying field is produced (dB/dt) or B-field and an electro-motive force (emf) is created as a finite impulse response. A current ring around the transmitter loop moves outward and downward as time progresses. When conductive rocks and mineralization are encountered, a secondary field is created by mutual induction and measured by the receiver at the centre of the transmitter loop.

VTEM measurements are made partly during the transmitter On but primarily during the Off-time, when only the secondary fields representing the conductive targets encountered in the ground are present. The secondary fields are displayed both as dB/dt and calculated B-field responses.

Efficient modeling of the results can be carried out on regularly shaped geometries, thus yielding close approximations to the parameters of the measured targets. The following is a description of a series of common models made for the purpose of promoting a general understanding of the measured results.

General Modeling Concepts

A set of models has been produced for the Geotech VTEM® system with explanation notes (see models C1 to C18). The reader is encouraged to review these models, so as to get a general understanding of the responses as they apply to survey results. While these models do not begin to cover all possibilities, they give a general perspective on the simple and most commonly encountered anomalies.

When producing these models, a few key points were observed and are worth noting as follows:

- For near vertical and vertical plate models, the top of the conductor is always located directly under the centre low point between the two shoulders in the classic **M** shaped response.

● As the plate is positioned at an increasing depth to the top, the shoulders of the **M** shaped response, have a greater separation distance.

● When faced with choosing between a flat lying plate and a prism model to represent the target (broad response) some ambiguity is present and caution should be exercised.

● With the concentric loop system and Z-component receiver coil, virtually all types of conductors and most geometries are most always well coupled and a response is generated. Only concentric loop systems can map these varieties of target geometries.

The Maxwell ™ EM modeling program (EMIT Technology Ltd. Pty., Midland WA, AU) used to generate the following dB/dt and B-field off-time responses all assume a conductive plate in an infinitely resistive half-spaced host rock

Variation of Plate Depth

Geometries represented by plates of different strike length, depth extent, dip, plunge and depth below surface can be varied with characteristic parameters like conductance of the target, conductance of the host and conductivity/thickness and thickness of the overburden layer.

Diagrammatic models for a vertical plate are shown in Figures C-1 & C-2 and C-5 & C-6 at two different depths, all other parameters remaining constant. With this transmitter-receiver geometry, the classic **M** shaped response is generated. Figures C-1 and C-2 show a plate where the top is near surface. Here, amplitudes of the duel peaks are higher and symmetrical with the zero centre positioned directly above the plate. Most important is the separation distance of the peaks. This distance is small when the plate is near surface and widens with a linear relationship as the plate (depth to top) increases. Figures C-5 and C-6 show a much deeper plate where the separation distance of the peaks is much wider and the amplitudes of the channels have decreased.

Variation of Plate Dip

As the plate dips and departs from the vertical position, the peaks become asymmetrical. Figures C-3 & C-4 and C-7 and C-8 show a near surface plate dipping 80º at two different depths. Note that the direction of dip is toward the high shoulder of the response and the top of the plate remains under the centre minimum.

As the dip increases, the aspect ratio (Min/Max) decreases and this aspect ratio can be used as an empirical guide to dip angles from near 90º to about 30º. The method is not sensitive enough where dips are less than about 30º. For example, for a plate dipping 45º, the minimum shoulder starts to vanish. In Figures C-9 & C-10 and C-11 & C-12, a flat lying plate is shown, relatively near surface. Note that the twin peak anomaly has been replaced by a symmetrical shape with large, bell shaped, channel amplitudes which decay relative to the conductance of the plate.

In the special case where two plates are positioned to represent a synclinal structure. Note that the main characteristic is that the centre amplitudes are higher (approximately double) compared to the high shoulder of a single plate. This model is very representative of tightly folded formations where the conductors where once flat lying.

Variation of Prism Dip

Finally, with thicker, prism models, another algorithm is required to represent current on the plate. A plate model is considered to be infinitely thin with respect to thickness and incapable of representing the current in the thickness dimension. A prism model is constructed to deal with this problem, thereby, representing the thickness of the body more accurately.

Figures C-13 & C-14 and C-15 & C-16 show the same prism at the same depths with variable dips. Aside from the expected differences asymmetry prism anomalies show a characteristic change from a double-peaked anomaly to single peak signatures.

I. THIN PLATE

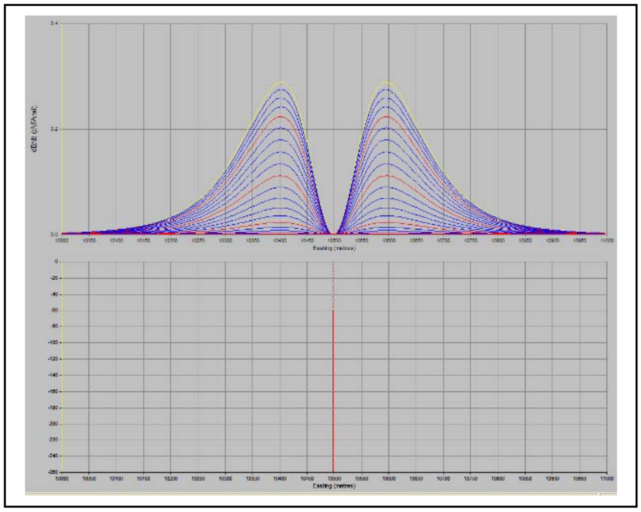

Figure C-1: dB/dt response of a shallow vertical thin plate. Depth=100 m, CT=20 S. The EM response is normalized by the dipole moment and the Rx area.

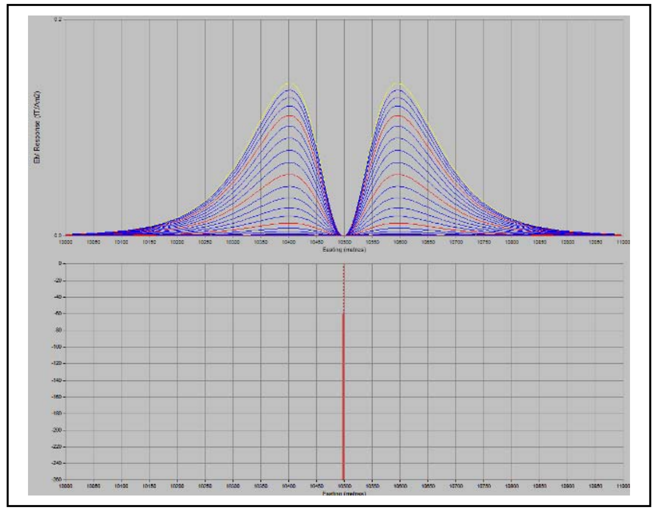

Figure C-2: B-field response of a shallow vertical thin plate. Depth=100 m, CT=20 S. The EM response is normalized by the dipole moment.

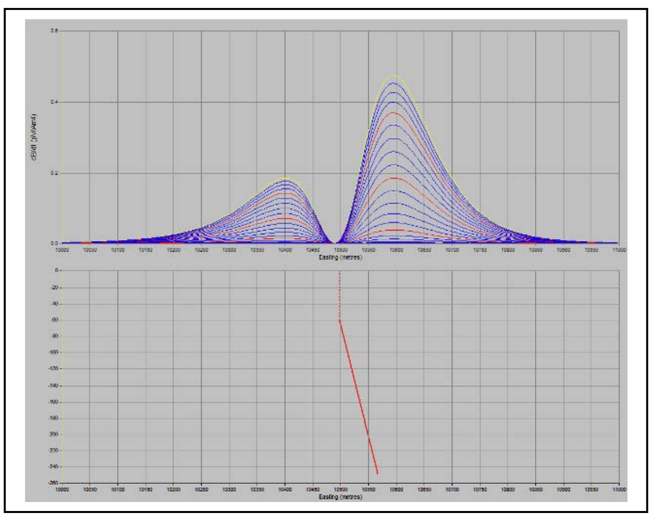

Figure C-3: dB/dt response of a shallow skewed thin plate. Depth=100 m, CT=20 S. The EM response is normalized by the dipole moment and the Rx area.

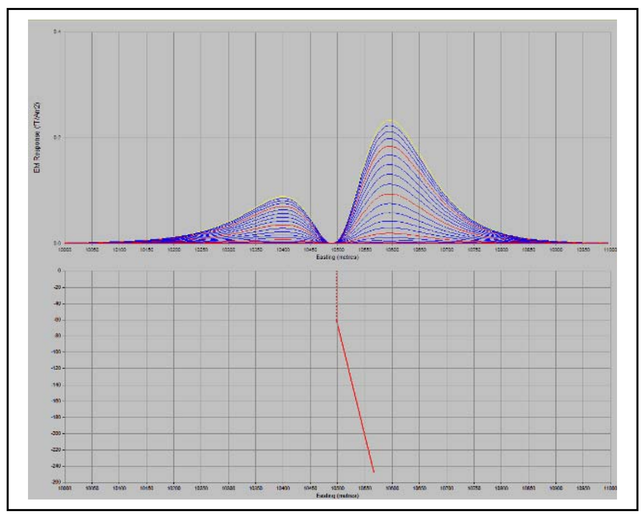

Figure C-4: B-field response of a shallow skewed thin plate. Depth=100 m, CT=20 S. The EM response is normalized by the dipole moment.

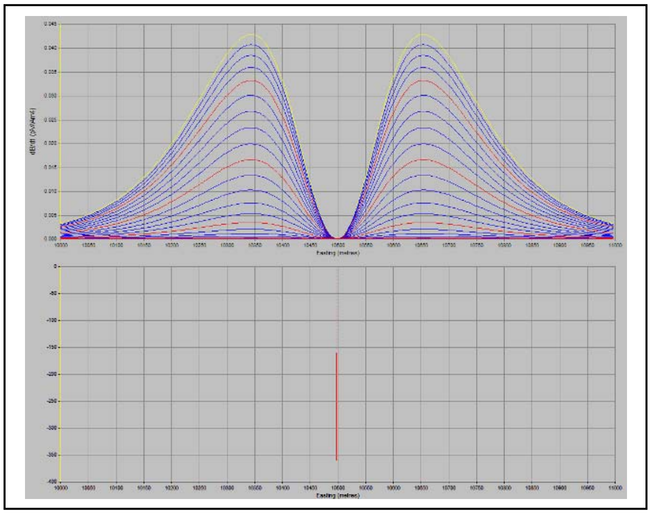

Figure C-5: dB/dt response of a deep vertical thin plate. Depth=200 m, CT=20 S. The EM response is normalized by the dipole moment and the Rx area.

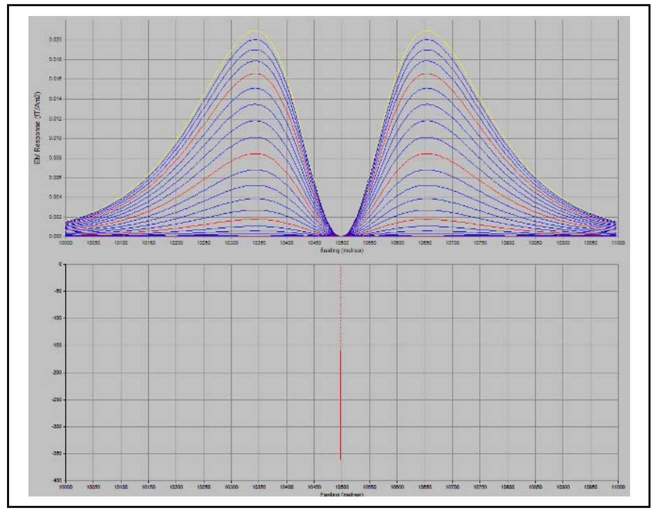

Figure C-6: B-Field response of a deep vertical thin plate. Depth=200 m, CT=20 S. The EM response is normalized by the dipole moment.

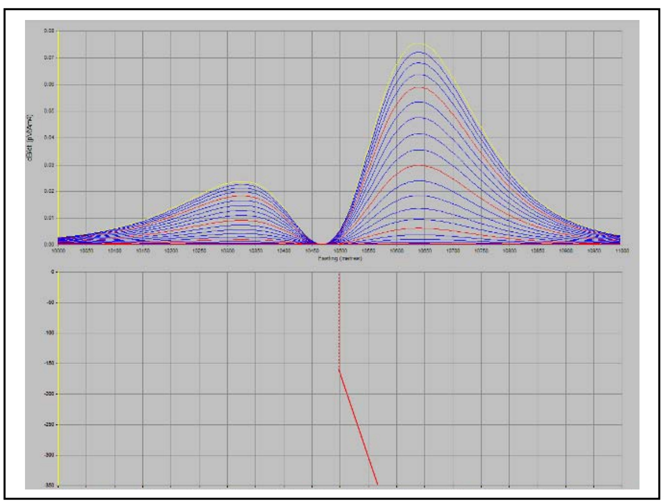

Figure C-7: dB/dt response of a deep skewed thin plate. Depth=200 m, CT=20 S. The EM response is normalized by the dipole moment and the Rx area.

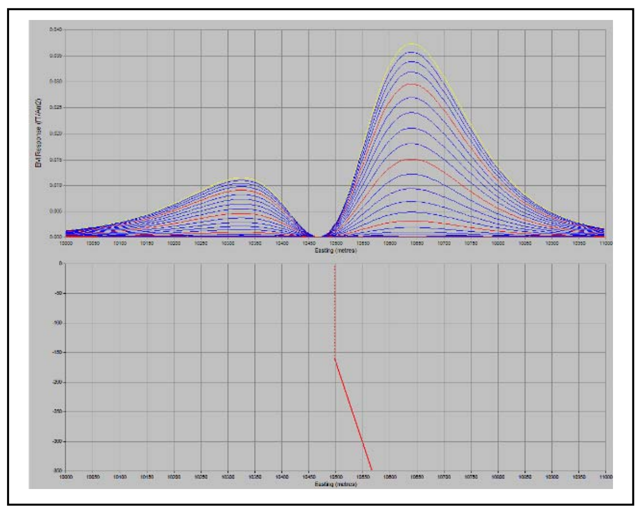

Figure C-8: B-field response of a deep skewed thin plate. Depth=200 m, CT=20 S. The EM response is normalized by the dipole moment.

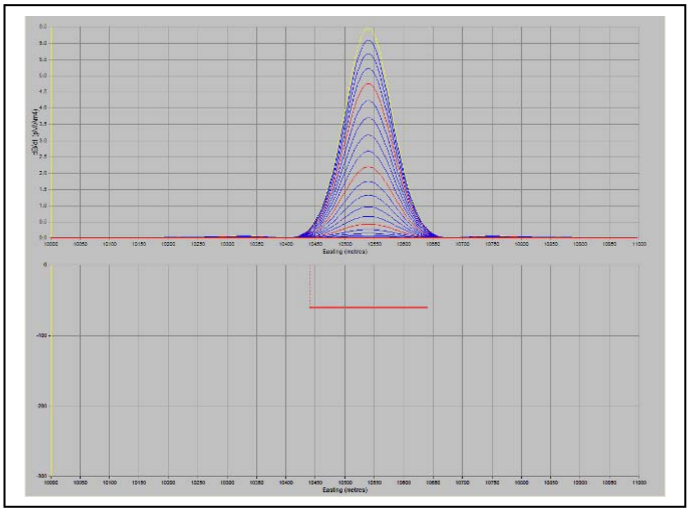

Figure C-9: dB/dt response of a shallow horizontal thin plate. Depth=100 m, CT=20 S. The EM response is normalized by the dipole moment and the Rx area.

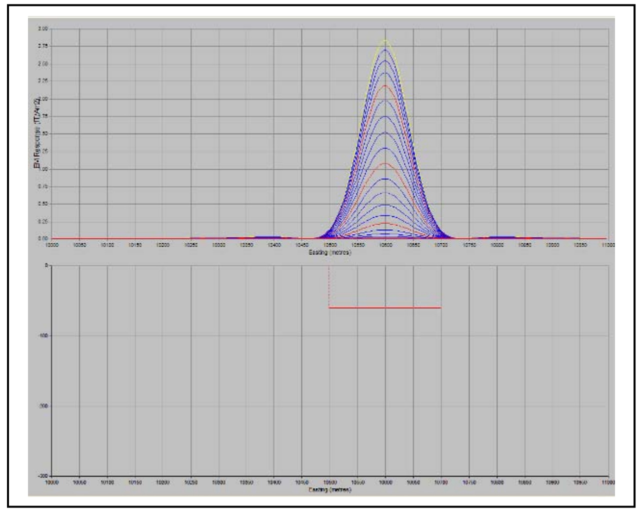

Figure C-10: B-Field response of a shallow horizontal thin plate. Depth=100 m, CT=20 S. The EM response is normalized by the dipole moment.

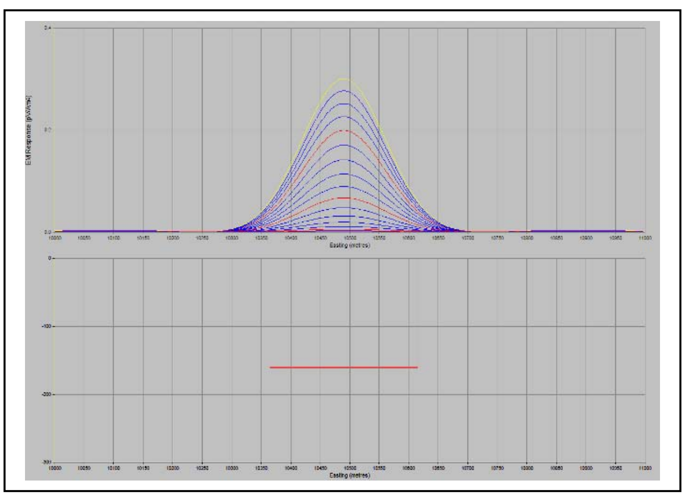

Figure C-11: dB/dt response of a deep horizontal thin plate. Depth=200 m, CT=20 S. The EM response is normalized by the dipole moment and the Rx area.

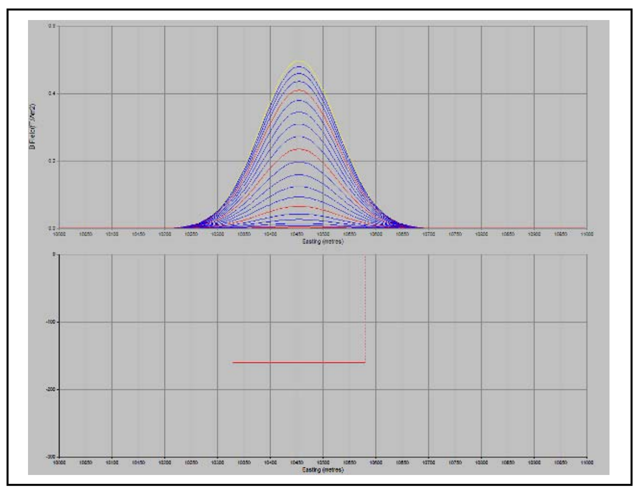

Figure C-12: B-Field response of a deep horizontal thin plate. Depth=200 m, CT=20 S. The EM response is normalized by the dipole moment.

II. THICK PLATE

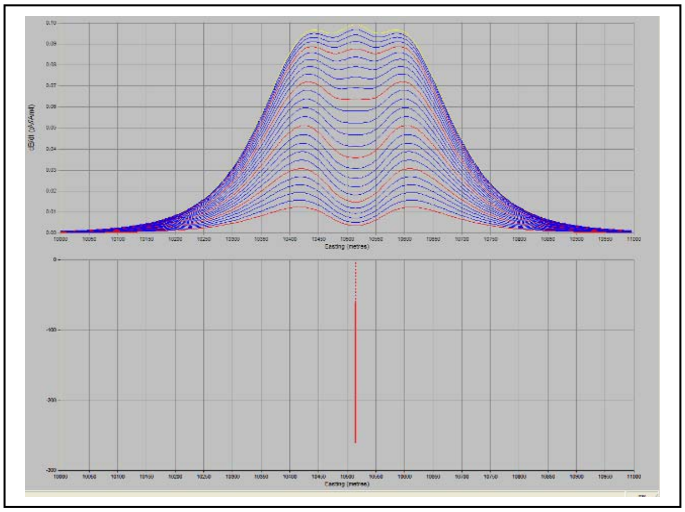

Figure C-13: dB/dt response of a shallow vertical thick plate. Depth=100 m, C=12 S/m, thickness=20 m. The EM response is normalized by the dipole moment and the Rx area.

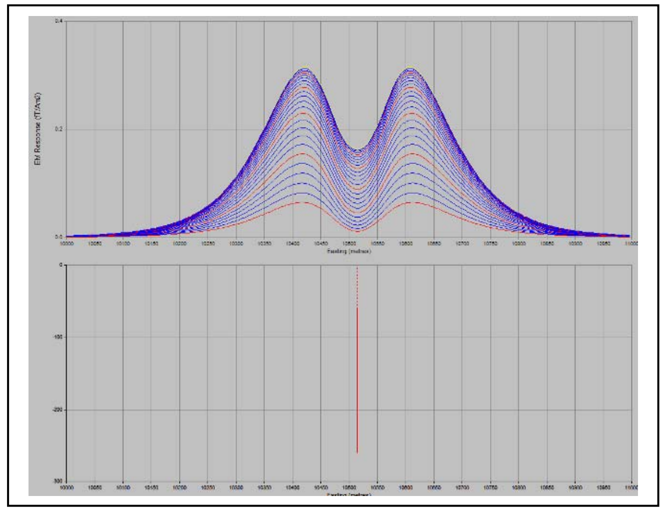

Figure C-14: B-Field response of a shallow vertical thick plate. Depth=100 m, C=12 S/m, thickness= 20 m. The EM response is normalized by the dipole moment.

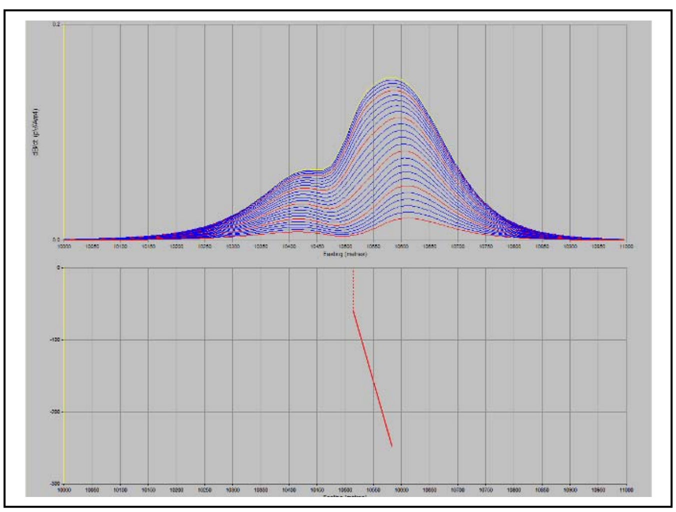

Figure C-15: dB/dt response of a shallow skewed thick plate. Depth=100 m, C=12 S/m, thickness=20 m. The EM response is normalized by the dipole moment and the Rx area.

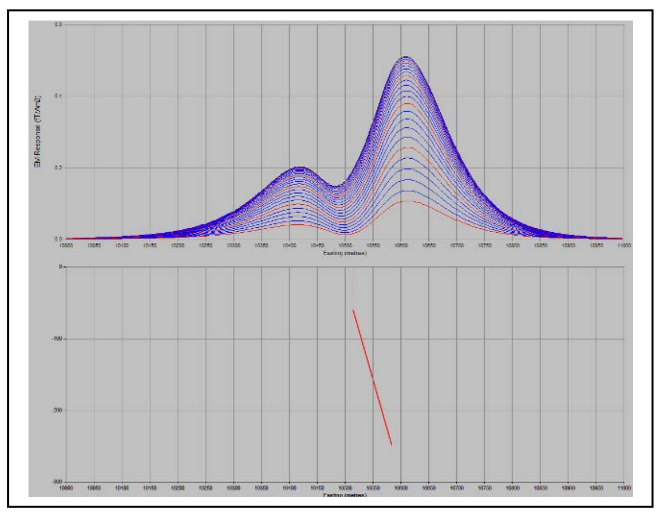

Figure C-16: B-Field response of a shallow skewed thick plate. Depth=100 m, C=12 S/m, thickness=20 m. The EM response is normalized by the dipole moment.

III. MULTIPLE THIN PLATES

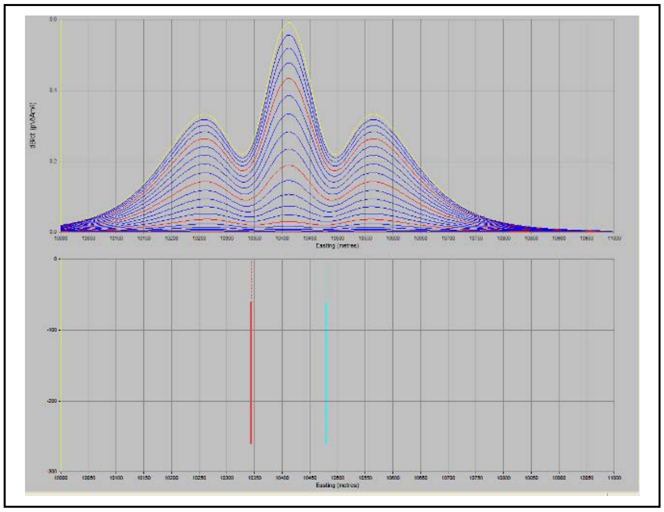

Figure C-17: dB/dt response of two vertical thin plates. Depth=100 m, CT=20 S. The EM response is normalized by the dipole moment and the Rx area.

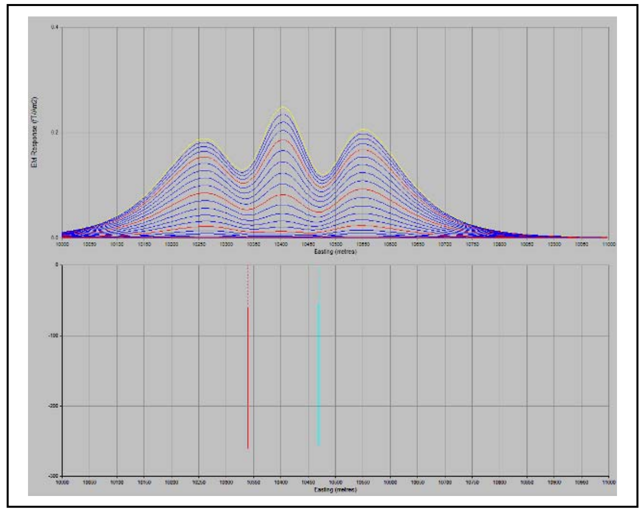

Figure C-18: B-Field response of two vertical thin plates. Depth=100 m, CT=20 S. The EM response is normalized by the dipole moment.

General Interpretation Principals

Magnetics

The total magnetic intensity responses reflect major changes in the magnetite and/or other magnetic minerals content in the underlying rocks and unconsolidated overburden. Precambrian rocks have often been subjected to intense heat and pressure during structural and metamorphic events in their history. Original signatures imprinted on these rocks at the time of formation have, it most cases, been modified, resulting in low magnetic susceptibility values.

The amplitude of magnetic anomalies, relative to the regional background, helps to assist in identifying specific magnetic and non-magnetic rock units (and conductors) related to, for example, mafic flows, mafic to ultramafic intrusives, felsic intrusives, felsic volcanics and/or sediments etc. Obviously, several geological sources can produce the same magnetic response. These ambiguities can be reduced considerably if basic geological information on the area is available to the geophysical interpreter.

In addition to simple amplitude variations, the shape of the response expressed in the wave length and the symmetry or asymmetry, is used to estimate the depth, geometric parameters and magnetization of the anomaly. For example, long narrow magnetic linears usually reflect mafic flows or intrusive dyke features. Large areas with complex magnetic patterns may be produced by intrusive bodies with significant magnetization, flat lying magnetic sills or sedimentary iron formation. Local isolated circular magnetic patterns often represent plug-like igneous intrusives such as kimberlites, pegmatites or volcanic vent areas.

Because the total magnetic intensity (TMI) responses may represent two or more closely spaced bodies within a response, the second derivative of the TMI response may be helpful for distinguishing these complexities. The second derivative is most useful in mapping near surface linears and other subtle magnetic structures that are partially masked by nearby higher amplitude magnetic features. The broad zones of higher magnetic amplitude, however, are severely attenuated in the vertical derivative results. These higher amplitude zones reflect rock units having strong magnetic susceptibility signatures. For this reason, both the TMI and the second derivative maps should be evaluated together.

Theoretically, the second derivative, zero contour or color delineates the contacts or limits of large sources with near vertical dip and shallow depth to the top. The vertical gradient map also aids in determining contact zones between rocks with a susceptibility contrast, however, different, more complicated rules of thumb apply.

Concentric Loop EM Systems

Concentric systems with horizontal transmitter and receiver antennae produce much larger responses for flat lying conductors as contrasted with vertical plate-like conductors. The amount of current developing on the flat upper surface of targets having a substantial area in this dimension, are the direct result of the effective coupling angle, between the primary magnetic field and the flat surface area. One therefore, must not compare the amplitude/conductance of responses generated from flat lying bodies with those derived from near vertical plates; their ratios will be quite different for similar conductances.

Determining dip angle is very accurate for plates with dip angles greater than 30º. For angles less than 30º to 0º, the sensitivity is low and dips can not be distinguished accurately in the presence of normal survey noise levels.

A plate like body that has near vertical position will display a two shoulder, classic **M** shaped response with a distinctive separation distance between peaks for a given depth to top.

It is sometimes difficult to distinguish between responses associated with the edge effects of flat lying conductors and poorly conductive bedrock conductors. Poorly conductive bedrock conductors having low dip angles will also exhibit responses that may be interpreted as surfacial overburden conductors. In some situations, the conductive response has line to line continuity and some magnetic correlation providing possible evidence that the response is related to an actual bedrock source.

The EM interpretation process used, places considerable emphasis on determining an understanding of the general conductive patterns in the area of interest. Each area has different characteristics and these can effectively guide the detailed process used.

The first stage is to determine which time gates are most descriptive of the overall conductance patterns. Maps of the time gates that represent the range of responses can be very informative.

Next, stacking the relevant channels as profiles on the flight path together with the second vertical derivative of the TMI is very helpful in revealing correlations between the EM and Magnetics.

Next, key lines can be profiled as single lines to emphasize specific characteristics of a conductor or the relationship of one conductor to another on the same line. Resistivity Depth sections can be constructed to show the relationship of conductive overburden or conductive bedrock with the conductive anomaly.

____

Roger Barlow
Consultant

____

Nasreddine Bournas, P. Geo.
Geophysicist
Geotech Ltd.

September 2008

APPENDIX F

EM TIME CONSTANT (TAU) CALCULATION

The EM Time-Constant (TAU) is a general measure of the speed of decay of the electromagnetic response and indicates the presence of eddy currents in conductive sources as well as reflecting the "conductance quality" of a source. Although Tau can be calculated using either the measured dB/dt decay or the calculated B-field decay, dB/dt is commonly preferred due to better stability (S/N) relating to signal noise. Generally, TAU calculated on base of early time response reflects both near surface overburden and poor conductors whereas, in the late ranges of time, deep and more conductive sources, respectively. For example early time TAU distributions in an area indicate of conductive overburden are shown in Figure 1.

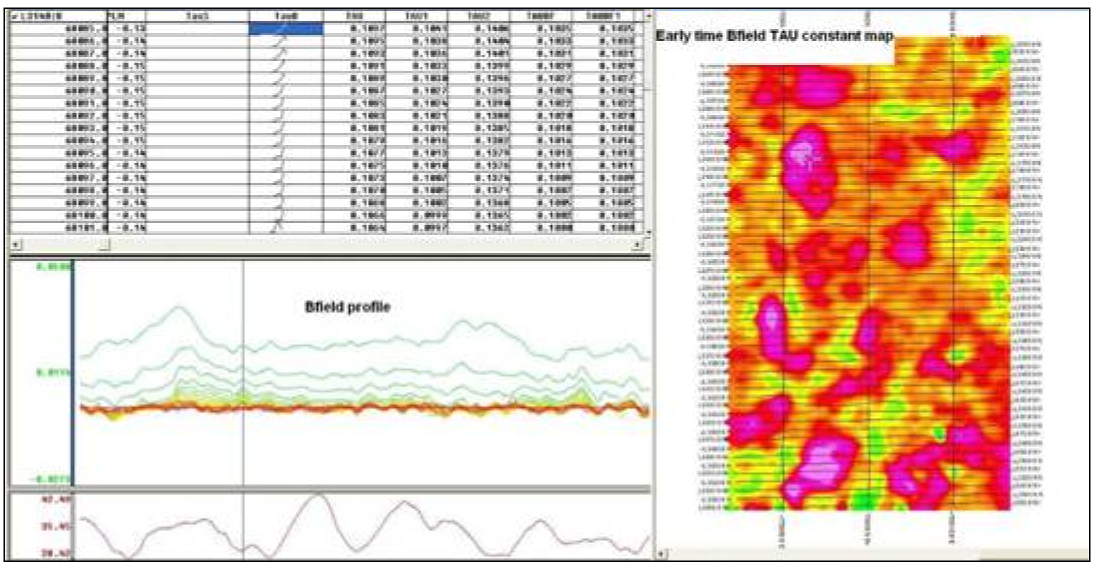

Figure 1 - Area with overburden conductive layer and local sources.

If TAU is calculated across a wide range of time it becomes an integrated parameter and can be used to differentiate conductive sources (Figure 2).

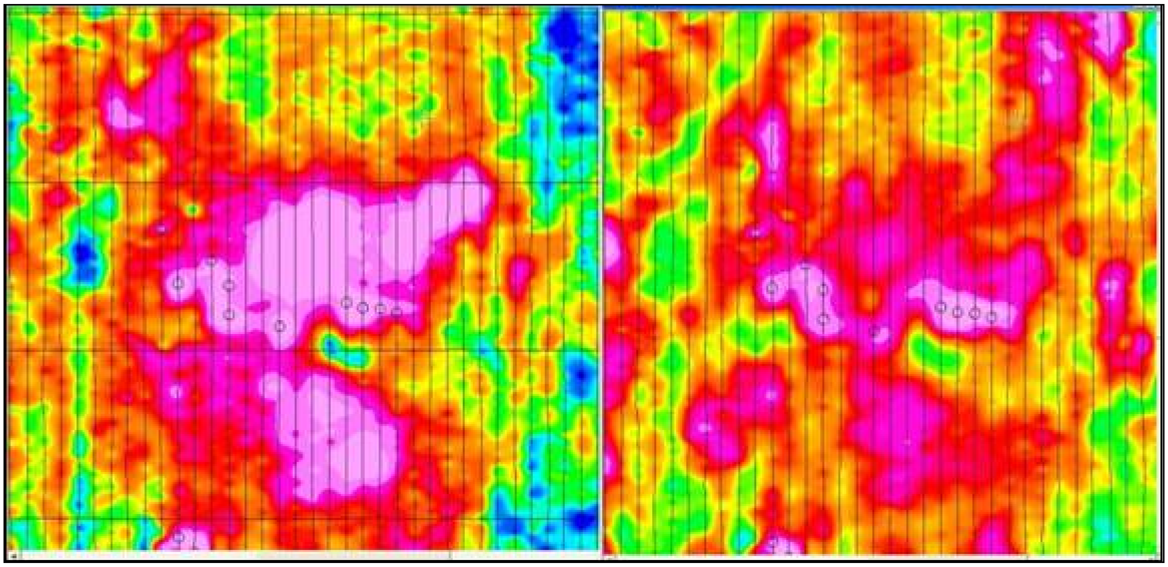

Figure 2 - Map of B-field (left) and TAU (right) with EM anomaly picks due to deep conductive targets.

There are many advantages of TAU maps:

- Because TAU is time integral parameter, all conductive zones and targets are displayed independently of their depth and conductivity on a single map.
- Very good differential resolution in complex conductive places with many sources with different conductivity.
- Signs of the presence of good conductive targets are amplified and emphasized independently of their depth and level of response accordingly.
- Targets which create negative responses in certain known geologic situations, for example due to the relative location of the target, the conductive cover and the coincident geometry of the VTEM system, will usually produce a positive TAU.

In the example shown in Figure 3, three local targets are defined, each of them with a different depth of burial, as indicated on the conductivity depth image (CDI). All are very good conductors but the deeper target (number 3) has a relatively weak dB/dt signal yet also features the strongest total TAU (Figure 4). This example highlights the benefit of Tau analysis in terms of an additional target discrimination tool.

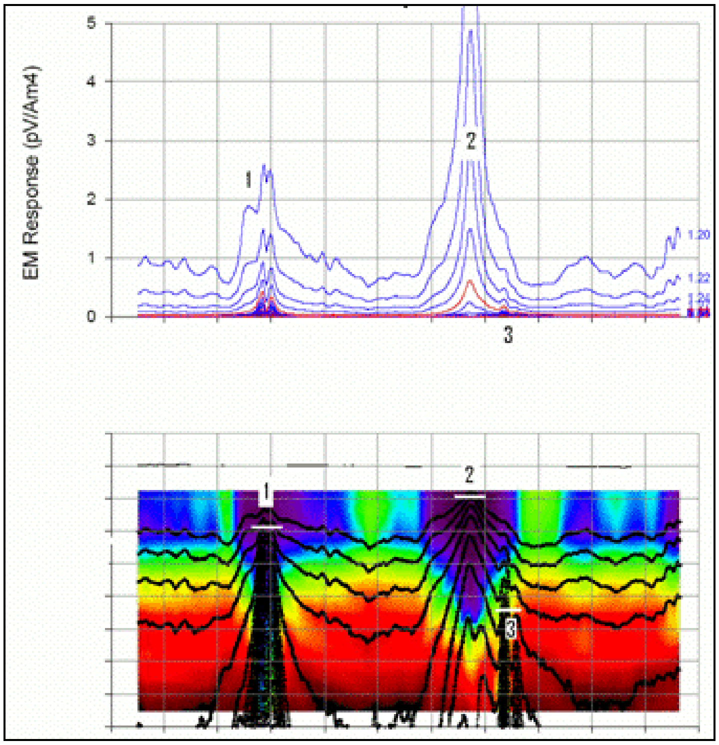

Figure 3 – dB/dt profile and CDI with different depths of sources (white lines).

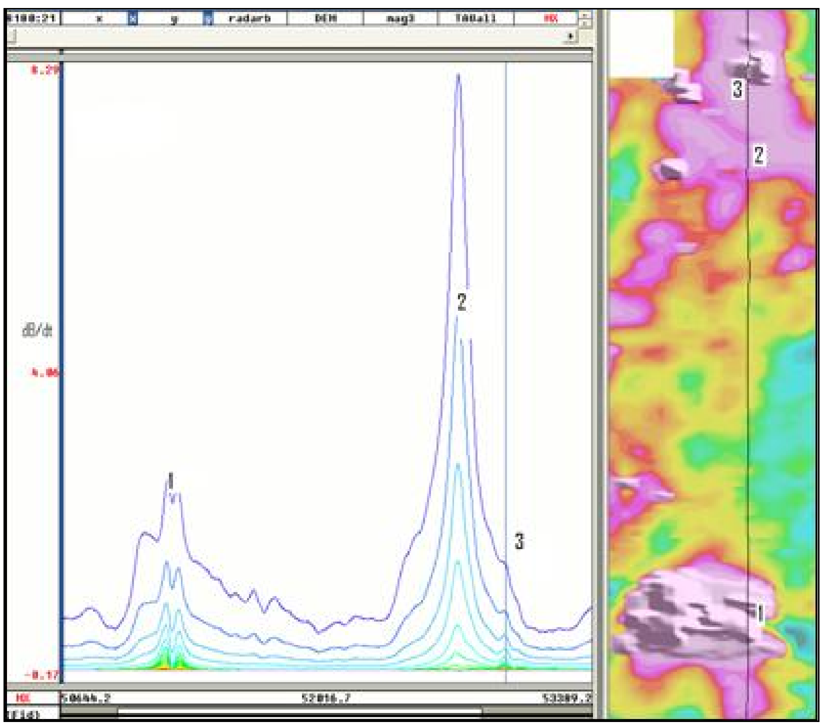

Figure 4 – Map of total TAU and dB/dt profile.

The EM Time Constants were calculated using an in-house program developed at Geotech, whose results are similar to Tau calculated using Maxwell[TM] Software (EMIT Technology Ltd. Pty., Midland WA, AU). The time constant was calculated for late mid and early time within 3 fixed windows (Figure 5). The best/highest Tau value from each window was then extracted and included as a database channel for dB/dt and B-Field. To avoid spikes and noisy data, a noise level was introduced as a threshold for tau calculation. Only Taus for which the mean squared error are less than that specified by the user were kept and the others were not considered in the computation process. Figure 6 illustrates the results of Tau calculation for the anomaly shown.

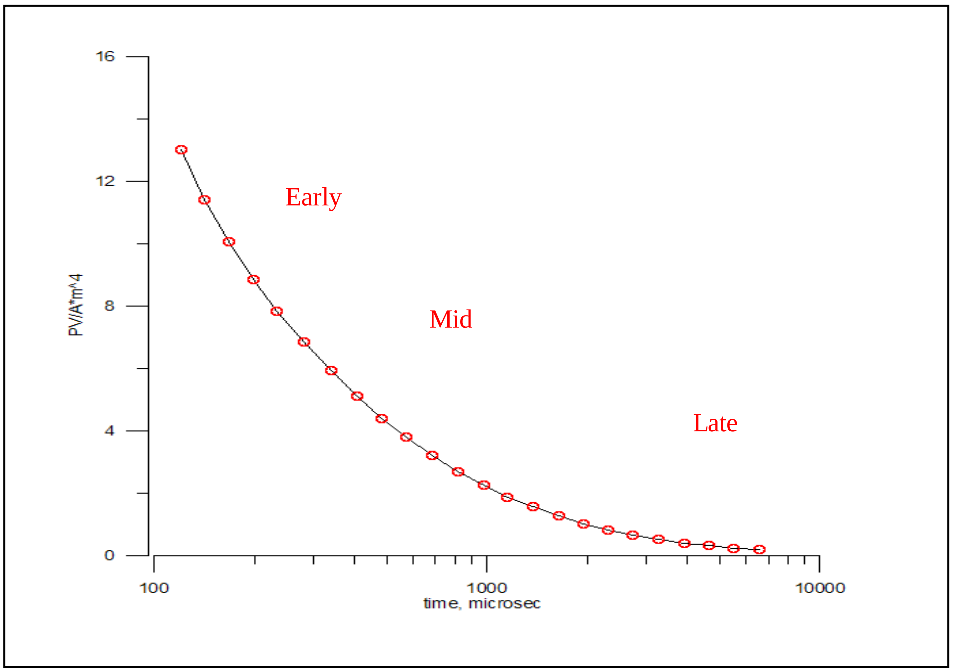

Figure 5 - Typical dB/dt decays of Vtem data

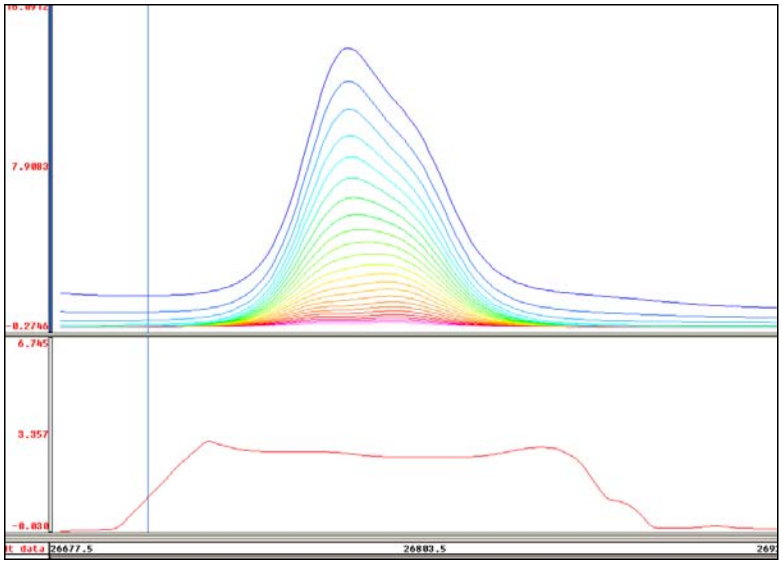

Figure 6 - Vtem anomaly and EM Time constant graph.

Alexander Prikhodko, PhD
Geotech Ltd.

Nasreddine Bournas, PhD, P. Geo (QC)
Geotech Ltd.

September 2008

APPENDIX G

EM ANOMALIES

Maki Property

Line	x	y	Cond_BF	Cond_SF	Dip1	ID	Peak	TauBF	TauSF
L1000	441636.5	5496930	15.04007769	10.9	72°	A	2	1.956	1.431
L1000	441635.5	5497495.5	32.48016637	18.95	77°	B	2	4.0945	2.3565
L1000	441637.5	5498001.5	22.00366632	15.35	80°	C	2	2.829	1.941
L1000	441637	5498960	25.27046114	16.35	67°	D	2	3.231	2.0565
L1000	441635	5499186	33.98484958	13.65		E		4.27	1.741
L1010	441740.5	5499120.5	29.76479406	14.15	70°	A	2	3.7735	1.8005
L1010	441739.5	5498556.5	26.37472729	8.05	81°	B	2	3.3655	1.105
L1010	441740	5497970	20.04607891	13.95	80°	C	2	2.5855	1.782
L1010	441739.5	5497558	44.40033164	23.45	76°	D	2	5.4345	2.892
L1010	441741	5496987	13.52038903	9.55	68°	E	2	1.7635	1.274
L1020	441837.5	5497029.5	15.49084054	11.6	67°	A	2	2.013	1.5135
L1020	441837	5497168	20.79608333	13.35		B		2.679	1.846
L1020	441835	5497561	44.14459389	24.8	82°	C	2	5.407	3.0565
L1020	441832	5498058	24.59199628	15.75	88°	D	2	3.148	1.982
L1020	441839	5499146.5	28.15320136	13.75	66°	E	2	3.5805	1.7515
L1030	441933	5499243	32.86884466	14.8		A		4.14	1.91
L1030	441936.5	5499086	30.8294425	17.3	81°	B	2	3.9	2.173
L1030	441938	5498849	74.30705067	22.1		C		8.279	2.827
L1030	441943.5	5498022	36.54037346	22	88°	D	2	4.564	2.72
L1030	441940	5497874	28.49015741	19.55		E		3.621	2.066
L1030	441941	5497603	21.5038524	15.15		F		2.767	1.76
L1030	441935.5	5497078	19.68981058	10.45	77°	G	2	2.541	1.3845

L1040	442036	5497114	26.72495377	18	72°	A	2	3.408	2.25
L1040	442038	5497609	31.63356567	19.65		B		3.995	2.374
L1040	442034.5	5498039	41.49684467	23.8	89°	C	2	5.119	2.9345
L1040	442035	5498208	35.71835943	20.5		D		4.47	2.251
L1040	442034	5499115	25.00044544	16.1	69°	E	2	3.198	2.032
L1040	442036	5499280	32.7149646	14.15		F		4.122	2.118
L1050	442138	5499289	32.46736944	18.75		A		4.093	2.546
L1050	442136.5	5499151	23.43620421	15.35	66°	B	2	3.006	1.9395
L1050	442141	5498230	32.48443225	17.9		C		4.095	2.15
L1050	442141.5	5498074	26.81983105	17.85	84°	D	2	3.4195	2.2275
L1050	442140	5497652	29.25799167	17.9		E		3.713	2.152
L1050	442137	5497545	41.39679065	20.7		F		5.108	2.983
L1050	442140	5497162	31.2098421	20.6	83°	G	2	3.945	2.5515
L1060	442238	5497199	29.42536316	21.3		A		3.733	2.634
L1060	442237	5497654	31.26062979	21.15		B		3.951	2.603
L1060	442235	5498098	32.34372013	19.45	86°	C	2	4.0785	2.4145
L1060	442239	5498267	33.55463962	18.9		D		4.22	2.365
L1060	442240	5498389	39.95905186	19.25		E		4.949	2.417
L1060	442238	5499176	24.82471496	18.8	73°	F	2	3.1765	2.3455
L1070	442340	5499369	24.89417213	16.15		A		3.185	2.141
L1070	442337.5	5499219.5	21.74557515	16.75	55°	B	2	2.797	2.109
L1070	442336	5498412	34.3471883	20.05		C		4.312	2.328
L1070	442340	5498257	28.36528459	17.3	75°	D	2	3.606	2.168
L1070	442341	5498145	34.67578656	19.55		E		4.35	2.508
L1070	442343	5497732.5	35.09625638	23.95	80°	F	2	4.3985	2.95
L1070	442343	5497613	35.07455296	22.5		G		4.396	2.668
L1070	442339	5497176	28.41938537	21.25	85°	H	2	3.6125	2.625
L1080	442434	5497016	31.58265943	20.2		A		3.989	2.462
L1080	442436	5497177	28.23218337	18.7		B		3.59	2.186
L1080	442440	5497347	27.01385828	17.85		C		3.443	2.27
L1080	442437.5	5497765	28.58178676	18.55	77°	D	2	3.632	2.3065

L1080	442435.5	5498202	28.82775555	19.35	84°	E	2	3.6615	2.4055
L1080	442441	5499238	15.92221595	12.8	82°	F	2	2.0675	1.6465
L1080	442436	5499478	18.98650935	11.75		G		2.453	1.583
L1090	442541.5	5499387.5	17.94634579	10.45	68°	A	2	2.3225	1.3825
L1090	442531.5	5498221.5	32.44604357	19.5	86°	B	2	4.0905	2.4165
L1090	442538.5	5497780.5	22.15703395	15.55	79°	C	2	2.848	1.963
L1090	442531	5497318	22.06823062	15.6	84°	D	2	2.837	1.968
L1090	442541	5497093.5	25.99636925	15.3	81°	E	2	3.3195	1.932
L1100	442635	5497157	21.29454192	13.75		A		2.741	1.72
L1100	442634	5497369.5	22.53278528	17.9	70°	B	2	2.8945	2.237
L1100	442636	5497676	42.45582656	22.2		C		5.224	3.059
L1100	442634.5	5497784	38.77275589	23.3	89°	D	2	4.8165	2.88
L1100	442634	5498170.5	29.69349918	16	83°	E	2	3.765	2.008
L1100	442632.5	5498423.5	30.17637813	17.1	77°	F	2	3.8225	2.1355
L1100	442630	5499410	23.27389725	11.9	68°	G	2	2.986	1.544
L1110	442736	5499475.5	21.19397132	15.85	70°	A	2	2.7285	1.998
L1110	442737	5498304	24.67362277	15.9	81°	B	2	3.158	2.005
L1110	442736	5498158	21.77782213	15.6		C		2.801	1.983
L1110	442740	5497800	43.89401078	24.95	78°	D	2	5.38	3.0765
L1110	442739	5497410.5	30.08809636	20.3	81°	E	2	3.812	2.5205
L1110	442736	5497164	29.04065169	15.2		F		3.687	1.51
L1120	442838	5497352	30.45835296	17.85	70°	A	2	3.856	2.2315
L1120	442845	5497812	32.6124633	20.45		B		4.11	2.727
L1120	442838.5	5498187.5	26.94365525	20.45	86°	C	2	3.4345	2.533
L1120	442837	5498364	36.40011859	20.8		D		4.548	2.529
L1120	442834	5498550	38.89314444	22.2		E		4.83	2.956
L1120	442829.5	5499508	22.12473815	15.7	74°	F	2	2.844	1.979
L1130	442940	5499567	20.71175787	14.2	77°	A	2	2.6685	1.8085
L1130	442933.5	5498559	44.12137079	22.75	55°	B	2	5.4045	2.809
L1130	442933	5498346	35.27434725	22.25		C		4.419	2.543
L1130	442933.5	5498219.5	46.8160291	29.45	90°	D	2	5.6915	3.6175

L1130	442936	5497841	30.45835296	24.6		E		3.856	2.498
L1130	442939.5	5497367	33.49021435	20.05	75°	F	2	4.2125	2.4835
L1140	443036	5497414.5	34.06241914	20.95	72°	A	2	4.279	2.587
L1140	443037	5497854	25.50804154	19.75		B		3.26	2.241
L1140	443037	5498227	40.56748863	25.9	89°	C	2	5.0165	3.1845
L1140	443037.5	5498393.5	44.22823259	27	88°	D	2	5.416	3.322
L1140	443038	5498585	51.18875463	25.55	69°	E	2	6.144	3.15
L1140	443031	5499195	39.1163709	19.6		F		4.855	1.877
L1140	443034	5499612.5	20.98892525	14.1	69°	G	2	2.703	1.7985
L1150	443139.5	5499654	20.57127276	14	71°	A	2	2.651	1.78
L1150	443138.5	5499292.5	26.49002571	15.4	87°	B	2	3.3795	1.9495
L1150	443142.5	5498613.5	49.72165811	26.6	61°	C	2	5.994	3.274
L1150	443141	5498429	34.33855087	23.4	84°	D	2	4.311	2.8885
L1150	443142	5497869.5	39.65363675	23.2	83°	E	2	4.915	2.8585
L1150	443146.5	5497444.5	24.21284218	17.5	78°	F	2	3.1015	2.1865
L1160	443230	5497441	21.27844805	15.45	80°	A	2	2.739	1.95
L1160	443235	5497869.5	32.31388848	21.95	82°	B	2	4.075	2.709
L1160	443236.5	5498259.5	26.7868249	19.4	84°	C	2	3.4155	2.4065
L1160	443236	5498411	31.84585102	20.45		D		4.02	2.806
L1160	443240	5498533	44.83395106	24.8		E		5.481	3.312
L1160	443241	5498597	42.39167155	25.45		F		5.217	2.957
L1160	443237	5499251	47.35350149	21.5		G		5.748	2.358
L1160	443236	5499683	20.18229595	14.9	69°	H	2	2.6025	1.8915
L1170	443333	5497246	19.02642735	11.45		A		2.458	0.91
L1170	443333	5497423	19.08232093	10.1		B		2.465	1.758
L1170	443333	5497658.5	20.50306276	14.95	71°	C	2	2.6425	1.8925
L1170	443329	5497871	35.59198097	21.7	84°	D	2	4.4555	2.686
L1170	443331	5498273	28.79438364	19.85	82°	E	2	3.6575	2.4655
L1170	443334	5498578.5	42.48791611	25.7	80°	F	2	5.2275	3.164
L1170	443337	5498747	44.29332342	24.9		G		5.423	2.935
L1170	443334	5499303	39.21470821	19.3		H		4.866	1.878

L1170	443333	5499706	17.91053402	13.35	75°	I	2	2.318	1.711
L1180	443440.5	5499734.5	19.53382694	14.3	78°	A	2	2.5215	1.8195
L1180	443438	5499332	42.59340988	14.45		B		5.239	2.167
L1180	443434.5	5499103.5	25.79104418	5.65	84°	C	2	3.2945	0.8235
L1180	443440	5498729	33.43440137	13.3		D		4.206	2.628
L1180	443440	5498658	34.54598895	22.05		E		4.335	2.824
L1180	443441	5498554	33.94177284	22.45		F		4.265	2.713
L1180	443441	5498474	31.82885771	20.3		G		4.018	2.31
L1180	443443	5498342	29.40861866	19		H		3.731	2.414
L1180	443444	5498258	29.46723161	20.4		I		3.738	2.647
L1180	443440	5497888.5	24.71036496	15.85	88°	J	2	3.1625	1.9945
L1180	443440.5	5497689.5	22.90507402	14.95	74°	K	2	2.9405	1.8945
L1180	443439	5497313	14.62128826	11	87°	L	2	1.903	1.437
L1190	443543	5497260	24.46145902	14.7		A		3.132	2.01
L1190	443542.5	5497426	22.33473663	15.35	89°	B	2	2.87	1.94
L1190	443535	5497909	29.94526276	20.4	76°	C	2	3.795	2.53
L1190	443535.5	5498408	34.28241991	22.85	88°	D	2	4.3045	2.821
L1190	443536.5	5498551.5	37.62772913	24.35	90°	E	2	4.6875	3.0005
L1190	443534	5498676	33.17706948	21.85		F		4.176	2.624
L1190	443536	5499098	31.78638242	13.55		G		4.013	0.847
L1190	443535	5499229	31.98186348	5.9		H		4.036	0.856
L1190	443532	5499362	43.92182875	12.55		I		5.383	2.381
L1190	443535	5499765	21.31868458	13.95	73°	J	2	2.744	1.7785
L1200	443640	5499864	22.22163824	14.75		A		2.856	1.774
L1200	443639	5499742	17.91849188	13.4		B		2.319	1.654
L1200	443640.5	5498770.5	22.24586922	16.85	80°	C	2	2.859	2.1125
L1200	443640.5	5498356.5	42.70358317	25.9	82°	D	2	5.251	3.194
L1200	443641.5	5497908.5	29.96206039	19	81°	E	2	3.797	2.3615
L1200	443644	5497505	29.62642553	18.85		F		3.757	2.373
L1200	443641.5	5497327.5	28.90286566	19.75	65°	G	2	3.6705	2.4525
L1210	443740	5497352.5	26.04978865	18.75	68°	A	2	3.326	2.331

L1210	443734	5497918.5	31.59962637	21.15	87°	B	2	3.991	2.6155
L1210	443733	5498319	31.45546497	21.4		C		3.974	2.632
L1210	443735	5498457	26.64249011	19.7		D		3.398	2.256
L1210	443737	5498643.5	30.8716651	20.75	87°	E	2	3.905	2.568
L1210	443738	5498846	34.40766445	22.25		F		4.319	2.828
L1210	443735	5499430	49.38189106	22.55		G		5.959	2.742
L1210	443733	5499815	22.32261645	15.15	76°	H	2	2.8685	1.9155
L1220	443842	5499794	22.10051906	15.65		A		2.841	1.891
L1220	443842	5498948	29.43373603	14.1		B		3.734	1.7
L1220	443844	5498733	35.68348527	17.4		C		4.466	2.663
L1220	443843	5498652	41.08801897	22.25		D		5.074	2.836
L1220	443840.5	5498437	28.71932007	18.25	82°	E	2	3.6485	2.2725
L1220	443837.5	5497941.5	38.55454674	24.05	88°	F	2	4.792	2.9605
L1220	443842.5	5497377.5	25.95528723	18	69°	G	2	3.3145	2.2465
L1230	443940	5497398	28.45268634	19.1	77°	A	2	3.6165	2.379
L1230	443938	5497988	32.44177875	17.8		B		4.09	2.256
L1230	443930	5498417.5	25.8608309	17.05	82°	C	2	3.303	2.1345
L1230	443931	5498707	33.62339031	19.4		D		4.228	2.679
L1230	443932	5499442	59.84079035	19		E		6.992	2.043
L1230	443935	5499775.5	26.0662283	17.05	89°	F	2	3.328	2.132
L1240	444040.5	5499816.5	31.98186348	22.1	79°	A	2	4.036	2.729
L1240	444040	5499427	49.74110227	17.5		B		5.996	1.259
L1240	444041	5498798	28.03271678	14.35		C		3.566	2.391
L1240	444040	5498729	26.01691346	18.2		D		3.322	2.135
L1240	444039	5498634	26.90649949	18.3		E		3.43	2.426
L1240	444040	5498439.5	29.71027175	23	84°	F	2	3.767	2.839
L1240	444040	5497988	37.69403849	21.45	86°	G	2	4.695	2.6465
L1240	444041.5	5497420.5	30.94346867	21.45	68°	H	2	3.9135	2.65
L1250	444138.5	5497452.5	27.28666011	19.15	83°	A	2	3.476	2.378
L1250	444137.5	5498006.5	26.11555548	16.35	79°	B	2	3.334	2.0555
L1250	444133.5	5498460	30.50469331	21.6	83°	C	2	3.8615	2.6675

L1250	444132.5	5498612	36.08505368	20.8	87°	D	2	4.512	2.5765
L1250	444131	5499844	37.05437754	22.7	79°	E	2	4.6225	2.8005
L1260	444241.5	5499859	32.55697017	20.1	79°	A	2	4.1035	2.496
L1260	444240.5	5498653	32.55697017	22.85	83°	B	2	4.1035	2.8215
L1260	444238.5	5498499.5	41.66073622	25.6	89°	C	2	5.137	3.151
L1260	444241	5498052	30.02086537	24.15		D		3.804	2.738
L1260	444240.5	5497475.5	23.04685986	16.25	80°	E	2	2.958	2.0445
L1270	444333	5497476	23.37532558	17.25	78°	A	2	2.9985	2.1565
L1270	444332.5	5498027	43.40818554	24.95	83°	B	2	5.3275	3.077
L1270	444334.5	5498527	44.59131214	24.45	89°	C	2	5.455	3.0115
L1270	444336	5498671	30.23525864	20.5	73°	D	2	3.8295	2.5355
L1270	444334	5498914	30.10490833	19.05		E		3.814	2.409
L1270	444337	5499404	32.82608474	12.7		F		4.135	0.865
L1270	444334	5499880.5	23.11575838	16.75	75°	G	2	2.9665	2.1
L1280	444440	5499914	26.84458942	18.6	82°	A	2	3.4225	2.3185
L1280	444436.5	5499386.5	15.41964099	8.75	83°	B	2	2.004	1.186
L1280	444438.5	5498629.5	37.02357191	22	87°	C	2	4.619	2.7175
L1280	444440.5	5498065.5	50.2428724	26.1	80°	D	2	6.0475	3.2145
L1280	444436	5497504.5	21.68915277	17.6	66°	E	2	2.79	2.197
L1290	444538	5497524.5	19.91392923	17.55	74°	A	2	2.569	2.194
L1290	444535	5498097.5	36.33880095	23.45	88°	B	2	4.541	2.8925
L1290	444537	5498581	32.08395005	24.5		C		4.048	2.773
L1290	444534.5	5498767.5	28.27376685	18.55	85°	D	2	3.595	2.3045
L1290	444534	5498894	22.93342432	16.7		E		2.944	2.049
L1290	444539	5499056	26.78269953	16.95		F		3.415	2.2
L1290	444541	5499319	37.81790161	12.65		G		4.709	1.06
L1290	444532	5499904	29.61804319	14		H		3.756	2.513
L1300	444640	5499932	31.0660305	19.95		A		3.928	2.427
L1300	444641	5499673	30.17217317	17.8		B		3.822	2.018
L1300	444635	5499023	20.70372823	15.3	80°	C	2	2.6675	1.9305
L1300	444639.5	5498793	36.68515799	23.9	79°	D	2	4.5805	2.946

L1300	444637.5	5498611.5	34.14434206	21.8	90°	E	2	4.2885	2.6935
L1300	444638.5	5498098	25.87314874	20.2	83°	F	2	3.3045	2.499
L1300	444638.5	5497544	16.98460733	12.45	85°	G	2	2.2015	1.6065
L1310	444731	5497558	6.197760695	9.25	89°	A	2	0.833	1.232
L1310	444736.5	5498114.5	30.44571694	21.3	88°	B	2	3.8545	2.635
L1310	444735	5498642	51.60277459	27.45	90°	C	2	6.186	3.375
L1310	444735.5	5498826	32.98007634	22.45	84°	D	2	4.153	2.773
L1310	444735.5	5499068	26.42413249	19.85	74°	E	2	3.3715	2.461
L1310	444727	5500037	23.71239296	18.85		F		3.04	2.126
L1320	444839.5	5499996	28.37776792	18.7	87°	A	2	3.6075	2.326
L1320	444841	5499102.5	35.48747605	23.8	69°	B	2	4.4435	2.936
L1320	444840	5498866	34.34286952	24.05	84°	C	2	4.3115	2.969
L1320	444836	5498714	42.35502595	26.15		D		5.213	3.057
L1320	444837	5498131	34.07966232	20.9	90°	E	2	4.281	2.5845
L1320	444838	5497591	9.942720489	8.85	83°	F	2	1.309	1.199
L1330	444932	5497598	7.721001366	8.15	76°	A	2	1.0265	1.1195
L1330	444933	5498154.5	42.91041465	26.45	78°	B	2	5.2735	3.258
L1330	444935.5	5498710.5	37.74710901	21.75	90°	C	2	4.701	2.6925
L1330	444935.5	5498893	33.46874538	20.8	84°	D	2	4.21	2.5725
L1330	444932	5499132.5	21.47566619	15.35	71°	E	2	2.7635	1.941
L1330	444933.5	5500033.5	33.25851066	22.65	76°	F	2	4.1855	2.7965
L1330	444942	5501467	20.73183301	16.9		G		2.671	1.762
L1330	444938	5501580	31.35378228	16		H		3.962	2.264
L1340	445041	5501616	23.85061507	16.5		A		3.057	1.87
L1340	445046	5501492	20.57127276	13.85		B		2.651	1.653
L1340	445039	5500324	27.99118904	16		C		3.561	2.368
L1340	445041	5500062.5	28.10749082	19.8	82°	D	2	3.575	2.4545
L1340	445041	5499152	22.65411986	18.15	69°	E	2	2.9095	2.259
L1340	445041	5498925	34.04948807	21.85	87°	F	2	4.2775	2.7045
L1340	445042	5498749	33.64058289	21.8	88°	G	2	4.23	2.6975
L1350	445133	5498767	39.37130288	21.4	85°	A	2	4.8835	2.6455

L1350	445138	5498963	33.76959009	21.15	74°	B	2	4.245	2.619
L1350	445136	5499159.5	28.81524034	20.8	74°	C	2	3.66	2.5785
L1350	445133	5499595	19.22609258	13.9		D		2.483	1.013
L1350	445134	5499752	37.21732079	14.7		E		4.641	2.729
L1350	445138	5500085.5	39.64915058	23.15	77°	F	2	4.9145	2.852
L1350	445138	5500348	34.0537983	21.85		G		4.278	2.738
L1350	445136	5501515	10.31232866	23.7		H		1.356	3.109
L1350	445135	5501646	26.3541455	20.1		I		3.363	1.898
L1360	445241	5501664	29.75221043	15.25		A		3.772	1.956
L1360	445239	5501535	16.64736796	10.8		B		2.159	0.876
L1360	445243	5500371	28.84027166	13.25		C		3.663	2.524
L1360	445241.5	5500115.5	39.78829212	26.6	72°	D	2	4.93	3.269
L1360	445244	5499974	61.80462804	30		E		7.176	3.669
L1360	445242.5	5499560.5	18.41223091	8.45	67°	F	2	2.381	1.1505
L1360	445244	5499250	27.2618435	18.45	63°	G	2	3.473	2.2965
L1360	445239	5499002	28.99053505	19.65	80°	H	2	3.681	2.4375
L1360	445236	5498771	45.65871058	21.7		I		5.569	2.956
L1370	445331	5498761	40.86144684	21.55		A		5.049	2.368
L1370	445334	5499070	33.53745685	19.95		B		4.218	2.572
L1370	445335	5499193	29.20781199	19.65		C		3.707	2.307
L1370	445332	5500140	32.76196717	22.7	72°	D	2	4.1275	2.8065
L1370	445335	5500404	30.50890672	21.05		E		3.862	2.637
L1370	445337	5501530.5	18.48396147	8.35	73°	F	2	2.39	1.1335
L1380	445437	5501601	20.03406283	7.8		A		2.584	0.779
L1380	445439	5500410	26.67547131	13.5		B		3.402	2.681
L1380	445436	5500125	30.51733385	21.35		C		3.863	2.604
L1380	445435	5499716	31.2098421	12.85		D		3.945	0.699
L1380	445431	5499540	13.30357516	5.1		E		1.736	0.796
L1380	445438	5499208	32.11799367	13.65		F		4.052	2.695
L1380	445434	5499097	27.85836427	19.45		G		3.545	2.144
L1380	445433	5498783	28.68180033	15.85		H		3.644	1.852

L1390	445538	5498932.5	25.24999301	18.1	84°	A	2	3.2285	2.259
L1390	445533.5	5499192	20.98892525	16.9	87°	B	2	2.703	2.1155
L1390	445534.5	5500161.5	40.66238767	23.7	69°	C	2	5.027	2.921
L1390	445533	5500412	28.39857543	17.15		D		3.61	1.529
L1390	445534.5	5501596	14.02128321	9.1	66°	E	2	1.827	1.2145
L1400	445637	5501640	12.59440964	13.05		A		1.646	1.649
L1400	445642	5500166.5	22.16510856	14	82°	B	2	2.849	1.7875
L1400	445641.5	5499209	26.2965281	19.6	73°	C	2	3.356	2.4315
L1400	445645	5498945.5	38.65692759	23.45	84°	D	2	4.8035	2.889
L1410	445733	5498918	38.76829912	24.8		A		4.816	3.144
L1410	445734	5499058	33.54604799	24.45		B		4.219	2.883
L1410	445733.5	5499256.5	39.49222994	22.1	71°	C	2	4.897	2.729
L1410	445735.5	5500185	21.63677172	17.15	79°	D	2	2.7835	2.148
L1420	445841	5500444	23.11170496	16.1		A		2.966	2.104
L1420	445839	5500203	30.36992113	21.05	82°	B	2	3.8455	2.6065
L1420	445834	5499273	41.21961139	25.05	78°	C	2	5.0885	3.0835
L1420	445833	5499121.5	31.04489254	21.45	90°	D	2	3.9255	2.6515
L1420	445837.5	5499000.5	31.30719928	21.85	86°	E	2	3.9565	2.7025
L1430	445935	5499021.5	41.50139442	25	89°	A	2	5.1195	3.084
L1430	445935	5499216.5	38.58124732	24.4	75°	B	2	4.795	3.0075
L1430	445939	5499335.5	33.3056808	22.45	71°	C	2	4.191	2.775
L1430	445936	5500211.5	31.11677291	19.45	83°	D	2	3.934	2.4205
L1430	445936	5500468	31.31990239	16.85		E		3.958	2.075
L1440	446039	5500478	30.62692592	15.35		A		3.876	1.81
L1440	446042.5	5500221.5	37.98618065	22.85	90°	B	2	4.728	2.8195
L1440	446036	5499347	42.60258736	28.15	64°	C	2	5.24	3.4565
L1440	446037	5499192	35.48312333	24.3		D		4.443	2.795
L1440	446036	5499036	32.63381212	22.6	85°	E	2	4.1125	2.79
L1450	446136	5499056	40.99734292	24.3	87°	A	2	5.064	2.993
L1450	446135	5499177	37.43781894	23.1		B		4.666	2.771
L1450	446135	5499309	38.46558277	23.85		C		4.782	3.116

L1450	446135.5	5500241.5	35.61811909	22	84°	D	2	4.4585	2.7205
L1450	446134	5500494	40.25615912	16.3		E		4.982	1.6
L1460	446242	5500269.5	27.21222017	19.05	75°	A	2	3.467	2.3685
L1460	446239	5499400	28.09087168	19.1		B		3.573	2.278
L1460	446239	5499245	31.72693618	21.1	85°	C	2	4.006	2.6115
L1460	446236	5499088	41.03360577	24.8	89°	D	2	5.068	3.0515
L1470	446334	5498634	52.26621487	16.7		A		6.253	1.051
L1470	446336	5498985	36.75980232	13.5		B		4.589	2.408
L1470	446339	5499056	32.91161651	19.5		C		4.145	2.43
L1470	446336.5	5499260.5	26.93952647	19.65	80°	D	2	3.434	2.4385
L1470	446334	5499412	26.87347827	17.85		E		3.426	2.17
L1470	446332.5	5499762	9.455183219	3.85	67°	F	2	1.247	0.5925
L1470	446330.5	5500290	27.30320636	19.35	62°	G	2	3.478	2.4005
L1480	446441	5500313.5	24.13546246	15.5	83°	A	2	3.092	1.956
L1480	446438	5499399	22.95772731	16	74°	B	2	2.947	2.014
L1480	446438.5	5499259.5	26.67547131	18.3	83°	C	2	3.402	2.283
L1480	446439	5499124	45.93642241	24.75	83°	D	2	5.5985	3.0465
L1490	446539	5499133	36.90481392	23.1	90°	A	2	4.6055	2.8525
L1490	446538	5499330	30.07128608	19.65		B		3.81	2.254
L1490	446538.5	5500340	37.11600928	21.9	69°	C	2	4.6295	2.7055
L1490	446532	5501602	1.548261843	10.45		D		0.245	0.333
L1500	446638	5500344	38.4033427	24.85	74°	A	2	4.775	3.06
L1500	446639.5	5499450	32.41192827	17.65	69°	B	2	4.0865	2.205
L1500	446637.5	5499154	56.61963361	29.55	85°	C	2	6.6835	3.631
L1510	446734.5	5499168	39.11190273	22.25	86°	A	2	4.8545	2.744
L1510	446738.5	5499332	29.32492067	19.4	83°	B	2	3.721	2.4055
L1510	446735	5500355	31.97761131	22.35	75°	C	2	4.0355	2.7615
L1510	446736	5500601	29.42536316	16.5		D		3.733	1.65
L1520	446838	5500633	38.33224609	14.3		A		4.767	1.99
L1520	446842	5500369	30.64379273	21	73°	B	2	3.878	2.5995
L1520	446837	5499983	27.09648359	5.8	88°	C	2	3.453	0.839

L1520	446839	5499399	25.76231556	10.85		D		3.291	2.158
L1520	446840	5499296	26.28829843	16.65		E		3.355	2.017
L1520	446841.5	5499196	44.04244428	23.75	84°	F	2	5.396	2.928
L1530	446935	5498642	54.22849086	19.5		A		6.449	1.91
L1530	446936	5498942	49.58563658	16.15		B		5.98	2.151
L1530	446936	5499171	52.67402575	23.75		C		6.294	3.716
L1530	446936	5499230	45.91286334	28.4		D		5.596	3.263
L1530	446937	5499303	38.75938602	24		E		4.815	2.653
L1530	446938	5499421	31.31143354	20.95		F		3.957	2.523
L1530	446940	5500378.806	32.86884466	21.2		G		4.14	2.712
L1530	446935	5500641	31.93084504	18.65		H		4.03	2.405
L1540	447040	5500657	36.63687988	13.95		A		4.575	1.152
L1540	447040.1087	5500379.813	28.1656699	14.55		B		3.582	2.552
L1540	447045	5499440	30.60162895	20.25		D		3.873	2.427
L1540	447044	5499320	35.5179488	20.8		E		4.447	2.719
L1540	447044	5499244	35.23958059	22.95		F		4.415	2.947
L1540	447045	5499173	37.66751091	23.9		G		4.692	2.941
L1540	447039	5498946	26.83220983	19		H		3.421	1.798
L1540	447037	5498869	27.92476449	15.45		I		3.553	2.109
L1550	447136	5498482	29.50911032	20.4		A		3.743	2.826
L1550	447137	5499022.5	23.14008039	13.65	90°	B	2	2.9695	1.7475
L1550	447133	5499233	46.82552146	28.1	89°	C	2	5.6925	3.4525
L1550	447134	5499335	45.724552	24.85		D		5.576	2.745
L1550	447134	5499440	33.57182435	19.75		E		4.222	2.164
L1550	447136	5500383	28.29872158	16.55	70°	F	2	3.598	2.0745
L1560	447242.5	5500377.5	35.14401536	17.7	72°	A	2	4.404	2.2145
L1560	447236	5500073	16.07665739	12.5		B		2.087	0.83
L1560	447238	5499570.5	22.26606352	13	69°	C	2	2.8615	1.672
L1560	447243	5499254	43.93110277	27.1	88°	D	2	5.384	3.332
L1560	447242.5	5499032	22.65007438	12.75	82°	E	2	2.909	1.6465
L1560	447237	5498491.5	40.73473782	23.65	85°	F	2	5.035	2.918

L1570	447335.5	5498513.5	35.25696288	22.6	85°	A	2	4.417	2.7905
L1570	447335	5498989	21.3911259	17.95		B		2.753	1.72
L1570	447333.5	5499262	31.3791969	20.7	85°	C	2	3.965	2.5655
L1570	447333.5	5499419.5	29.33328863	17.95	71°	D	2	3.722	2.237
L1570	447335	5499623	25.39331295	15.65		E		3.246	1.985
L1570	447337	5500061	21.01705953	6.1	79°	F	2	2.7065	0.874
L1570	447337	5500410	35.24392597	18.65	66°	G	2	4.4155	2.321
L1580	447442	5500423	37.09399481	21.25	74°	A	2	4.627	2.6295
L1580	447440.5	5500076.5	40.24714604	6.5	87°	B	2	4.981	0.919
L1580	447441	5499848	18.79497177	7.65		C		2.429	1.421
L1580	447440	5499562.5	28.87782537	20.15	80°	D	2	3.6675	2.497
L1580	447443	5499373	31.57417664	17.9		E		3.988	2.038
L1580	447444	5499280	32.23294561	19.05	86°	F	2	4.0655	2.3715
L1580	447435.5	5498544	25.98404375	19.25	86°	G	2	3.318	2.388
L1590	447538.5	5498574	19.48984604	13.5	83°	A	2	2.516	1.7275
L1590	447536	5498985	29.81094208	13.8		B		3.779	1.782
L1590	447535	5499315	27.08821943	16.05		C		3.452	2.251
L1590	447532	5499584.5	29.96626007	18.15	62°	D	2	3.7975	2.263
L1590	447536.5	5500438	32.8089841	19.35	62°	E	2	4.133	2.405
L1600	447636.5	5500440	23.34286362	15.75	68°	A	2	2.9945	1.982
L1600	447640	5499673	29.26635637	14.15		B		3.714	1.591
L1600	447640	5499498	29.09078283	14.8		C		3.693	2.16
L1600	447637	5499307	28.11164584	20.9	88°	D	2	3.5755	2.583
L1600	447635	5498983	32.98863597	19.1		E		4.154	2.042
L1600	447640.5	5498599	28.55679222	19.5	83°	F	2	3.629	2.4225
L1610	447738.5	5498607	38.30115301	24.85	85°	A	2	4.7635	3.0635
L1610	447735.5	5499045.5	41.06534404	14.9	76°	B	2	5.0715	1.8905
L1610	447736.5	5499344	35.24392597	21.15	88°	C	2	4.4155	2.6165
L1610	447737.5	5499620.5	25.87725486	13	71°	D	2	3.305	1.6715
L1610	447734	5500056	17.98216116	8.95		E		2.327	0.861
L1610	447739.5	5500451.5	22.09648278	14.4	75°	F	2	2.8405	1.8265

L1610	447741	5500779	14.70818106	11.8		G		1.914	1.402
L1610	447739	5500953	9.502363658	9.15		H		1.253	1.066
L1620	447836	5500924	18.00604007	9.25		A		2.33	1.417
L1620	447834	5500765	15.28518042	11.2		B		1.987	1.514
L1620	447836	5500465	29.65995904	17.6	79°	C	2	3.761	2.2015
L1620	447837	5499627.5	20.86034875	12.55	82°	D	2	2.687	1.62
L1620	447837.5	5499368.5	26.2965281	17.25	84°	E	2	3.356	2.1575
L1620	447840	5499185	48.60884455	21.75		F		5.879	3.214
L1620	447839	5498988	31.69297691	19.15		G		4.002	1.575
L1620	447838	5498613.5	31.2098421	20.85	80°	H	2	3.945	2.577
L1630	447934.5	5498625	40.40496395	21.55	90°	A	2	4.9985	2.661
L1630	447934	5499027	46.60264463	18.35		B		5.669	1.99
L1630	447933	5499202	48.40673355	21.15		C		5.858	3.259
L1630	447936.5	5499381	38.44779698	21.5	83°	D	2	4.78	2.656
L1630	447937	5499563	18.31661368	15.65		E		2.369	1.547
L1630	447936	5499695	19.51383484	12.2		F		2.519	1.609
L1630	447932	5500078	34.97042165	8.8		G		4.384	0.757
L1630	447937	5500440	35.59633699	12.9		H		4.456	2.563
L1630	447936	5500530	21.02911798	17.75		I		2.708	1.881
L1630	447940	5500941	16.73462691	13.95		J		2.17	1.684
L1640	448037	5500931	22.9739307	13.7		A		2.949	1.819
L1640	448042	5500534	20.87641748	14.45		B		2.689	1.856
L1640	448044	5500445	24.74711354	16.05		C		3.167	2.188
L1640	448043.5	5499641	23.23739403	14.25	75°	D	2	2.9815	1.8155
L1640	448043	5499387.5	42.39625298	25.3	82°	E	2	5.2175	3.116
L1640	448043	5499280	45.57410864	25.1		F		5.56	2.925
L1640	448040	5499196	47.09636244	23.3		G		5.721	2.825
L1640	448037	5498612	42.91501472	24.05	83°	H	2	5.274	2.961
L1650	448130	5498620.5	43.67168754	23.9	81°	A	2	5.356	2.947
L1650	448139	5499214	40.16605604	23.75		B		4.972	2.741
L1650	448133.5	5499396.5	35.35260284	22.85	78°	C	2	4.428	2.822

L1650	448134.5	5499689	17.58043636	13.05	82°	D	2	2.2765	1.6765
L1650	448138	5500519.5	22.92937407	17	69°	E	2	2.9435	2.132
L1650	448137	5500963	24.95138949	16.2		F		3.192	2.134
L1660	448242	5500947	24.3391526	16.4		A		3.117	1.973
L1660	448243	5500781	18.36441895	13.5		B		2.375	1.476
L1660	448243	5500575	21.23821766	13.05		C		2.734	1.873
L1660	448244	5500482	21.51190617	16.1		D		2.768	2.17
L1660	448245	5500164	61.02159152	11.2		E		7.103	0.74
L1660	448239.5	5499696.5	18.12944012	14.5	82°	F	2	2.3455	1.846
L1660	448241	5499427	36.95318459	17.9		G		4.611	2.731
L1660	448242	5499306	45.92228643	24.05		H		5.597	3.205
L1660	448244	5499217	49.32374107	26.2		I		5.953	3.254
L1660	448231.5	5498624.5	44.44688543	24.55	79°	J	2	5.4395	3.0225
L1670	448334	5498641	37.45106001	18.65	85°	A	2	4.6675	2.3225
L1670	448337	5498877	58.22185086	15.7		B		6.838	1.649
L1670	448335	5499106	53.18325705	17.9		C		6.345	2.841
L1670	448334	5499279.5	40.18407174	27.4	78°	D	2	4.974	3.367
L1670	448338	5499488.5	37.22613398	24.9	72°	E	2	4.642	3.072
L1670	448338	5499718.5	20.97284984	17	66°	F	2	2.701	2.1275
L1670	448333	5500507	24.89417213	17.65		G		3.185	2.215
L1670	448338	5500659	22.43980352	16.3		H		2.883	1.875
L1670	448341	5500797	16.52047825	12.7		I		2.143	1.403
L1670	448340	5500976	26.71670581	12.25		J		3.407	1.776
L1680	448444	5500950	32.53563196	15.05		A		4.101	2.038
L1680	448441	5500793	18.57962598	14.2		B		2.402	1.576
L1680	448437	5500604	26.33768165	14.9		C		3.361	2.192
L1680	448437	5500550	35.27434725	19.65		D		4.419	2.679
L1680	448445	5499808	23.98078524	19.45		E		3.073	2.156
L1680	448444.5	5499499	37.37163261	22.15	79°	F	2	4.6585	2.7395
L1680	448445.5	5499296	45.54122345	25.7	79°	G	2	5.5565	3.164
L1680	448443	5498682	24.67362277	19.75		H		3.158	1.798

L1690	448533	5498666.5	21.18994929	13.85	84°	A	2	2.728	1.7665
L1690	448537	5498884	31.17599254	13.4		B		3.941	1.668
L1690	448541	5499301	48.82094131	20.65		C		5.901	3.481
L1690	448539	5499373	40.1120237	26.8		D		4.966	3.121
L1690	448539	5499446	36.89162483	24		E		4.604	2.797
L1690	448537	5499559	28.66512745	20.65		F		3.642	2.316
L1690	448537	5499838	14.20280219	15.3		G		1.85	1.553
L1690	448535	5500486	24.80429075	14.65		H		3.174	2.166
L1690	448535	5500711	26.86522387	18.1		I		3.425	2.353
L1690	448534	5500817	20.36268262	17.15		J		2.625	1.944
L1700	448631.5	5498670.5	15.46315062	11.35	84°	A	2	2.0095	1.479
L1700	448630	5498887	29.60127974	12.85		B		3.754	1.869
L1700	448634	5499300	41.82483564	19.7		C		5.155	3.044
L1700	448635	5499377	35.21351109	24.3		D		4.412	2.95
L1700	448636	5499471	34.60654687	21.25		E		4.342	2.31
L1700	448635	5499547	32.41619227	17.4		F		4.087	2.033
L1700	448630	5499880	29.80255059	11.15		G		3.778	0.877
L1700	448634	5500502	21.40722669	9.9		H		2.755	1.75
L1700	448634	5500597	32.77478854	16.4		I		4.129	2.37
L1700	448636	5500713	30.51733385	19.95		J		3.863	2.572
L1700	448636	5500815	26.13200063	20		K		3.336	2.389
L1710	448738	5500724	45.0583444	22.05		A		5.505	3.068
L1710	448732	5500604	37.44664618	22.7		B		4.667	2.533
L1710	448732	5500514	24.33100132	17.3		C		3.116	1.79
L1710	448742	5499634.5	24.26987647	19.65	84°	D	2	3.1085	2.437
L1710	448737	5499368	39.95905186	23.75	87°	E	2	4.949	2.9265
L1710	448733	5499174	46.41327959	22.05		F		5.649	2.553
L1710	448739.5	5498671	21.34685382	15.9	82°	G	2	2.7475	1.9985
L1720	448835	5498501	15.24959384	13	81°	A	2	1.9825	1.6725
L1720	448836	5498703	23.1765682	15.4	79°	B	2	2.974	1.944
L1720	448836	5499385.5	35.4918289	22.15	89°	C	2	4.444	2.737

L1720	448835	5499648	17.35788564	14.6	82°	D	2	2.2485	1.8525
L1720	448830	5500205	47.31537274	10.55		E		5.744	0.932
L1720	448836	5500539	25.05769203	11.5		F		3.205	2.063
L1720	448837	5500642	34.97042165	17.05		G		4.384	2.215
L1720	448838	5500734	39.90510397	20.9		H		4.943	2.965
L1720	448837	5501620	18.61949426	15.1		I		2.407	0.871
L1730	448940	5500727	29.08242663	11.8		A		3.692	2.181
L1730	448940	5500632	26.56006191	16.25		B		3.388	1.9
L1730	448941	5500545	22.83623752	15.7		C		2.932	2.054
L1730	448942	5500210	16.81396918	11.15		D		2.18	0.851
L1730	448944	5499873	31.14215009	12.1		E		3.937	2.282
L1730	448943	5499713	24.6246431	17.35		F		3.152	2.06
L1730	448941.5	5499630.5	24.06625125	16.75	84°	G	2	3.0835	2.0975
L1730	448940	5499464	32.20313514	18.95		H		4.062	2.483
L1730	448941	5499228	27.25357202	18.2		I		3.472	2.057
L1730	448940	5499143	26.93952647	17		J		3.434	2.193
L1730	448938.5	5498709.5	36.3431799	22.55	89°	K	2	4.5415	2.7835
L1730	448939	5498616	21.60051419	18.3		L		2.779	1.966
L1730	448939	5498547	18.44410928	13.6		M		2.385	1.507
L1730	448941	5498480	20.29051426	13.5		N		2.616	1.942
L1740	449031	5498535	27.4107929	15.45		A		3.491	1.96
L1740	449031.5	5498724.5	30.06288157	18.7	86°	B	2	3.809	2.326
L1740	449032	5499402	26.08266932	17.8		C		3.33	2.129
L1740	449033	5499477	25.84440829	16.75		D		3.301	2.066
L1740	449032.5	5499650.5	25.97582717	18.1	90°	E	2	3.317	2.2565
L1740	449030	5499859	33.49450851	18.8		F		4.213	2.499
L1740	449034	5500252	21.31063678	13.25		G		2.743	0.9
L1740	449034	5500548	25.27046114	13.05		H		3.231	2.461
L1740	449032	5500650	23.81808449	17.45		I		3.053	1.915
L1740	449033	5500746	27.52672527	16.2		J		3.505	2.168
L1750	449146	5500656	26.20602086	17.25		A		3.345	2.153

L1750	449145	5500555	32.08395005	19.05		B			4.048	2.584
L1750	449140	5499871	35.87539858	20.65		C			4.488	2.523
L1750	449140.5	5499640	27.31561701	18.3	76°	D		2	3.4795	2.2815
L1750	449141	5499486	27.63444209	19.55		E			3.518	2.487
L1750	449143	5499411	30.18058319	20.5		F			3.823	2.59
L1750	449140	5498737	34.4595209	19.8		G			4.325	2.321
L1750	449143	5498173	5.724972486	11.2		H			0.773	0.579
L1760	449233	5497980	6.481312877	4.6		A			0.869	0.802
L1760	449233	5498210	10.6033235	6.8		B			1.393	1.111
L1760	449234	5498370	15.84699393	9.15		C			2.058	1.348
L1760	449235	5498739.5	30.34045436	18.95	73°	D		2	3.842	2.3555
L1760	449238	5499469.5	30.78301028	22.2	80°	E		2	3.8945	2.744
L1760	449237	5499557	38.37667711	22.1		F			4.772	2.807
L1760	449237	5499686	31.09139971	20.05		G			3.931	2.176
L1760	449238	5499885	36.79494284	15.95		H			4.593	1.844
L1760	449234.5	5500618.5	28.33616021	17.6	88°	I		2	3.6025	2.1995
L1770	449333	5500896	39.49222994	20.3		A			4.897	2.659
L1770	449336	5500625	25.02906676	16.65	89°	B		2	3.2015	2.0845
L1770	449334	5499689	33.08282361	18.1		C			4.165	2.522
L1770	449337	5499568	27.69246965	19.15		D			3.525	2.232
L1770	449341	5499407	28.02441047	17.65		E			3.565	2.18
L1770	449338	5498867	52.29600749	21		F			6.256	3.033
L1770	449336	5498768	35.78813329	22.6		G			4.478	2.551
L1770	449339	5498391	15.18238143	16.1		H			1.974	1.506
L1770	449340	5498171	8.472201814	9.85		I			1.122	1.108
L1770	449338	5497973	8.189056874	6.7		J			1.086	0.776
L1780	449433	5498236	17.51286243	7.15		A			2.268	1.216
L1780	449439	5498408	16.77429613	10.45		B			2.175	1.547
L1780	449435	5498745.5	49.91137251	27.5	81°	C		2	6.0135	3.377
L1780	449431	5499553	26.90649949	19.85	86°	D		2	3.43	2.458
L1780	449436	5499921	20.60337736	12.95		E			2.655	0.922

L1780	449431.5	5500676	28.78604166	20.1	90°	F	2	3.6565	2.4915
L1790	449537	5500929	32.23720472	22.35		A		4.066	3.065
L1790	449539.5	5500674	34.09259601	23.7	78°	B	2	4.2825	2.9195
L1790	449543	5499891	27.25357202	15.3		C		3.472	0.822
L1790	449543.5	5499512	26.85284293	16.75	86°	D	2	3.4235	2.099
L1790	449538	5498750.5	30.47941514	20.4	80°	E	2	3.8585	2.525
L1790	449534	5498464	21.11756319	17.1		F		2.719	1.759
L1790	449538	5498227	8.88900707	11.65		G		1.175	1.274
L1800	449631	5498254	21.83426421	10.75		A		2.808	1.558
L1800	449634	5498440	22.10859183	11.1		B		2.842	1.35
L1800	449635.5	5498754.5	34.77537602	21.05	85°	C	2	4.3615	2.605
L1800	449632	5499276	39.18788179	20.05		D		4.863	2.451
L1800	449635	5499481	30.44150515	20.8		E		3.854	2.689
L1800	449636	5499562	26.46119466	21.1		F		3.376	2.531
L1800	449635	5499676.5	29.26217397	22.5	85°	G	2	3.7135	2.7775
L1800	449635.5	5500712.5	30.18478836	21.3	90°	H	2	3.8235	2.632
L1810	449741	5500932	30.5931975	22.7		A		3.872	2.743
L1810	449743.5	5500700	29.40024702	21.9	86°	B	2	3.73	2.7085
L1810	449739	5499629	26.01691346	20.95		C		3.322	2.322
L1810	449739.5	5499526.5	26.40354546	19	89°	D	2	3.369	2.365
L1810	449736	5499278	42.08965774	20.3		E		5.184	2.607
L1810	449743.5	5498771	34.17022186	22.65	77°	F	2	4.2915	2.796
L1810	449741	5498247	6.189883013	13.8		G		0.832	0.676

Solomon Pillars Property

Line	x	y	Cond_BF	Cond_SF	dIP1	ID	Peak	TauBF	TauSF
L2000	452722.1	5504735.25	17.05	10.7	76°	A	2	2.21	1.41
L2010	452823.45	5504730.65	17.3	10.1	83°	A	2	2.24	1.34
L2020	452919.3	5504735.35	13.4	9.25	74°	A	2	1.75	1.24
L2020	452920.4	5502635	12.45	10.55		B		0.81	1.3

L2030	453027.65	5504719.4	11	5.55	80°	A	2	1.445	0.805
L2040	453122.45	5504733.6	7.15	4.75	78°	A	2	0.955	0.71
L2050	453223.9	5504708.95	8.5	4.75	87°	A	2	1.125	0.71
L2060	453323.1	5504696.6	7.3	4.9	85°	A	2	0.975	0.73
L2070	453424.7	5504671.65	8.35	5.9	88°	A	2	1.11	0.845
L2080	453520.5	5504664.3	7.65	6	83°	A	2	1.015	0.86
L2090	453620.35	5504635.95	7.25	5.35	81°	A	2	0.97	0.78
L2100	453724.4	5504620.9	6.5	4.95	85°	A	2	0.87	0.73
L2110	453824.7	5504506	12.25	7.95	90°	A	2	1.605	1.09
L2120	453923.05	5504516.25	13.05	8.7	88°	A	2	1.705	1.185
L2130	454020.65	5504481.8	11.05	7.15	84°	A	2	1.445	1
L2140	454123.5	5504656.7	13.05	7.6		A		1.92	1.1
L2140	454123.95	5504480.05	12.85	7.25	85°	B	2	1.67	1.015
L2150	454225.45	5504462.15	14.9	7.05	89°	A	2	1.935	0.985
L2160	454320.75	5504447.1	15.05	7.3	86°	A	2	1.955	1.02
L2170	454422.9	5504442.15	13.05	6.6	89°	A	2	1.7	0.935
L2180	454522.85	5505132.3	7.85	5.3	90°	A	2	1.04	0.775
L2180	454518.05	5504434.2	13	7.35	90°	B	2	1.7	1.02
L2190	454623.8	5504430.2	14.7	7.75	84°	A	2	1.915	1.07
L2190	454621.6	5504706.8	16.15	8.65	85°	B	2	2.1	1.175
L2190	454621.9	5505016.95	10.3	6.65	86°	C	2	1.36	0.935
L2200	454723.6	5505077.75	7.85	5.35	65°	A	2	1.04	0.785
L2200	454719.8	5504400.45	12.75	8.3	90°	B	2	1.665	1.135
L2210	454829.3	5504391.6	13.5	9.75	78°	A	2	1.765	1.3
L2210	454821.6	5505098.05	9.5	6.55	75°	B	2	1.25	0.925
L2220	454922.25	5505153.7	10.9	6.8	84°	A	2	1.43	0.955
L2220	454922.6	5504372.85	11.85	9.4	76°	B	2	1.555	1.26
L2230	455022.8	5504372.85	12.45	8.95	79°	A	2	1.62	1.21
L2230	455020.4	5505208.3	8.05	5.5	64°	B	2	1.075	0.8
L2240	455123.85	5504868.05	20.95	8.9	85°	A	2	2.675	1.205
L2240	455120.8	5504367.75	11.95	8.05	81°	B	2	1.57	1.105
L2250	455222.9	5504364.85	12.55	6.85	85°	A	2	1.635	0.97

L2250	455226.5	5504877.2	9.05	7	83°	B	2	1.195	0.985
L2260	455321.05	5505353.8	8.75	4.65	67°	A	2	1.15	0.7
L2260	455321.9	5504927.55	9.8	6.35	81°	B	2	1.295	0.9
L2260	455319.3	5504381.05	10.95	6.75	78°	C	2	1.44	0.955
L2270	455425.4	5504551	11.4	6.6		A		1.57	0.9
L2270	455426.1	5504735.45	20.05	10.45	89°	B	2	2.59	1.38
L2270	455422.3	5505117.35	7.2	4.95	85°	C	2	0.955	0.735
L2270	455422.6	5505444.8	6.6	4.35	77°	D	2	0.885	0.655
L2280	455524.95	5505484.1	7.75	5.7	48°	A	2	1.03	0.82
L2280	455524.8	5505156.15	10.7	4.35	81°	B	2	1.41	0.66
L2280	455519.9	5504823.6	16.6	7.45		C		2.53	1.41
L2280	455518.1	5504620.4	16.3	9.6	83°	D	2	2.12	1.28
L2290	455620.1	5504638.8	14.85	8.85		A		1.9	1.16
L2290	455621.15	5504815.9	18.6	9.85	86°	B	2	2.405	1.31
L2300	455720.9	5504846.5	16.75	9.85	83°	A	2	2.18	1.315
L2300	455723.5	5504631.7	15	9.15		B		1.69	1.15
L2310	455821.1	5504633.4	14.45	9.1		A		2.07	1.3
L2310	455819.65	5504886.45	31.2	13.95	74°	B	2	3.94	1.78
L2310	455824.2	5505275.1	12.4	6.65	85°	C	2	1.62	0.945
L2320	455927.2	5505497.7	9.35	6.1		A		0.8	0.78
L2320	455925.3	5505047.3	19.1	9.75		B		4.07	1.8
L2320	455923.3	5504518.4	27.65	13.1	67°	C	2	3.515	1.675
L2330	456019.5	5504441.3	30.95	12.5		A		3.81	1.48
L2330	456019.25	5504671.55	28.55	14	80°	B	2	3.62	1.79
L2330	456022.2	5505021	30.5	13.3	75°	C	2	3.86	1.7
L2330	456022.75	5505479.95	6.05	4.7	87°	D	2	0.81	0.705
L2340	456124.1	5505483.2	6.5	4.85		A		0.98	0.73
L2340	456120.95	5505085.7	23.8	9.6	90°	B	2	3.045	1.285
L2340	456127.5	5504723.7	29.3	14.55	79°	C	2	3.71	1.845
L2340	456126	5504490.6	28.65	14.85		D		4.22	2.08
L2350	456226.45	5504786.25	27.45	13.6	77°	A	2	3.485	1.735
L2350	456221.1	5505130.85	27.75	11.75	62°	B	2	3.515	1.525

L2360	456325.15	5505649.75	17.6	8.6	78°	A	2	2.28	1.165
L2360	456321.5	5505189.6	34.75	14.65	82°	B	2	4.355	1.86
L2360	456321	5504851.55	30.05	13.7	82°	C	2	3.795	1.75
L2370	456425	5504928		13.3		A	2	3.3	1.8
L2370	456424.15	5505225.7	28.2	14.15	77°	B	2	3.585	1.795
L2370	456425.6	5505615.7	29.2	13.65		C		4.06	1.76
L2380	456524.1	5505462	35.65	13.45		A		4.85	1.68
L2380	456522.5	5505246.5	32.15	12.5	82°	B	2	4.035	1.615
L2380	456525.5	5504983.5	26.35	13.15	77°	C	2	3.36	1.685
L2390	456624	5505011.5	26	12.8	84°	A	2	3.3	1.6
L2390	456626	5505250.5	32	17.55	82°	B	2	4.035	2.19
L2400	456718.75	5505276.35	31.2	14.2	72°	A	2	3.945	1.805
L2400	456720.55	5505112.2	29.5	14.15	82°	B	2	3.74	1.795
L2410	456820.85	5505067.7	27.55	14	82°	A	2	3.505	1.78
L2410	456828.1	5505304.4	28.35	14	86°	B	2	3.605	1.78
L2420	456922.8	5505623.9	19.8	10.6		A		2.51	1.31
L2420	456923.4	5505330.55	18.35	10.35	80°	B	2	2.38	1.37
L2420	456926.05	5505113	28.2	14.75	84°	C	2	3.585	1.87
L2420	456927	5503321.4	40.25	18.25		D		6.13	2.55
L2430	457021.1	5505135.95	23.5	12	84°	A	2	3.01	1.56
L2430	457022	5505358.2	19.25	10.3	69°	B	2	2.485	1.37
L2430	457022	5505674.4	20.95	11.1		C		2.78	1.54
L2440	457121.15	5505362.15	27.2	15.55	72°	A	2	3.465	1.96
L2440	457121.15	5505184.1	23.15	12.4	86°	B	2	2.97	1.605
L2450	457286.8	5502870.8	21.05	12.5		A		2.37	1.59
L2450	457223.6	5504940.45	25.05	10.45	81°	B	2	3.2	1.38
L2450	457225.4	5505198.6	23.55	11.65	70°	C	2	3.02	1.51
L2450	457226.9	5505385	31.1	13.3	87°	D	2	3.92	1.705
L2460	457327	5505615.15	29.05	14.45	80°	A	2	3.69	1.835
L2460	457322.7	5505365.2	30.65	11.5	88°	B	2	3.875	1.5
L2460	457328.5	5504969.35	16.95	8.7	90°	C	2	2.2	1.18
T2500	455494.3	5505562	9.85	6.35		A		0.72	0.74

T2500	456041.5	5505572	5.9	5.3		B		0.87	0.82
T2500	456357.4	5505558.5	16.5	9.1		C		3.38	1.62
T2500	456671.5	5505559.4	29.35	9.6		D		4.07	0.93
T2500	456980.3	5505561.6	27.65	9.85		E		2.97	1.68
T2510	457364.2	5504609.3	28.8	12.3		A		4.33	1.5
T2510	455828.7	5504612.6	18.85	10.45		B	2	2.43	1.375

West Geraldton Property

Line	X	y	Cond_BF	Cond_SF	Dip1	ID	Peak	TauBF	TauSF
L3010	493015	5508388.5	17.65	12.7343329	68°	A	2	2.28	1.64
L3010	493020.5	5508911	39.8	23.88592249	88°	B	2	4.93	2.945
L3020	493120.5	5508905	29.5	17.66384968	87°	A	2	3.745	2.205
L3020	493119.5	5508373	23.7	14.84260902	72°	B	2	3.035	1.88
L3030	493217	5508380	25.5	16.45471537	79°	A	2	3.26	2.065
L3030	493221.5	5508854.5	34.3	21.0175808	82°	B	2	4.305	2.6
L3040	493320.5	5508807.5	28.85	20.47150666	85°	A	2	3.665	2.535
L3040	493320.5	5508372.5	22.65	16.06396913	82°	B	2	2.91	2.02
L3050	493417	5508314	26	19.83868199	80°	A	2	3.315	2.46
L3050	493414	5508757	31.8	21.22704956	84°	B	2	4.015	2.625
L3060	493522	5508723	32.9	22.81002443	84°	A	2	4.145	2.815
L3060	493517.5	5508293	26.7	21.77029671	84°	B	2	3.405	2.69
L3070	493612.5	5508273.5	29.5	21.0175808	74°	A	2	3.735	2.6
L3070	493617	5508695	29.8	20.47150666	83°	B	2	3.775	2.535
L3080	493723.5	5508681.5	25.7	18.00739604	85°	A	2	3.285	2.245
L3080	493720.5	5508186	15	11.36927954	77°	B	2	1.955	1.485
L3090	493821	5508166.5	18.95	13.65829585	89°	A	2	2.445	1.745
L3090	493818	5508642.5	22.55	17.01736734	88°	B	2	2.895	2.13
L3100	493921.5	5508617.5	20.15	15.10499386	90°	A	2	2.595	1.91
L3100	493920.5	5508197.5	19.55	12.11777038	86°	B	2	2.52	1.57
L3110	494018	5508169.5	21.55	13.0424958	84°	A	2	2.77	1.675
L3110	494016	5508591	25.1	18.43558333	90°	B	2	3.215	2.295

L3120	494122	5508563.5	23.15	16.67137203	84°	A	2	2.97	2.09
L3120	494122	5508663.5							
L3130	494221	5508523	22.95	16.4113471	86°	A	2	2.94	2.06
L3130	494221	5508623							
L3140	494322	5508508.5	23.2	16.80121597	85°	A	2	2.975	2.105
L3140	494322	5508608.5							
L3150	494421.5	5508089.5	26	13.70224609	87°	A	2	3.315	1.75
L3150	494419	5508471	24.8	15.97700739	86°	B	2	3.17	2.01
L3160	494521	5508571	22.4	19.75407614		A		2.87	2.45
L3160	494526	5508067.5	22.45	14.44843952	80°	B	2	2.885	1.835
L3170	494619	5508028	26.8	19.92323328	87°	A	2	3.415	2.47
L3170	494619	5508128							
L3180	494719.5	5507990.5	26.6	20.93370784	79°	A	2	3.39	2.59
L3180	494719.5	5508090.5							
L3190	494817	5507961	26.45	21.39440944	79°	A	2	3.375	2.645
L3190	494817	5507801							
L3200	494918	5507947.5	25.35	19.7963859	75°	A	2	3.235	2.455
L3200	494918	5507997.5							
L3210	495019.5	5507925.5	27.1	20.55565843	88°	A	2	3.45	2.545
L3210	495019.5	5508025.5							
L3220	495114	5507925	25.95	19.6694155	87°	A	2	3.31	2.44
L3220	495114	5508025							
L3230	495217	5507933.5	28.1	21.31075306	79°	A	2	3.575	2.635
L3230	495217	5508033.5							
L3240	495318.5	5507905.5	29.05	20.34518115	83°	A	2	3.685	2.52
L3240	495318.5	5508005.5							
L3250	495415	5507870	27.5	18.43558333	82°	A	2	3.505	2.295
L3250	495415	5507970							
L3260	495515	5507873	26.75	19.3302208	90°	A	2	3.41	2.4
L3260	495515	5507973							
L3270	495614	5507833.5	26.05	16.71466597	79°	A	2	3.32	2.095
L3270	495615	5508248	27.5	15.45430189		B		3.5	1.95

L3280	495717	5508166	25.8	16.10743267	84°	A	2	3.28	2.025
L3280	495721	5507836.5	25.55	18.17883803	87°	B	2	3.265	2.265
L3290	495816	5507823.5	32.3	20.47150666	83°	A	2	4.07	2.535
L3290	495814.5	5508130	19.75	12.64626554	90°	B	2	2.55	1.63
L3300	495915	5508133	16.55	11.14930604	89°	A	2	2.15	1.46
L3300	495918.5	5507839	27.65	19.5423213	86°	B	2	3.52	2.425
L3310	496017	5507836	16.45	13.92191145	90°	A	2	2.135	1.775
L3310	496013	5508202	16.8	11.5013125		B		2.17	1.5
L3320	496117.5	5507897.5	5.45	3.350549124	85°	A	2	0.745	0.53
L3320	496117.5	5507997.5							
L3330	496219.5	5507907.5	13.6	11.23728195	90°	A	2	1.775	1.47
L3330	496219.5	5508007.5							
L3340	496316	5508313	18.4	12.9104419		A		2.38	1.66
L3340	496316.5	5507917	20.8	12.69030014	88°	B	2	2.68	1.635
L3350	496418	5507908.5	19.25	14.31690448	81°	A	2	2.49	1.82
L3350	496418	5508283	27	16.4113471		B		3.44	2.06
L3360	496521	5508221	23.1	16.49807142	87°	A	2	2.965	2.07
L3360	496517.5	5507955	19.25	15.0175693	75°	B	2	2.485	1.9
L3370	496624	5507964.5	22.2	15.0612863	73°	A	2	2.855	1.905
L3370	496622.5	5508223	22.75	16.58474657	86°	B	2	2.925	2.08
L3380	496716.5	5507968	24.7	15.62871056	74°	A	2	3.15	1.97
L3380	496721	5508239	24.7	19.28775899	89°	B	2	3.16	2.395
L3390	496818	5508246	23.9	17.53479432	83°	A	2	3.065	2.19
L3390	496825	5507967	25.45	13.96582636	72°	B	2	3.25	1.78
L3400	496916	5507969	26.75	14.53609063	79°	A	2	3.4	1.845
L3400	496914	5508232	21.65	15.4106736	90°	B	2	2.785	1.945
L3410	497024	5508212.5	23.95	16.67137203	86°	A	2	3.065	2.09
L3410	497022.5	5507981.5	29.3	16.71466597	76°	B	2	3.705	2.095
L3420	497118	5507937.5	31.15	17.49174879	73°	A	2	3.94	2.185
L3420	497113.5	5508201.5	27	18.90497389	86°	B	2	3.435	2.35
L3430	497218	5508181.5	25.5	20.63975849	83°	A	2	3.265	2.555
L3430	497223	5507909	32.5	13.2625193	68°	B	2	4.1	1.7

L3440	497314.5	5507863	29.35	11.5013125	64°	A	2	3.715	1.5
L3440	497316	5508173.5	21.95	17.40561733	81°	B	2	2.825	2.175
L3450	497422.5	5508181.5	19.75	15.97700739	84°	A	2	2.545	2.01
L3450	497422	5507821	24.3	11.45729793	80°	B	2	3.08	1.495
L3460	497517.5	5507825.5	27.5	14.71129505	78°	A	2	3.425	1.865
L3460	497518	5508181.5	21.6	16.67137203	88°	B	2	2.78	2.09
L3470	497617	5508199.5	25.7	17.87866923	86°	A	2	3.28	2.23
L3470	497621.5	5507854.5	30.9	14.84260902	76°	B	2	3.86	1.88
L3470	497620	5505937	1.6	2.172927179		C		0.25	0.37
L3480	497715	5505966	1.5	1.821414318		A		0.24	0.32
L3480	497718	5507842.5	36.05	13.52641341	78°	B	2	4.45	1.73
L3480	497720.5	5508198.5	31.85	22.56102747	87°	C	2	4.02	2.785
L3490	497820	5508194	35.4	24.25747378	88°	A	2	4.435	2.99
L3490	497816.5	5507877	25.1	15.0612863	80°	B	2	3.205	1.905
L3500	497919	5507879.5	20.7	13.79012984	85°	A	2	2.665	1.76
L3500	497916.5	5508201.5	30.15	20.59771489	90°	B	2	3.82	2.55
L3510	498018.5	5508230	21.7	16.23775311	85°	A	2	2.79	2.04
L3510	498017	5507858.5	20.9	15.10499386	84°	B	2	2.69	1.91
L3520	498118	5507839.5	20.1	13.08650757	87°	A	2	2.585	1.68
L3520	498117	5508216.5	16.9	11.85353058	80°	B	2	2.185	1.54
L3530	498218.5	5508224	13.95	10.79762012	79°	A	2	1.815	1.42
L3530	498220	5507842	15.45	10.35863767	88°	B	2	2.01	1.37
L3540	498318.5	5507812.5	12.55	8.527833467	83°	A	2	1.64	1.16
L3540	498316.5	5508208.5	11.85	9.440041605	84°	B	2	1.55	1.265
L3550	498422.5	5508190	6.1	7.156	89°	A	2	0.815	1
L3550	498419	5507678	8.2	5.650465106		B		1.09	0.82
L3560	498519	5507847	6	4.200920289		A		0.81	0.64
L3560	498515.5	5508166.5	5.75	4.398228441	84°	B	2	0.78	0.665
L3570	498618	5508285	6.6	4.596920535		A		0.88	0.69
L3570	498618.5	5507939.5	5.65	5.4863168	74°	B	2	0.765	0.8
L3580	498722	5507884	9.95	8.225623779	72°	A	2	1.305	1.125
L3580	498722	5507984							

L3590	498822.5	5507860	11.4	8.614366263	83°	A	2	1.495	1.17
L3590	498822.5	5507960							
L3600	498916	5507746.5	24.15	10.57802965	70°	A	2	3.1	1.395
L3600	498916	5507846.5							
L3610	499019	5507698	23.9	13.39448652	60°	A	2	3.06	1.715
L3610	499019	5507798							
L3620	499117	5507506	28.3	17.53479432		A		3.6	2.19
L3620	499117	5507699.5	24.8	15.49791983	76°	B	2	3.17	1.955
L3630	499220	5507689	25.95	16.84447191	67°	A	2	3.315	2.11
L3630	499220	5507789							
L3640	499318	5507662.5	19.5	14.53609063	68°	A	2	2.515	1.845
L3640	499318	5507762.5							
L3650	499417	5507628	21.6	17.7927825	85°	A	2	2.78	2.22
L3650	499417	5507728							
L3660	499514	5507609	19.3	15.67228614	88°	A	2	2.495	1.975
L3660	499514	5507609							
L3670	499618	5507591	19.15	16.15088457	84°	A	2	2.475	2.03
L3670	499618	5507691							
L3680	499719	5507566	28.65	18.09314479	83°	A	2	3.635	2.255
L3680	499719	5507566							
L3690	499810.5	5507621.5	16.25	8.744312662	82°	A	2	2.1	1.185
L3690	499810.5	5507721.5							
L3700	499915.5	5507596	22.6	17.49174879	70°	A	2	2.905	2.185
L3700	499915.5	5507696							
L3710	500017.5	5507550.5	19	11.01738025	77°	A	2	2.45	1.445
L3710	500017.5	5507650.5							
L3720	500118.5	5507493	25.55	15.93350936	52°	A	2	3.26	2.005
L3720	500118.5	5507593							
L3730	500221.5	5507429.5	34.55	23.3899049	73°	A	2	4.32	2.885
L3730	500221.5	5507529.5							
L3740	500313.5	5507415	29.8	19.83868199	84°	A	2	3.775	2.46
L3740	500313.5	5507515							

L3750	500417.5	5507336	24.6	15.93350936	78°	A	2	3.145	2.005
L3750	500417.5	5507436							
L3760	500522.5	5507310.5	26.05	9.876821182	79°	A	2	3.33	1.315
L3760	500522.5	5507410.5							
L3770	500622.5	5507281	26.05	10.70976198	84°	A	2	3.33	1.41
L3770	500622.5	5507381							
L3780	500713	5507116	26.7	14.57990414		A		3.41	1.85
L3780	500716	5507506.5	24.95	14.97384296	82°	B	2	3.19	1.895
L3790	500817	5507213.5	25.35	15.27972757	81°	A	2	3.24	1.93
L3790	500817	5507313.5							
L3800	500919.5	5507219	24.35	15.45430189	73°	A	2	3.12	1.95
L3800	500917	5507468	27	17.36253148		B		3.45	2.17
L3810	501017.5	5507399.5	24.9	16.62806554	61°	A	2	3.185	2.085
L3810	501021	5507097	23.2	14.05363689		B		2.97	1.79
L3820	501122	5507091	21.1	12.29394311		A		2.72	1.59
L3820	501121	5507363.5	27.55	19.07524057	85°	B	2	3.51	2.37
L3830	501221	5507290	18	13.08650757		A		2.33	1.68
L3830	501219	5507080	24.2	12.47011207		B		3.1	1.61
L3840	501318	5507257	23.8	13.2625193	55°	A	2	3.035	1.7
L3840	501318	5507246							
L3850	501420	5507199	29.9	20.42941125	89°	A	2	3.78	2.53
L3850	501420	5507299							
L3860	501514	5506930	23.3	12.9104419		A		2.99	1.66
L3860	501517.5	5507147	31.2	19.58469983	70°	B	2	3.94	2.43
L3870	501617.5	5507509	22.75	7.838694984	86°	A	2	2.885	1.08
L3870	501617	5506985	11.95	12.3820288	68°	B	2	1.565	1.6
L3880	501718	5506337	13.3	7.838694984		A		1.74	1.08
L3880	501714	5506959.5	13.8	12.16181327	82°	B	2	1.805	1.575
L3890	501822.5	5506940	18.1	15.58512426	70°	A	2	2.34	1.965
L3890	501822.5	5507040							
L3900	501923	5506900.5	20.75	17.53479432	77°	A	2	2.675	2.19
L3900	501923	5507000.5							

L3910	502019.5	5506875	22.35	17.49174879	87°	A	2	2.88	2.185
L3910	502017	5507137	25.1	16.7579473		B		3.21	2.1
L3910	502019	5507341	13.5	7.156		C		1.76	1
L3920	502115.5	5506872.5	23.3	17.70684095	82°	A	2	2.985	2.21
L3920	502115.5	5506972.5							
L3930	502219	5506806	19.2	16.06396913		A		2.48	2.02
L3930	502221	5506945.5	23.25	15.67228614	86°	B	2	2.98	1.975
L3940	502323	5506854	26.15	18.22166378	89°	A	2	3.32	2.27
L3940	502323	5506954							
L3950	502422	5506834	17.3	14.49226905		A		2.24	1.84
L3950	502422	5506934							
L3960	502566	5509107	29.6	21.10140466		A		3.75	2.61
L3960	502520	5506877	26.7	17.7927825	84°	B	2	3.39	2.22
L3970	502619.5	5506837.5	26.95	18.69182495	85°	A	2	3.43	2.325
L3970	502621	5507086	38.4	24.00981007		B		4.78	2.96
L3980	502723	5507089	25.95	16.23775311	73°	A	2	3.305	2.04
L3980	502719.5	5506842.5	26.5	20.72380726	82°	B	2	3.375	2.565
L3990	502817.5	5506879.5	27.45	20.63975849	83°	A	2	3.495	2.555
L3990	502817.5	5506979.5							
L4000	502921.5	5506866.5	29.2	20.72380726	77°	A	2	3.71	2.565
L4000	502921.5	5506966.5							
L4010	503018	5506814	25	16.23775311		A		3.2	2.04
L4010	502983	5508091	40.5	44.64866975		B		5.01	5.07
L4040	503313	5508593	56.1	12.29394311		A		6.64	1.59
L4040	503313	5508593							